



**UCGE Reports
Number 20344**

Department of Geomatics Engineering

Geoid Investigations for the New Vertical Datum in Canada

(URL: <http://www.geomatics.ucalgary.ca/graduatetheses>)

by

Elmas Sinem Ince

December 2011



UNIVERSITY OF CALGARY

Geoid Investigations for the New Vertical Datum in Canada

by

Elmas Sinem Ince

A THESIS

SUBMITTED TO THE FACULTY OF GRADUATE STUDIES
IN PARTIAL FULFILMENT OF THE REQUIREMENTS FOR THE
DEGREE OF MASTER OF SCIENCE

DEPARTMENT OF GEOMATICS ENGINEERING

CALGARY, ALBERTA

DECEMBER, 2011

© Elmas Sinem Ince 2011

ABSTRACT

The aim of this study is to investigate the current vertical datums in North America and to assess the possible improvements to them coming from the recently obtained satellite gravity models. The study is conducted in two steps. First, the geoid models computed from the first and the second generation GOCE-only and GRACE-GOCE combined satellite-only models and truncated for different spherical harmonic degrees are compared to the GPS/leveling geoid heights which are reduced to the same spectral band of the gravity field. The GPS/leveling-derived geoid heights are used as independent controls in the assessment of the geoid models. The comparison results indicate that the GOCE models show a full power of gravity signal in terms of geoid undulation up to about spherical harmonic degree 150. Second, one of the first generation GOCE satellite-only models developed by the time-wise approach, TW01, is complemented with local terrestrial data and tested against the GPS/leveling-derived geoid undulations in full spectrum of the gravity field and compared with the official global and regional geoid models. Based on these results there is not enough evidence indicating significant improvement (cm level) from the first generation GOCE models to the geoid modeling in Canada and the two sub-regions, the Great Lakes area and Rocky Mountains investigated, compared to EGM2008 and the existing regional geoid models. One important contribution is the evaluation of the GOCE-only and complementary terrestrial data combined geoid model in Canada without any effect of the other satellite and geodetic techniques. The preliminary investigations on the second generation GOCE models show that the future GOCE-only and combined GRACE-GOCE models can provide more accurate and consistent geoid solutions for Canada.

ACKNOWLEDGEMENTS

I would like to express my gratitude to my supervisor, Professor Michael G. Sideris, for his professional supervision during my studies. His patience during the last few years was exceptional and much appreciated. His experience, knowledge and concerns on the topic have helped me further my studies. I would like to thank my co-supervisor Dr. Jianliang Huang from the Geodetic Survey Division of Natural Resources Canada. His continuous support and understanding during my studies are also much appreciated. He never avoided sharing his wide knowledge and ideas with me. I am grateful to Dr. Elena Rangelova for being a third “supervisor” during my studies from day to night and on weekends.

Funding for my studies was provided by NSERC and GEOIDE NCE grants to my supervisor, awards from the Department of Geomatics Engineering and the Schulich School of Engineering, and the Research Affiliate Program (RAP) Scholarship of the Geodetic Survey Division (GSD) of Natural Resources Canada. The RAP was an excellent opportunity for me to continue my studies without time restriction. I would like to thank Mr. Marc Véronneau from GSD for his continuous support during the RAP, and for the datasets and source codes he provided. Also, many thanks go to GSD for their hospitality and help during my stay at GSD, Ottawa. I am thankful to Dr. Franz Barthelmes, Dr. Svetozar Petrovic and Dr. Christoph Förste, who made a visit to GFZ, Potsdam, available to me during the last stage of my studies. It was an excellent experience for me to be there. Many thanks go to Dr. Bihter Erol from the Istanbul Technical University who helped me during making decision of studying graduate studies.

Many thanks go to the past and current members of the gravity group. From the first day that I arrived Wouter has been there with his continuous support in making decisions, Sina has been there for any open discussions and Steffens have been there for the wings nights and conferences. I would like to thank Jin for being a great office mate, and many thanks to Babak, Feng, Meda, Vidya, Tas and all other friends.

Last, but not least, I am thankful to my parents Songül and Ilyas, and my sister Sibel, who have given their continuous and endless love, patience and encouragement in my entire life regardless of the circumstances.

PEACE AT HOME, PEACE IN THE WORLD.

M. Kemal ATATÜRK

TABLE OF CONTENTS

Abstract	ii
Acknowledgements	iii
Table of Contents	vi
List of Tables	viii
List of Figures and Illustrations	xi
List of Symbols and Abbreviations.....	xv
 CHAPTER 1	 1
1. INTRODUCTION	1
1.1. Background and statement of the problem	1
1.2. Thesis Objectives	7
1.3. Thesis Outline	7
 CHAPTER 2	 10
2. HEIGHTS AND VERTICAL DATUMS IN NORTH AMERICA.....	10
2.1. Introduction.....	10
2.2. Heights	10
2.2.1. Geopotential numbers.....	10
2.2.2. Dynamic height	12
2.2.3. Orthometric height.....	12
2.2.4. Normal height.....	15
2.2.5. Relationship between H , H^* and H^{dyn}	17
2.3. Vertical Datum.....	19
2.3.1. Realization of vertical datum.....	21
2.3.2. Global vertical datum	22
2.3.3. Regional vertical datum.....	27
2.4. Current Vertical Datums in North America.....	28
2.4.1. The Canadian Geodetic Vertical Datum of 1928 (CGVD28)	28
2.4.2. The North American Vertical Datum of 1988 (NAVD88)	30
2.4.3. Great Lakes Vertical Datums	31
2.5. A Geoid-based Height System.....	34
 CHAPTER 3	 39
3. GRAVIMETRIC GEOID DETERMINATION	39
3.1. Introduction.....	39
3.2. Global Gravity Field Modeling.....	44
3.3. Regional Geoid Modeling in Helmert’s Space	48
3.3.1. Remove-compute-restore technique	48
3.3.2. Helmert’s Method.....	52
3.3.2.1. Terrestrial data	54
3.3.2.2. Global Gravitational Model	58

3.3.3. Stokes`s integration	59
3.3.4. Indirect effect of the topography	64
3.3.5. Error of the combined gravimetric geoid model	65
3.3.5.1. Errors due to GGM	65
3.3.5.2. Errors due to terrestrial gravity anomalies.....	66
3.4. Validation of a Gravimetric Geoid Model	67
3.4.1. Simple outlier detection.....	67
3.4.2. Validation by using GNSS/leveling-derived geoid undulations in absolute and relative sense	68
3.4.3. Geoid fitting to the GPS/leveling benchmarks.....	69
 CHAPTER 4	 72
4. EVALUATION OF THE SATELLITE-ONLY GEOID SOLUTIONS	72
4.1. Introduction.....	72
4.2. Overview of the satellite gravity missions.....	72
4.2.1. CHAMP	73
4.2.2. GRACE.....	75
4.2.3. GOCE	76
4.3. Investigation of the satellite-only global geopotential models	80
4.3.1. GOCE-based geopotential models	80
4.3.2. Assessment of the absolute agreement of the satellite-only geoid models ...	88
4.3.3. Assessment of the relative agreement of the geoid models.....	105
4.4. Summary.....	109
 CHAPTER 5	 111
5. COMBINED GRAVIMETRIC GEOID MODELS FOR CANADA AND THEIR ASSESSMENT	111
5.1. Introduction.....	111
5.2. Evaluation of the Existing Global and Regional Geoid Models.....	113
5.2.1. Earth Gravitational Model of 2008 (EGM2008).....	113
5.2.2. Canadian Gravimetric Geoid Model of 2005 (CGG2005).....	116
5.2.3. An Experimental Canadian Geoid Model of 2010 (ECG10)	120
5.3. Investigations of the GOCE and Terrestrial Data Combined Models	121
5.4. Summary.....	137
 CHAPTER 6	 139
6. CONCLUSIONS AND RECOMMENDATIONS	139
6.1. Conclusions.....	139
6.2. Recommendations.....	142
 REFERENCES	 145

LIST OF TABLES

Table 2.1: Height types and their definitions.....	19
Table 4.1: Specifications of the CHAMP mission.....	74
Table 4.2: Specifications of the GRACE mission.....	75
Table 4.3: Specifications of the GOCE mission	77
Table 4.4: First generation GOCE based models.....	83
Table 4.5: Second generation GOCE based models.	83
Table 4.6: Specifications of the first generation GRACE and GOCE combined model, GOCO01S.....	83
Table 4.7: Specifications of the second generation GRACE and GOCE combined model, GOCO02S.....	83
Table 4.8: Expected overall RMS errors of geoid heights and gravity anomalies at different resolutions for GOCE solutions.	85
Table 4.9: GPS/leveling differences, in m, of the highest expansions of GOCE solutions in Canada.....	93
Table 4.10: GPS/leveling differences, in m, of the highest expansions of GOCE solutions in the Great Lakes area.....	93
Table 4.11: GPS/leveling differences, in m, of the highest expansions of GOCE solutions in the Rocky Mountains.....	93
Table 4.12a: GPS/leveling differences, in m, of the different expansions of the GOCE-only solutions in Canada.....	98
Table 4.12b: GPS/leveling differences, in m, of the different expansions of the GRACE and GOCE combined solutions in Canada.....	99
Table 4.12c: GPS/leveling differences, in m, of the different expansions of the two latest GRACE-only solutions in Canada.....	99
Table 4.12d: GPS/leveling differences, in m, of the different expansions of EGM2008 in Canada.....	99
Table 4.13a: GPS/leveling differences, in m, of the different expansions of the GOCE-only solutions in the Great Lakes area.....	100

Table 4.13b: GPS/leveling differences, in m, of the different expansions of the GRACE and GOCE combined solutions in the Great Lakes area.....	101
Table 4.13c: GPS/leveling differences, in m, of the different expansions of the two latest GRACE-only solutions in the Great Lakes area.....	101
Table 4.13d: GPS/leveling differences, in m, of the different expansions of EGM2008 in the Great Lakes area.....	101
Table 4.14a: GPS/leveling differences, in m, of the different expansions of the GOCE-only solutions in the Rocky Mountains.	102
Table 4.14b: GPS/leveling differences, in m, of the different expansions of the GRACE and GOCE combined solutions in the Rocky Mountains.....	103
Table 4.14c: GPS/leveling differences, in m, of the different expansions of the two latest GRACE-only solutions in the Rocky Mountains.	103
Table 4.14d: GPS/leveling differences, in m, of the different expansions of EGM2008 in the Rocky Mountains.	103
Table 4.15: The statistics of the relative agreement over baseline distances 20km to 800km.	106
Table 5.1: The statistics of the agreement of EGM2008 geoid with the GPS/leveling-derived geoid undulations tested on 2579, 652 and 659 benchmarks in Canada, the Great Lakes and the Rocky Mountains regions, respectively. The values in paranthesis are obtained after the 4-parameter corrector surface is applied. The statistics are given in meter.	114
Table 5.2: The statistics of the agreement of CGG2005 geoid with the GPS/leveling-derived geoid undulations tested on 2579, 652 and 659 benchmarks in Canada, the Great Lakes and the Rocky Mountains regions, respectively. The values in paranthesis are obtained after the 4-parameter corrector surface is applied. The statistics are given in meter.....	118
Table 5.3: The statistics of the agreement of ECG10 geoid with the GPS/leveling-derived geoid undulations tested on 2579, 652 and 659 benchmarks in Canada, the Great Lakes and the Rocky Mountains regions, respectively. The values in paranthesis are obtained after the 4-parameter corrector surface is applied. The statistics are given in meter.	121
Table 5.4: Statistics of the gridded Helmert gravity anomalies in Canada, the Great Lakes and the Rocky Mountains given in mGal.	123
Table 5.5: Summary of the GGM only and combined models investigated.....	126

Table 5.6: The statistics of the components used in remove-compute-restore technique are given in meters.	129
Table 5.7: Comparisons of the combined models with GPS/leveling-derived geoid undulations in Canada. The values in parenthesis are obtained after the 4-parameter corrector surface is applied. The statistics are given in meter.	131
Table 5.8: Comparisons of the combined models with GPS/leveling-derived geoid undulations in the Great Lakes area. The values in parenthesis are obtained after the 4-parameter corrector surface is applied. The statistics are given in meter.	132
Table 5.9: Comparisons of the combined models with GPS/leveling-derived geoid undulations in the Rocky Mountains region. The values in parenthesis are obtained after the 4-parameter corrector surface is applied. The statistics are given in meter.	133
Table 5.10: Explanation, comparison and interpretation of result of each model developed.	134

LIST OF FIGURES AND ILLUSTRATIONS

Figure 1.1: The geoid, ellipsoid and Earth’s surface.	2
Figure 1.2: Illustration of the ellipsoidal height, geoid height and their relation.	3
Figure 1.3: Current and future vertical datums in Canada.	6
Figure 2.1: The principles of leveling and equipotential surfaces.	11
Figure 2.2: The difference of orthometric heights as lengths along the curved plumb line and the straight ellipsoidal normal.	14
Figure 2.3: Normal height, height anomaly, telluroid and quasi-geoid.	16
Figure 2.4: The reference surfaces, geoid, quasi-geoid, and ellipsoid and height systems.	18
Figure 2.5: The relation between the reference tide gauge station and the collocated GPS benchmark.	21
Figure 2.6: Depiction of the Canadian Geodetic Vertical Datum of 1928, CGVD28 and its relation with the equipotential surfaces representing the MSLs at the tide gauges that the datum is constrained to.	29
Figure 2.7: A representation of dynamic and orthometric heights of a lake.	33
Figure 3.1: Illustration of the geoid, reference ellipsoid, and the vectors of the gravity and normal gravity.	41
Figure 3.2: Computation of the local gravimetric geoid model using heterogeneous data.	50
Figure 3.3: The flow chart of the regional geoid determination in Helmert’s space.	51
Figure 3.4: Helmert’s second condensation method.	55
Figure 3.5: The $\beta_n(\psi_0)$ coefficients determined for different integration cap size vs to spherical harmonic degree of expansion.	61
Figure 3.6: The modified transition coefficients $\beta_n^M(\psi_0)$ are shown vs to spherical harmonic degree of expansion.	63
Figure 4.1: Concept of satellite-to-satellite tracking in high-low mode (SST-hl) for CHAMP.	74
Figure 4.2: Concept of inter-satellite link (SST-II) coupled with SST-hl for GRACE. ..	76

Figure 4.3: Schematic illustration of the combined electrostatic gravity gradiometer (EGG) and satellite-to-satellite (high-low) tracking (SST-hl) mission concepts.....	77
Figure 4.4: Expected performances of the satellite gravity missions.	78
Figure 4.5: Overview of GOCE applications.....	79
Figure 4.6: Geoid error per degree by error coefficients. The solid lines represent the geoid signal whereas the dashed lines illustrate the noise.	84
Figure 4.7: Cumulative geoid error by error coefficients. The solid lines represent the geoid signal whereas the dashed lines illustrate the noise.	84
Figure 4.8: Differences in the geoid undulations obtained from EGM2008 and TW01 models both expanded up to spherical harmonic degree 150.	87
Figure 4.9: Differences in the geoid undulations obtained from EGM2008 and TW01 models both expanded up to spherical harmonic degree 210.	87
Figure 4.10: Distribution of the GPS/leveling benchmarks in Canada and the two sub-regions, the Great Lakes area and Rocky Mountains.....	89
Figure 4.11: Standard deviations (std, solid) and root mean squares (rms, dashed) values of the differences in meter as functions of the spherical harmonic degree of the three first generation GOCE-only solutions (DS01, TW01, and SW01), the combined GRACE-GOCE model GOCO01S and EGM2008 with GPS/leveling-derived geoid undulations on 2579 benchmarks in Canada.....	90
Figure 4.12: Standard deviations (std, solid) and root mean squares (rms, dashed) values of the differences in meter as functions of the spherical harmonic degree of the three first generation GOCE-only solutions (DS01, TW01, and SW01), the combined GRACE-GOCE model GOCO01S and EGM2008 with GPS/leveling-derived geoid undulations on 652 benchmarks in the Great Lakes area.....	91
Figure 4.13: Standard deviations (std, solid) and root mean squares (rms, dashed) values of the differences in meter as functions of the spherical harmonic degree of the three first generation GOCE-only solutions (DS01, TW01, and SW01), the combined GRACE-GOCE model GOCO01S and EGM2008 with GPS/leveling-derived geoid undulations on 659 benchmarks in the Rocky Mountains.	92
Figure 4.14: Standard deviations of the differences in meter as a function of the spherical harmonic degree of the three first, two second generation GOCE-only solutions (DS01, TW01, SW01, DS02, and TW01), the combined GRACE-GOCE models GOCO01S and GOCO02S, the latest GRACE-only model ITG10S and EGM2008 with the GPS/leveling-derived geoid undulations on 2579 benchmarks in Canada.	94

Figure 4.15: Standard deviations of the differences in meter as a function of the spherical harmonic degree of the three first, two second generation GOCE-only solutions (DS01, TW01, SW01, DS02, and TW01), the combined GRACE-GOCE models GOCO01S and GOCO02S, the latest GRACE-only model ITG10S and EGM2008 with the GPS/leveling-derived geoid undulations on 652 benchmarks in the Great Lakes area.	95
Figure 4.16: Standard deviations of the differences in meter as a function of the spherical harmonic degree of the three first, two second generation GOCE-only solutions (DS01, TW01, SW01, DS02, and TW01), the combined GRACE-GOCE models GOCO01S and GOCO02S, the latest GRACE-only model ITG10S and EGM2008 with the GPS/leveling-derived geoid undulations on 659 benchmarks in the Rocky Mountains.	96
Figure 4.17: Relative undulation accuracy [ppm] as a function of baseline distance [km] for Canada from EGM2008, three first generation GOCE solutions (DS01, TW01, and SW01) and the GRACE-GOCE combined satellite-only model GOCO01S.	107
Figure 4.18: Relative undulation accuracy [ppm] as a function of baseline distance [km] for the Great Lakes area from EGM2008, three first generation GOCE solutions (DS01, TW01, and SW01) and the GRACE-GOCE combined satellite-only model GOCO01S.	107
Figure 4.19: Relative undulation accuracy [ppm] as a function of baseline distance [km] for the Rocky Mountains from EGM2008, three first generation GOCE solutions (DS01, TW01, and SW01) and the GRACE-GOCE combined satellite-only model GOCO01S.	108
Figure 5.1: The GPS/leveling benchmarks in Canada and 24 outliers (shown with red markers) detected by a 3-sigma technique.	112
Figure 5.2: The GPS/leveling benchmarks in the Great Lakes area and 8 outliers (shown with red markers) detected by a 3-sigma technique.	112
Figure 5.3: The GPS/leveling benchmarks in the Rocky Mountains region and 9 outliers (shown with red markers) detected by a 3-sigma technique.	113
Figure 5.4: EGM2008 geoid in Canada.	115
Figure 5.5: Differences between the geoid undulations derived from GPS/leveling and EGM2008 up to the maximum spherical harmonic degree 2190.	116
Figure 5.6: Differences between the official Canadian geoid, CGG2005, and the official Canadian vertical datum, CGVD28.	118

Figure 5.7: The existing official geoid models, CGG2005 and EGM2008, are compared with undulations obtained from Canadian GPS/leveling. The residuals (CGG2005 shown with blue, EGM2008 shown with green) versus latitude and longitude are shown in Figures 5.7(a) and (b), respectively.....	119
Figure 5.8: Differences between EGC10 and EGM2008. The differences occur due to the different and higher resolution of EGC10, as well as different data included in its development such as GRACE new solutions and the use of ship-borne data in coastal area.....	120
Figure 5.9: The point gravity measurements in Canada.....	122
Figure 5.10: The 2'x 2' gridded Helmert gravity anomalies in Canada.....	123
Figure 5.11: The geoid undulations predicted from HTW01 included in the combined solution.....	128
Figure 5.12: The residual geoid undulations obtained from residual gravity anomalies used in M6.....	128
Figure 5.13: The indirect topographic effect on the geoid.....	129
Figure 5.14: The combined model M6.....	130
Figure 5.15: The difference between EGM2008 and M6.....	137

LIST OF SYMBOLS AND ABBREVIATIONS

a	Semi-major axis of the ellipsoid
\mathbf{A}	Design matrix
b	Semi-minor axis of the ellipsoid
C_{CGVD28}	Geopotential number of CGVD28
C^n	Normal geopotential number
C_{NAVD88}	Geopotential number of NAVD88
$\bar{C}_{nm}, \bar{S}_{nm}$	Fully-normalized spherical harmonic coefficients
C_P	Geopotential number at point P
dH	Orthometric height difference
dH^*	Normal height difference
dn	Vertical differential differences
dv	An element of volume inside the Earth
$d\sigma$	Surface integration element in Stokes's integration
f_{DC}	Downward continuation operation
g	Gravity (measured on the Earth's surface)
g_0	Gravity computed at the corresponding point of P on the geoidal point P_0
\bar{g}_P	Averaged gravity value along the plumb line from point P to P_0
\mathbf{g}_{P_0}	Gravity vector at point P_0 on the geoid surface
g_P	Gravity measured at point P on the Earth's surface
G	Newton's gravitational constant
GM	Geocentric gravitational constant
GM_0	Geocentric gravitational constant of the gravity field
GM_e	Gravitational constant of the ellipsoid
h	Ellipsoidal height
h_{GNSS}	Ellipsoidal, GNSS or GPS height
H	Orthometric height
$(H^2)_{nm}$	Harmonic coefficients of squared topography

H_{CGVD28}^*	CGVD28 normal-orthometric height
H_{IGLD85}^{dyn}	IGLD85 dynamic height
H_{NAVD88}	NAVD88 Helmert-orthometric height
H_P	Orthometric height of point P
H_P^{dyn}	Dynamic height of point P
H_P^{no}	Normal-orthometric height of point P
H_P^*	Normal height of point P
J_2	Dynamic form factor of the Earth
l	Selected upper limit for spherical harmonic degree of the satellite-only gravity model
$l(r, \psi, r')$	Spatial distance between the computation and integration points, r_i and r' , respectively
l_i	Misclosures ($h_{GNSS} - H - N = 0$)
\bar{l}	Misclosures averaged
m_{TG}	π / Δ where Δ is sampling interval of the terrestrial gravity data
\mathbf{n}	Normal of the geoidal surface
n_{max}	Maximum spherical harmonic degree of GGM
N	Geoid undulation, geoid height
N_0	Zero-degree term geoid component
N_{GM}	Geoid undulation obtained from GGM
N_{grav}	Gravimetric geoid undulation
N_{ind}	Indirect effect of the gravity reduction on the geoid undulation
P	Point at the Earth's surface
P_0	Corresponding point of P on the geoidal surface
\bar{P}_{nm}	Fully normalized associated Legendre functions for degree n and order m
$Q_n^{DB}(\psi_0)$	Degree-banded Stokes kernel truncation coefficients
$Q_n^M(\psi_0)$	Modified Stokes kernel truncation coefficients

r_t	Geocentric radius of the computation point
r_p	Geocentric distance of point P
R	Mean radius of the sphere
$s_n(\psi_0)$	Coefficients corresponding to the modified degree-banded Stokes kernel
S_0	Global ocean surface
$S(\psi)$	Standard Stokes kernel
$S_{DB}(\psi)$	Degree-banded Stokes kernel
$\bar{S}_{DB}(\psi, \psi_0)$	Degree-banded Stokes kernel within a limited cap
S_{ij}	Baseline distance between benchmark points
$S_M(\psi, \psi_0)$	Modified degree-banded Stokes kernel
$\bar{S}_M(\psi, \psi_0)$	Modified degree-banded Stokes kernel within a limited cap
$t_n(\psi_0)$	Coefficients corresponding to the modified degree-banded Stokes kernel
T	Disturbing potential
T^h	Disturbing potential in the Helmert's Space
T_p	Disturbing potential at point P
u	Transition band in the modified Stokes kernel chosen as 60
U_0	Normal gravity potential of the ellipsoid
U_p	Normal gravity potential at the point P
$\hat{\mathbf{v}}$	Adjusted residuals
v	Transition band in the modified Stokes kernel chosen as 120
V	Gravitational potential of the Earth
V^{ct}	Gravitational potential of the condensed layer
V_{CG}	Error contribution coming from satellite-combined GGM
V_e	Gravitational potential of the ellipsoid
V_{SG}	Error contribution coming from satellite-only GGM
V^t	Gravitational potential of the topography

V_{TG}	Errors due to the terrestrial gravity anomalies
W	Constant potential value
W_0	Constant potential value of the geoid
W^h	Helmert's gravity field potential value
W_P	Potential of the equipotential surface through the point P at the Earth's surface
x	Cartesian coordinate
$\hat{\mathbf{x}}$	Vector of unknown parameters of the corrector surface model
y	Cartesian coordinate
Y_{nm}	Surface spherical harmonics
$\partial\gamma / \partial h$	Normal gravity gradient
$\alpha_n(\psi_0)$	Weights introduced in the Stokes band modification
$\beta_n(\psi_0)$	Coefficients corresponding to the degree-banded Stokes kernel
$\beta_n^M(\psi_0)$	Coefficients corresponding to the degree-banded modified Stokes kernel
δg	Gravity disturbance
δh	Physical height differences
δn	Leveling increment
δV_{GM}^h	Direct effect of the Helmert condensation to the gravitational potential at the geoid
$\delta\rho$	Anomalous density
$\delta V'$	Gravitational potential difference created by the condensation
Δg	Gravity anomaly
Δg_B	Bouguer gravity anomaly
Δg_h	Helmert gravity anomaly on the geoid
Δg_{GM}	Gravity anomaly predicted from GGMs
Δg_F	Free-air gravity anomaly
$\Delta g_{SRB}(r_g)$	Spherical refined Bouguer anomaly on the geoid
Δh_{GNSS}	Ellipsoidal height difference

Δl_{ij}	Misclosure differences
Δg_{res}	Residual gravity anomaly
Δg_{SITE}	Second indirect effect of the topography on the gravity anomalies
ΔH	Orthometric height difference
ΔN	Geoid undulation height difference
γ	Normal gravity
$\bar{\gamma}$	Normal gravity averaged
γ_0	Normal gravity value used for dynamic height determination
γ_{45°	The normal gravity value determined on latitude of 45 degree
$\bar{\gamma}_P$	Mean normal gravity along the plumb line
γ_Q	Vector of the normal gravity computed at point Q on the ellipsoid
γ_Q	Absolute normal gravity computed at point Q on the ellipsoid
Φ	Centrifugal potential of the Earth
Φ_e	Centrifugal potential of the ellipsoid
ζ_P	Height anomaly
λ	Geocentric spherical coordinate (longitude) of the computational point
λ_P	Geocentric co-longitude of point P
θ	Geocentric spherical coordinate (latitude) of the computational point
θ_P	Geocentric co-latitude of point P
ρ	Crust density
σ	Earth's surface
ω	Angular velocity of the Earth
ω_e	Angular velocity of the ellipsoid
ψ	Spherical distance between the computation point and running point in Stokes
ψ_0	Limited spherical cap

AGBVP	Altimetry gravimetry boundary value problem
AHD71	Australian Height Datum of 1971
BVP	Boundary value problem
CDED	Canadian Digital Elevation Data
CGG2005	Canadian Gravimetric Geoid of 2005
CGG2010	Canadian Gravimetric Geoid of 2010
CGVD28	Canadian Geodetic Vertical Datum of 1928
CHAMP	CHALLENGING Minisatellite Payload
CSR	University of Texas at Austin Center for Space Research
DEM	Digital Elevation Model
DORIS	Doppler Satellite Tracking System
DOT	Dynamic Ocean Topography
DS01	First generation GOCE Direct Solution
DS02	Second generation GOCE Direct Solution
DTED	Digital Terrain Elevation Data (USA)
ECG10	Experimental Canadian Geoid 2010
EGG	Electrostatic Gravity Gradiometer
EGM	Earth Gravitational Model
EGM96	Earth Gravitational Model of 1996
EGM2008	Earth Gravitational Model of 2008
EGMXX	Future Earth Gravitational Model
EIGEN05C	Global mean Gravity Field Model from Combination of Satellite Mission and Altimetry/Gravimetry Surface data
ESA	European Space Agency
GGM	Global Gravitational Model
GGM02C	Earth gravity field model from GRACE and surface data
GBVP	Geodetic Boundary Value Problem
GLONASS	Global Navigation Satellite System
GNSS	Global Navigation Satellite Systems
GOCE	Gravity field and steady-state Ocean Circulation Explorer
GOCO01S	First generation GRACE and GOCE combined solution
GOCO02S	Second generation GRACE and GOCE combined solution

GPS	Global Positioning System
GRACE	Gravity Recovery and Climate Experiment
GRS80	Geodetic Reference System of 1980
GSD	Geodetic Survey Division
HTW01	First generation GOCE time-wise solution in Helmert's space
IAG	International Association of Geodesy
ICGEM	International Center for Global Gravity Field Models
IGN69	France Institute Geoprahique National 1969
IGLD55	International Great Lakes Datum of 1955
IGLD85	International Great Lakes Datum of 1985
INS	Inertial Navigation System
ITG-Grace2010s	Grace-based Satellite-only Model
KMS	National Survey and Cadastre of Denmark
LEO	Low Earth orbiting satellite
MSL	Mean Sea Level
MSST	Mean Sea Surface Topography
MWL	Mean water level
NA	North America
NAVD88	North American Vertical Datum of 1988
NGA	National Geospatial-Intelligence Agency
NGS	National Geodetic Survey
NIMA	National Imagery and Mapping Agency
NOAA	National Oceanic and Atmospheric Service
NOS	National Ocean Service
NRCan	Natural Resources Canada
SGG	Satellite Gravity Gradiometer
SLR	Satellite Laser Ranging
SSH	Sea Surface Height
SST	Sea Surface Topography
SST-l1	Satellite-to-satellite tracking between low and low orbiting satellites
SST-h1	Satellite-to-satellite tracking between high and low orbiting satellites
SW01	First generation of GOCE Space-wise Solution

VLBI	Very Long Baseline Interferometry
USGG2009	United States Gravimetric Geoid of 2009
TDRSS	Tracking Data and Relay Satellite System
T/P	Topex/Poseidon altimeter
TW01	First generation of GOCE Time-wise solution
TW02	Second generation of GOCE Time-wise solution
WHS	World Height System

CHAPTER 1

1. INTRODUCTION

1.1. Background and statement of the problem

Height observations are one of the most fundamental measurement types in geodesy and geodetic science related areas. Scientists have been working on the development of the new geodetic techniques and equipment for many years to obtain more accurate height information. In the last 200 years, spirit-leveling has been the most accurate and widely used geodetic method to determine height differences. However, leveling only provides relative heights between the associated points rather than their absolute heights. Therefore, to obtain the absolute heights one needs a defined zero reference point/surface. Traditionally, this has been accomplished by fixing a tide-gauge station as the zero-height reference point and the leveling observations are tied to this station. As the spirit-leveling technique used in height measurements requires the observation of rod-readings point by point, data collection is mostly performed along routes easy to access, such as highways/roads, valleys, etc. This poses a limitation in the spatial distribution of the leveling network, and also a lack of efficiency and cost benefit in data collection.

With the invention of the Global Navigation Satellite Systems (GNSS), observing heights of any arbitrary points on the Earth's surface or above has become possible. The GNSS technique can be used in any terrain (such as in mountainous regions) and at any time. Over water, satellite radar altimetry can measure sea surface and large water body surface height. However, the heights obtained from these techniques are referred to a reference ellipsoid, a mathematical surface, and they do not have any physical meaning but only a geometrical one. This type of heights is fundamentally different from the leveling heights which are referred to a specific equipotential surface, namely the *geoid*, and defined by the Earth's gravity field.

The ellipsoid is a geometrically defined figure or model of the Earth, whose center is usually assumed to be at the center of mass of the Earth. The semi-minor axis of the ellipsoid is aligned with the Earth's reference pole (Hofmann-Wellenhof and Moritz, 2005, Jekeli, 2000). The ellipsoid is a well-defined smooth surface and it can be used as a reference surface for mathematical operations, and also to obtain the horizontal and vertical coordinates (Seeber, 1993). A point at the Earth's surface can be defined by its three coordinates; latitude, φ , longitude, λ , and the distance, h , from the ellipsoid to the point along the perpendicular to the ellipsoid (see Figure 1.1). In Figure 1.1, the ellipsoidal height is represented by h , whereas N is the geoid height representing the separation between the geoidal and ellipsoidal surfaces. The semi-major and minor axes of the ellipsoid are represented by a and b , respectively.

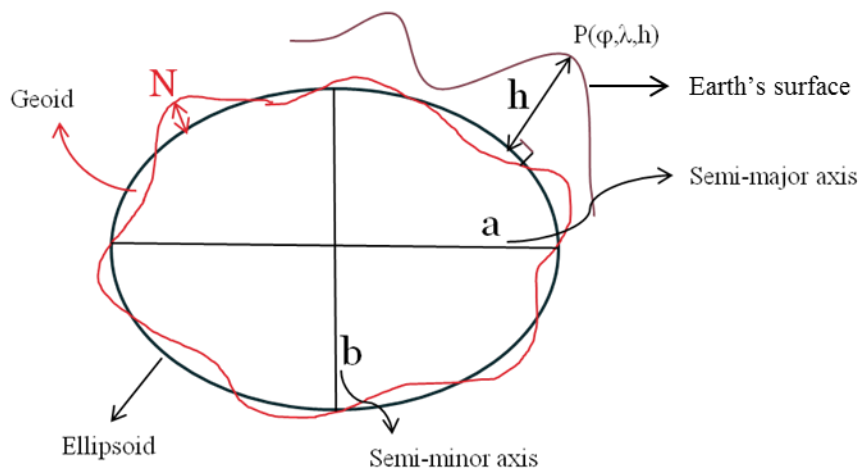


Figure 1.1: The geoid, ellipsoid and Earth's surface.

The geoid is a closed, continuous and constant gravity potential surface. Unlike the ellipsoid, the geoid is not defined analytically (Torge, 2001). According to Gauss-Listing, *geoid* is defined as an equipotential surface of the Earth's geopotential field which coincides with the Mean Sea Level (MSL) in a least-squares sense. It can be obtained by means of MSL records from tide gauge observations. However, today it is a known fact that the MSL differs from the geoid up to 2 meters due to the Sea Surface Topography

(SST) which occurs as a result of temperature, salinity, tides, waves and other quasi-stationary effects (Torge, 2001). Moreover, SST needs to be accounted for in order to refer the leveling heights to the geoid surface.

The geoid is not a regular surface but a very complicated one. Thus it is not suitable for mathematical computations. However, the surface of the geoid can be approximated by using an analytically defined surface such as the ellipsoid. The vital question is: “*How do we relate these two surfaces, the ellipsoid and the geoid?*” Figure 1.2 illustrates the relation between these two height types in terms of the *geoid height*. Chapter 3 in this thesis deals with the methodology for the computation of the geoid height.

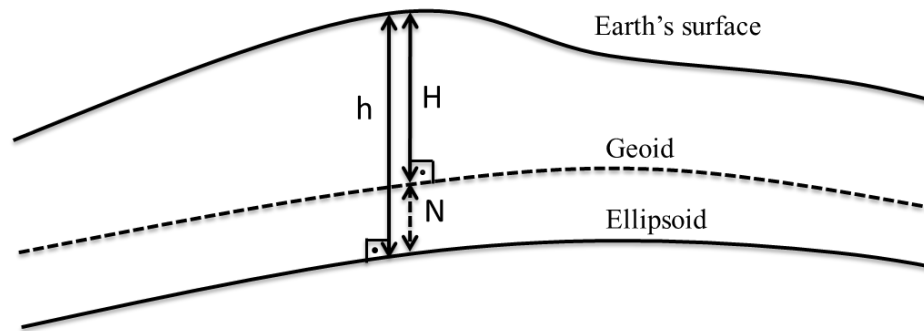


Figure 1.2: Illustration of the ellipsoidal height, geoid height and their relation.

The relation between the GNSS and leveling heights can be expressed by the well-known formula:

$$h_{GNSS} - H - N = 0, \quad (1.1)$$

where h_{GNSS} is the ellipsoidal height obtained by GNSS observations, H is the orthometric height obtained by leveling and gravity observations, and N is the geoid height which is also called geoid undulation. This formula can also be investigated in the relative sense as below:

$$\Delta h_{GNSS} - \Delta H - \Delta N = 0. \quad (1.2)$$

These expressions provide the basic relationships used in the conversion of the ellipsoidal heights to the orthometric heights.

In this study, the terms geoid, geoid undulation, and geoid height are used interchangeably and refer to the separation between the geoid and the ellipsoid surface (see Figure 1.2). Also, GNSS, GPS or geometric heights are used interchangeably and refer to the ellipsoidal height, which is represented by h_{GNSS} or h .

With the recently developed technologies, the most practical and the easiest way to collect height information is by using the Global Positioning Systems (GPS), GLONASS and GALILEO (ESA, 2005), Very Long Baseline Interferometry (VLBI), Satellite Laser Ranging (SLR), and Doppler Satellite Tracking System (DORIS). Moreover, satellite altimetry also provides geodetic height information over the oceans. However, as mentioned in the previous paragraphs, these height measurements are all referred to the geometrically defined reference ellipsoid. They do not have physical meaning but only a geometric one and therefore they do not directly provide the necessary information for physical heights necessary in such application areas as topographic mapping, water system observations, coastal studies, transportation, etc. For instance, in the water flow example, the water can flow from a lower ellipsoidal height to a higher height, which is a contradiction to reality (Hofmann-Wellenhof and Moritz, 2005). In these kinds of applications, it is necessary to introduce physically meaningful height types which are described in Chapter 2.

Equations 1.1 and 1.2 have been used for the determination of orthometric heights from ellipsoidal heights and a geoid model. This is called GNSS/leveling (Huang and Véronneau, 2004) and is currently in the process of replacing the traditional leveling techniques in many countries, such as Canada, US, Australia, New Zealand and Brazil. In this methodology when two of the heights are known, the third one can easily be computed. The important part of this procedure is the desired accuracy level of the orthometric heights. It is a known fact that ellipsoidal heights can be obtained more accurately than geoid undulations. Accordingly, this degrades the determination of

accurate orthometric heights. Therefore, precise geoid determination is crucial for the application of GNSS/leveling in practice. By having a centimeter-accurate geoid model, a direct conversion between the ellipsoidal and orthometric heights can be obtained at any arbitrary point on the Earth's surface. This is crucial for the determination of physical heights in applications such as establishment of a new height control in remote areas, connection of different height systems, connection of engineering projects between two or more countries with different heights systems, etc. In relative height determinations, the geoid has a good precision at small distances so the orthometric height can be obtained with relatively good precision depending on the application requirements.

With the recent developments in the gravity field satellite missions, pure gravimetric geoid determination has become an important research topic. It has become possible to determine the geoid accurately using satellite gravity models from the GOCE and GRACE satellite missions combined with high-resolution and high-quality terrestrial gravity and topographic data. The determination of an accurate geoid model has always been desirable as it can provide a continuous equipotential reference surface that is a natural vertical datum for heights. With this new definition and realization of the vertical reference surface based on a gravimetric geoid, height datum information will be available at any point on the Earth's surface with respect to a common reference surface.

A depiction of two differently defined vertical datums, the current official datum and the future geoid-based datum for Canada, is depicted in Figure 1.3. The upper map represents the current datum realized by traditional leveling whereas the lower map is a geoid model for the proposed future geoid-based vertical datum in Canada. The leveling-based vertical datum can be used efficiently in countries such as Germany, Switzerland, etc., where the leveling network covers the entire country densely and leveling benchmarks are well distributed. However, in Canada this method is inadequate to provide a quick, easy, and accurate access to the national vertical datum as one can easily notice that the leveling network exists and is accessible only in the southern part of the country. The Geodetic Survey Division (GSD), Natural Resources Canada, has been working on the

development of a newly defined “*geoid-based vertical datum*” in collaboration with US and Mexico for the whole North America.

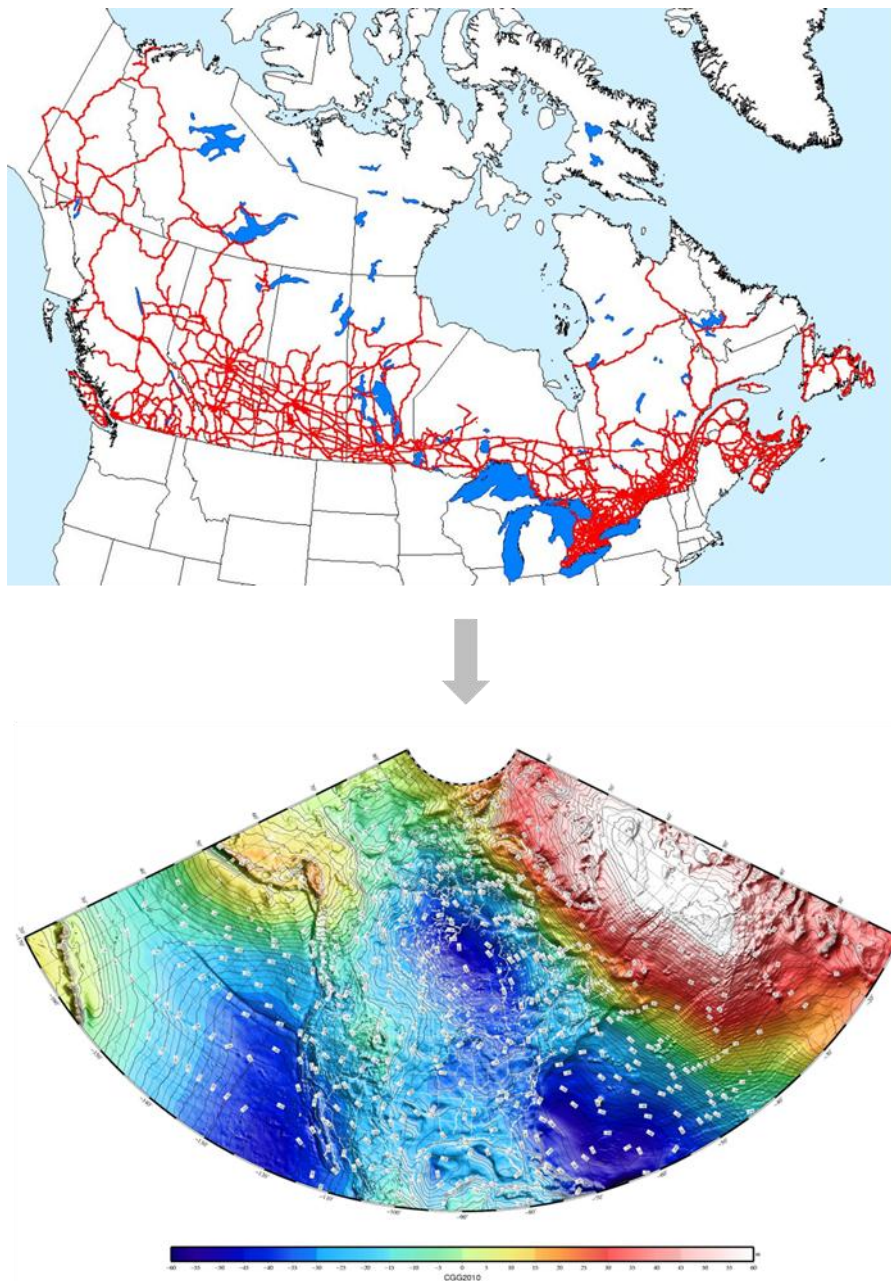


Figure 1.3: Current and future vertical datums in Canada (Huang et al., 2011).

1.2. Thesis Objectives

Main objectives of the research are the following:

- The first and primary objective of this study is to explore the current vertical datums in North America and express the necessity of a newly defined geoid-based height system in Canada. Methods to overcome the existing problems of the Canadian, American and Great Lakes vertical datums are investigated and a prototype of a geoid-based height system for Canada is introduced.
- The second objective is to investigate the possible contribution of the recent satellite-only gravity field solutions from the GOCE and GRACE missions to the existing global and regional geoid models in Canada. The first and the second generation GOCE-only and GRACE and GOCE combined satellite-only solutions are evaluated by comparing with GPS/leveling-derived geoid undulations and the latest global gravity field model, Earth Gravitational Model of EGM2008 (EGM2008).
- The final objective is to develop an accurate regional gravimetric geoid model in Canada by optimally combining the recent satellite-only gravity field solution and regional terrestrial data.

1.3. Thesis Outline

This thesis consists of six chapters. Chapter 2 describes various height types, discusses a number of different ways of realizing a vertical datum, and proposes a prototype of a geoid-based vertical datum in Canada. Chapter 3 deals with the theory and methodology used in geoid determination with satellite-only models and terrestrial gravity data. Chapter 4 evaluates the recent GOCE-only and GRACE-GOCE combined satellite-only gravity models. Chapter 5 contains investigations made on the combined geoid models from satellite and terrestrial data. Finally, Chapter 6 gives the conclusions, recommendations and the key discussions on the possible benefit of this study in the development of the new geoid model and the choice of the new vertical datum of Canada.

In Chapter 2, it is aimed to include the background information of the height systems and the vertical datums used in North America. The definition of the height systems, the realization and the maintenance of a vertical reference system, and the advantages and disadvantages of each option are explained. Descriptions and the definitions of the existing vertical datums of Canada, US and the Great Lakes area are included, as well as the existing problems of these datums and the proposed ways to overcome these problems. The need for this research is given and, more importantly, the idea for a geoid-based vertical datum for North America is introduced and a prototype of the geoid-based height system in Canada is discussed in this chapter.

Chapter 3 starts with the fundamentals of potential theory and continues with the geoid modeling. Global gravitational and regional geoid modeling and main aspects of the remove-compute-restore technique used in the development of the combined regional geoid in Helmert space are described in details. The treatment of the datasets used in the combined gravimetric geoid model is given in this chapter. The Stokes integration used in the geoid computation and the Stokes kernel modification are also described in this chapter. Lastly, the methodology used for the validation of the gravimetric geoid models is given.

In Chapter 4, the evaluation results of the assessment of the accuracy and precision of the satellite-only geoids are given. The geoid heights derived from the global satellite-only geoid models developed up to different spherical harmonic degrees are compared with the GNSS/leveling-derived geoid undulations which are reduced to the same spectral band of the gravity field as the satellite-only model geoids. By this a fair comparison is provided and it has been performed in the absolute and relative sense. This provides the information about the GOCE models and their behaviour over Canada for different gravity wavelength intervals.

In Chapter 5, the combined models from the satellite-only solutions and the terrestrial data are developed and compared with the full spectrum of the GNSS/leveling-derived geoid undulations as well as with the latest official Canadian and global geoid models

publicly released. The possible improvement of the Canadian geoid model from GOCE is assessed.

In Chapter 6, besides discussions on how the results will help the choice of the new vertical datum, conclusions and recommendations are provided. This part is important for future studies and contributes to the current development of the geoid model and vertical datum in Canada.

CHAPTER 2

2. HEIGHTS AND VERTICAL DATUMS IN NORTH AMERICA

2.1. Introduction

This chapter aims to define and describe different height systems and reference surfaces, and existing vertical datums in North America (NA). In the first section of this chapter, the height systems are defined, and the relations among them are given. In the second part of this chapter, the definition, realization and maintenance of global and regional vertical systems are discussed. The third section describes the current vertical datums in NA. Existing problems of the North American vertical datums and proposed ways to overcome these also are explained in this section. In the last section, a prototype of the geoid-based vertical datum for Canada is introduced.

2.2. Heights

Different types of heights are used in different engineering and science applications. Hence, it is necessary to ensure the conversion among the height types in order to do comparisons and provide compatibility at a national and global range. The descriptions of the dynamic, orthometric, and normal heights are given in this section. Before defining the height types, it is necessary to introduce the geopotential number since it is fundamental in the calculation of the height values.

2.2.1. Geopotential numbers

As mentioned in the previous chapter, equipotential surfaces are closed and continuous surfaces with a unique constant gravity potential value, W . Since the height differences obtained from leveling are dependent on the leveling path, the potential values are used to determine the heights by obtaining the difference between the potentials of the geoid and the equipotential surface that passes through the point at the Earth surface. This

difference is called geopotential number in equation (2.1) and it is defined to be always positive (Hofmann-Wellenhof and Moritz, 2005).

$$C_P = W_0 - W_P = \int_{P_0}^P g dn , \quad (2.1)$$

where W_0 value is the constant potential value of the geoid whereas W_P represents the potential of the equipotential surface through the point P at the Earth's surface and P_0 is the corresponding point on the geoid. In practice, P_0 is a benchmark at which the W_0 value is defined.

A representation of leveling and equipotential surfaces is given in Figure 2.1. As it is seen from the figure, the leveled height differences are path dependent and not the same as physical height differences ($\sum \delta n \neq H_B - H_A$).

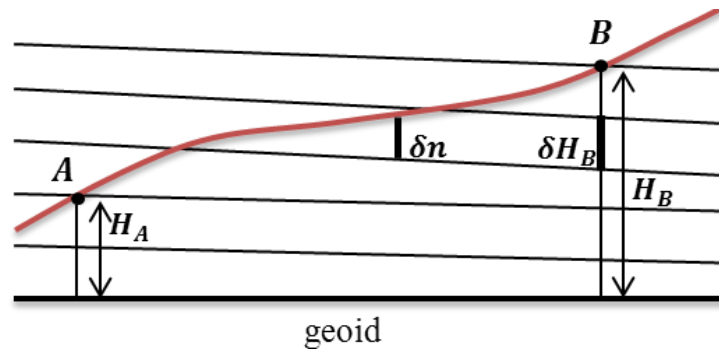


Figure 2.1: The principles of leveling and equipotential surfaces (Hofmann-Wellenhof and Moritz, 2005).

The value of the geopotential number depends on the vertical differential distances, dn , obtained from leveling between the equipotential surfaces and on the value of the gravity, g , measured at the leveling points. The geopotential number C_P is independent of any particular leveling line connecting point P to sea level (geoid). The geopotential numbers are measured in geopotential units (g.p.u.) where $1 \text{ g.p.u} = 1 \text{ kGal m} = 1000 \text{ gal m}$

(Hofmann-Wellenhof and Moritz, 2005). Subsequently they are scaled by the gravity to obtain the height. Evidently, different height values can be obtained at the same point P depending on the gravity value used in its computation.

2.2.2. Dynamic height

Dynamic heights are the scaled geopotential numbers by a normal gravity γ_0 at the reference ellipsoid surface computed for latitude 45° . They do not have a definite geometric interpretation. Like the geopotential numbers, they are physical quantities in distance units relative to the geoid and the points with the same dynamic heights are on the same equipotential surface. To determine dynamic heights one needs to scale the geopotential number as follows:

$$H_p^{dyn} = \frac{C_p}{\gamma_0} . \quad (2.2)$$

The normal gravity value used in Canada for dynamic height determination is $\gamma_{45^\circ} = 9.806199203 \text{ m s}^{-2} = 980.6199203 \text{ Gal}$ for the GRS 1980 ellipsoid (Moritz, 1992; Hofmann-Wellenhof and Moritz, 2005). The International Great Lakes Datum which will be addressed later in this chapter is realized based on the dynamic height.

2.2.3. Orthometric height

The distance along the plumb line between the geoid and the point located on the Earth's surface is defined as the orthometric height (Hofmann-Wellenhof and Moritz, 2005, Jekeli, 2000). Figure 2.2 shows a representation of the orthometric height and Figure 2.4 at the end of this section illustrates a comparison with the other types of heights. The orthometric height of a point P on the Earth's surface is denoted by H_p and can be computed by the following equation:

$$H_p = \frac{C_p}{\bar{g}_p} , \quad (2.3)$$

where \bar{g}_p is the averaged gravity value along the plumb line computed as follows:

$$\bar{g}_P = \frac{1}{H_P} \int_{P_0}^P g dH . \quad (2.4)$$

The \bar{g}_P cannot be determined exactly due to the lack of complete knowledge of the mass density of the crust. It is not practical to measure the gravity everywhere along the plumb line. Thus, the determination of the orthometric heights depends on the approximation used in computing the mean value of gravity (Hofmann-Wellenhof and Moritz, 2005). One needs to be cautious when combining different types of heights or working with orthometric heights from different national sources since they can be computed by different approaches (Fotopoulos, 2003; Erol, 2007).

Helmert heights are one of the most common orthometric height types that are based on the Poincaré-Prey reduction model (Hofmann-Wellenhof and Moritz, 2005). In this commonly used approximation, a constant crustal density and a constant gravity gradient are assumed for the terrain point P .

In practice, the mean gravity value is approximated (Hofmann-Wellenhof and Moritz, 2005), as follows:

$$\bar{g}_P = g_P - 2\pi G\rho H_P + \frac{1}{2} \frac{\partial \gamma}{\partial h} H_P , \quad (2.5)$$

where G is the Newton's gravitational constant of $66.7 \times 10^{-9} \text{ cm}^3 \text{ g}^{-1} \text{ sec}^{-2}$. The expression is simplified by using a crust density of $\rho = 2.67 \text{ g cm}^{-3}$ and a normal gravity gradient $\frac{\partial \gamma}{\partial h} = 0.3086 \text{ mGal m}^{-1}$. After substitution of these numerical values, the simplified expression is

$$\bar{g}_P = g_P + 0.0424 H_P . \quad (2.6)$$

Consequently, equation (2.6) for the Helmert orthometric height can be rewritten as

$$H_P = \frac{C_P}{g_P + 0.0424 H_P} . \quad (2.7)$$

This equation is solved by iterations due to the fact that the computation of gravity along the plumb line always requires H_p information (Hofmann-Wellenhof and Moritz, 2005; Jekeli, 2000). This practical approach assumes that g varies linearly along the plumb line. Thus \bar{g}_p can be calculated by averaging the g_p measured at the surface point P and g_0 computed at the corresponding geoidal point at P_0 by the Prey reduction (Hofmann-Wellenhof and Moritz, 2005):

$$\bar{g}_p = \frac{1}{2}(g_p + g_0). \quad (2.8)$$

In summary, the orthometric height is the distance along the plumb line from the geoid to the point on the Earth's surface which is called Pizzetti's projection. However, in practice, to simplify the computations, orthometric heights are assumed as the distance along the ellipsoidal normal instead of the plumb line and this is called Helmert's projection (see Figure 2.2).

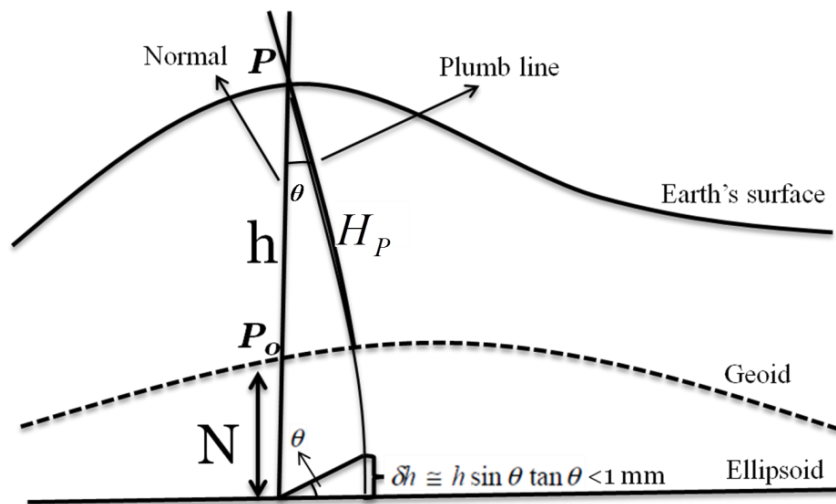


Figure 2.2: The difference of orthometric heights as lengths along the curved plumb line and the straight ellipsoidal normal (Hofmann-Wellenhof and Moritz, 2005; Jekeli, 2000).

The error that occurs due to the difference between the plumb line and the ellipsoidal normal is negligible for the topographic heights on the Earth's surface (Jekeli, 2000). The difference between the plumb line and the ellipsoidal normal is called deflection of the vertical and is denoted by θ . This value can reach 1 arc minute at maximum and according to the approximate relation between the vertical deflection and the height $\delta h \cong h \sin \theta \cos \theta$, it can affect the height only by less than a millimeter. It is negligible even for the extreme cases where $\theta = 1$ arc minute and $h = 10000$ m, where the height difference becomes $\delta h = 0.8462 \text{ mm} < 1 \text{ mm}$ (Jekeli, 2000).

Normal-orthometric height: This type of heights is an approximation to the normal or orthometric heights. Averaged normal gravity value is used in its computation instead of any actual gravity value.

$$H_P^{no} = \frac{C^n}{\bar{\gamma}}. \quad (2.9)$$

Normal geopotential number C^n used in its computation is obtained by using the averaged normal gravity value in eq. (2.1) instead of the actual gravity.

This type of heights is used in Canada, Norway, former Yugoslavia and Turkey and was formerly used in USA.

2.2.4. Normal height

Normal height is introduced in order to avoid any hypothesis or modeling of the mass distribution of the topographic masses. This is attained by using the normal gravity field which can exactly be calculated at any point. The normal height is computed as follows:

$$H_P^* = \frac{C_P}{\gamma_R}, \quad (2.10)$$

where

$$\bar{\gamma}_R = \frac{1}{H_R^*} \int_Q^{H_R^*} \gamma dH^*, \quad (2.11)$$

is the mean normal gravity along the plumb line and R is located on the telluroid where $U_R = W_P$ (see Figure 2.3). The distance between the telluroid and the Earth's surface is the height anomaly at point P , ζ_P . Often, the distances H_P^* and ζ_P are reversed along the plumb line; the normal height of the point P , H_P^* , is represented by the distance between the point on the Earth's surface and the quasi-geoid. The surface obtained by plotting ζ_P above the ellipsoid is called *quasi-geoid*. It is a geoid-like surface obtained by Molodensky's solution (Hofmann-Wellenhof and Moritz, 2005). Unlike the geoid, the quasi-geoid is not an equipotential surface either in the normal or the actual gravity field and has no physical meaning.

The normal heights are widely used in many countries in the world. There are two advantages of using normal heights: 1) the exact value of the normal height can be calculated by using the normal gravity field, 2) density information is not required to compute the normal height (Hofmann-Wellenhof and Moritz, 2005; Jekeli, 2000).

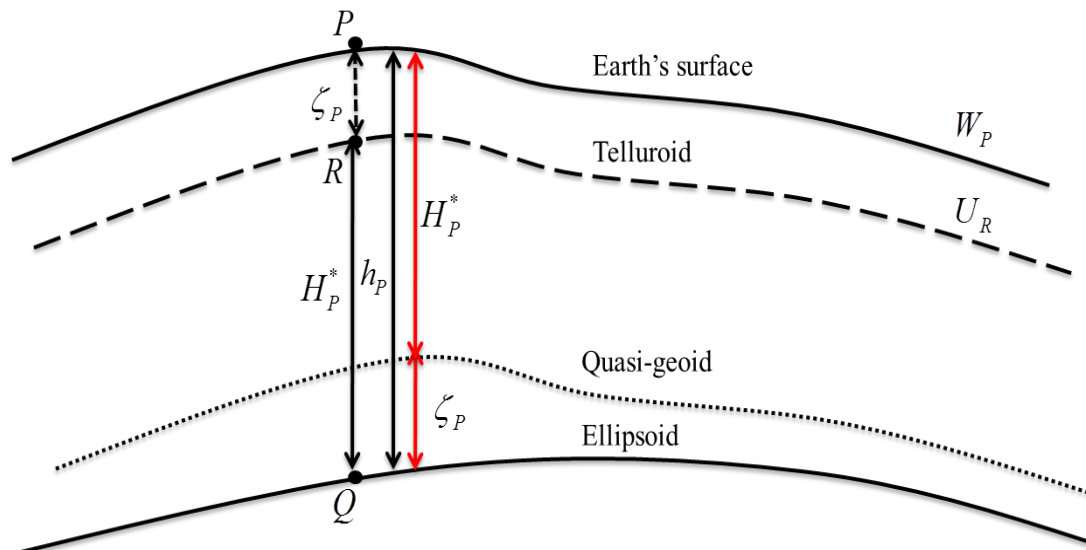


Figure 2.3: Normal height, height anomaly, telluroid and quasi-geoid.

2.2.5. Relationship between H , H^* and H^{dyn}

In Canada and North America, the orthometric heights are the official height system referring to the geoid. In contrast, most European countries use normal heights and the quasi-geoid as a vertical reference surface (Augath and Ihde, 2002). In theory, the geoid height and the height anomaly, as well as all other type of heights, can be linked by the geopotential number. For example, equation (2.12) can be written expressing the relationship between the geoid height and height anomaly by the help of equations (2.7) and (2.10):

$$h_p = H_p + N = H_p^* + \zeta_p , \quad (2.12)$$

and

$$N - \zeta_p = H_p^* - H_p = \frac{\bar{g} - \bar{\gamma}}{\bar{\gamma}} H_p \approx \frac{\Delta g_B}{\bar{\gamma}} H_p , \quad (2.13)$$

where Δg_B is the Bouguer gravity anomaly and $\bar{\gamma}$ is the mean normal gravity along the normal plumb line (Hofmann-Wellenhof and Moritz, 2005).

The orthometric and normal heights are defined geometrically. The calculation of the orthometric height requires the knowledge of the mass density of the crust. In the contrary the exact value of the normal height can be determined exactly with no density knowledge.

Unlike the orthometric, normal or ellipsoidal heights, the dynamic heights are physically meaningful and indicate the direction of the flow of water. They are used in the Great Lakes area to determine the lake water level, and can be converted into other height types when required:

$$H_p = \frac{H_p^{dyn} \gamma_0}{\bar{g}_p} = \frac{H_p^{dyn} \gamma_0}{g_p + 0.0424 H_p} . \quad (2.14)$$

The orthometric and normal heights and the associated reference surfaces discussed above are depicted in Figure 2.4. The geoid undulation or geoid height, N , represents the

separation between the ellipsoid and the geoid along the ellipsoidal normal, and the height anomaly, ζ_P , represents the separation between the ellipsoid and the quasi-geoid along the ellipsoidal normal (see Figure 2.4). In flat areas, the height anomaly is close to the geoid height.

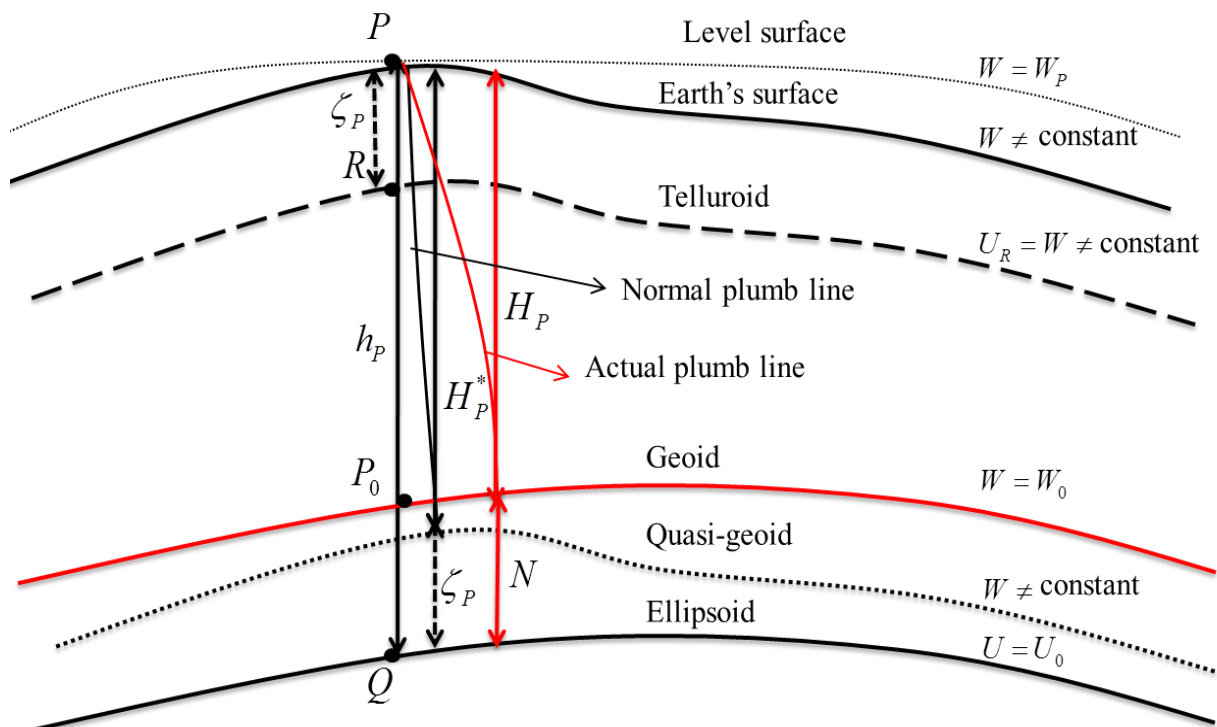


Figure 2.4: The reference surfaces, geoid, quasi-geoid, and ellipsoid and height systems.

A summary of the heights discussed above is given in Table 2.1. More details can be found in Hofmann-Wellenhof and Moritz (2005) and Jekeli (2000).

Table 2.1: Height types and their definitions.

Height Type	Definition	Meaning	Usage/ Characteristic
Ellipsoidal height	h_p	Geometrically meaningful.	Geometrically defined along the perpendicular to the ellipsoid.
Dynamic height	$H_p^{dyn} = \frac{C_p}{\gamma_0}$	Physically meaningful and associates with a value computed at a fixed latitude.	Indicates the direction of water flow.
Orthometric height	$H_p = \frac{C_p}{\bar{g}_p}$	Geometrically meaningful and cannot be determined exactly.	The distance along the plumb line between the geoid and point on the Earth's surface. The calculation requires the complete knowledge of the mass density of the crust.
Normal height	$H_p^* = \frac{C_p}{\bar{\gamma}_p}$	Geometrically meaningful and can be determined exactly.	The distance between the quasi-geoid and the point on Earth's surface. There is no need to make approximations for the density of the Earth's crust.
Normal-orthometric height	$H_p^{no} = \frac{C^n}{\bar{\gamma}}$	Approximates to either orthometric or normal heights.	Makes use of normal geopotential number. It is not compatible with geoid or quasi-geoid.
Geoid height	$h_p - H_p = N_p$	The separation between the geoid and the reference ellipsoid.	Used in the conversion of the geometrically defined heights into physical heights.
Height anomaly	$h_p - H_p^* = \zeta_p$	The separation between the quasi-geoid and the reference ellipsoid.	Approximation of the geoid undulation according to the Molodensky's theory.

2.3. Vertical Datum

The definition and realization of the vertical reference system is essential in height determination. Vaníček (1991) defines the vertical datum as a coordinate surface where the vertical coordinates are referred to. According to Vaníček, geoid, quasi-geoid, and the ellipsoid are three different conventional vertical datums. For many scientific and practical applications such as engineering, geodynamics, precise navigation, flooding protection, and coastal research, physical height information is required (Ihde and Sánchez, 2005).

Today most of the countries around the world use regional vertical datums without a link to a global datum. Over 100 regional vertical datums realized by spirit leveling related to different tide gauge stations exist all over the world (Pan and Sjöberg, 1998). The development of a unique global vertical datum for all lands and oceans around the world is the subject of ongoing research (Burša et al., 2007; Ihde et al., 2007; Ihde and Sánchez, 2005; Sánchez 2007; and Sánchez, 2009). The realization of a global reference surface for physical height systems, the relation of the individual tide gauge records with respect to the reference surface, the separation of the sea level changes and vertical crustal movements observed from tide gauge measurements, and the connection with the terrestrial reference system are some of the problems that need to be resolved. According to Ihde and Sánchez (2005), to develop a unified physical height system the followings are needed to be known at the centimeter accuracy level:

- a unique global height datum,
- consistent parameters, models and processing procedures of terrestrial reference frame and gravity field,
- a closed theory for the combination of parameters (space techniques, gravity),
- consideration of time dependent influences,
- concepts for the realization.

A height system is a one-dimensional coordinate system used to express the height of a point with respect to a reference surface. The height of a point can be defined in different ways leading different height coordinates for the same point. Its definition changes according to the reference surface chosen and the path along which the height is measured (Featherstone, 2006). There are two main height systems: one that ignores the Earth's gravity field and linked with the normal of the ellipsoid, and one that follows the curved plumbline and linked to the equipotential surfaces (see section 2.2).

A vertical datum is the practical realization of a height system and its reference surface. The realization of a vertical datum has always been a basic task of height determination at the global or a regional level. In this section more details on the realization of a vertical datum, solution of the global and regional vertical datums problems are given.

2.3.1. Realization of vertical datum

Traditionally, averaging approximately 18.6 years (corresponding to the longest tidal component period) of sea level observations in order to obtain the MSL at one or more fundamental tide gauges was a common approach to determine the regional vertical datum (Torge, 2001). This requires the assumption that the MSL coincides with the geoid. As stated in the previous section, there exist discrepancies between the MSL and the geoid due to the sea surface topography (SST) (Torge, 2001). Besides the regular tidal components, meteorological, hydrological and oceanographic effects are the other factors responsible for the existence of the SST (Torge, 2001). Therefore, the MSL is not an equipotential surface. In this approach, one of the tide gauge stations is linked to a reference benchmark nearby (Fotopoulos, 2003) or directly on the tide gauge (see Figure 2.5). Thereby, the height of the reference benchmark above the sea level can be obtained from the link with the tide gauge. The benchmark with the known height is the initial point of the leveling network.

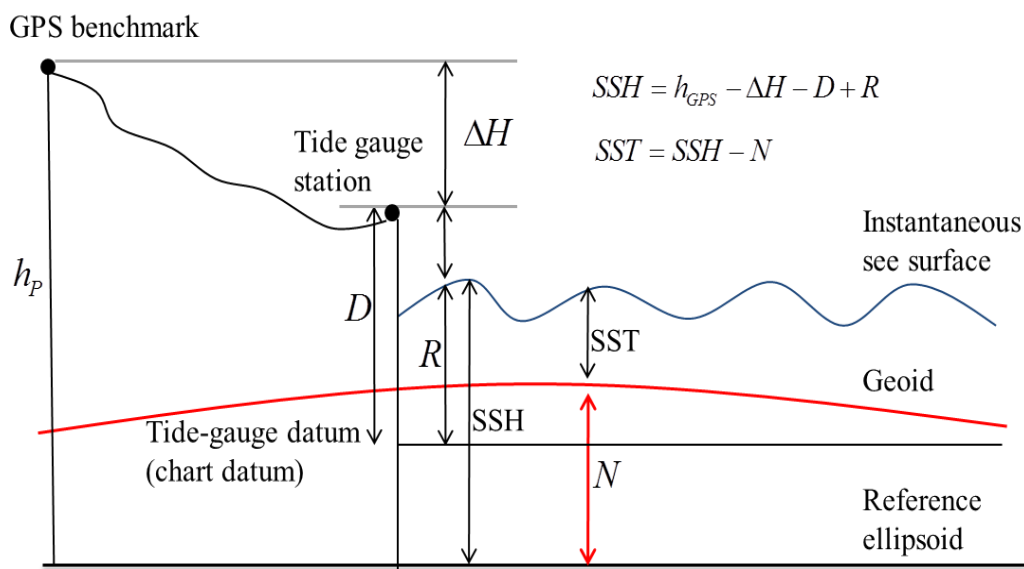


Figure 2.5: The relation between the reference tide gauge station and the collocated GPS benchmark.

For large networks, the vertical datum can be fixed to several tide gauge stations (Heck and Rummel, 1990), such as the Canadian Geodetic Vertical Datum of 1928, CGVD28 (Cannon, 1929). Orthometric, dynamic, and normal heights are determined by adding small gravity dependent corrections to the levelled height increments and can be computed by the combination of leveling height increments and measured gravity potential differences (Rummel and Teunissen, 1988).

There are different methods used in the realization of a global or regional vertical datum. Globally, a common reference surface is defined which is associated with the same potential surface. Regionally, the reference surface is defined and specified based on regional data. The descriptions of these two are given in the following sections.

2.3.2. Global vertical datum

A global vertical datum can be defined as a height reference surface for the all continents and oceans. Many studies addressed this topic during the last century when the theory of the realization of a global datum was developed. However, the lack of accurate geodetic data did not allow the realization of a global datum. The need for a global vertical datum is even more pressing today and a common international vertical datum or “World Height System (WHS)” is still to be realized and adopted by the International Association of Geodesy (IAG) for all related height applications. The advances made in accurate determination of the global geopotential, as well as the availability of highly accurate GPS/GNSS heights, allow the realization of the global datum at a cm-level accuracy, which is necessary for many science applications such as global change monitoring, MSL changes, polar ice-cap volume monitoring, post glacial rebound studies, etc. A global network providing information on a common system on both land and ocean is essential.

A well-established global vertical datum could provide many advantages in different application areas. For example:

- National and/or regional vertical datums can be connected accurately and consistently.

- Inconsistencies that exist in the gravity anomalies and height measurements due to different vertical datums can be eliminated by using a common reference surface.
- Geodetic leveling and oceanographic procedures used in sea surface determination can be compared (Balasubramania, 1994).

Indeed, besides information collected on land, measurements over the oceans are necessary. Satellite altimetry is the most important development providing the ellipsoidal height information on the ocean, large water bodies and polar ice-sheets (Rummel and Sansò, 1993).

Many researchers have reviewed the connection of regional datums as a practical solution to create a unified global vertical datum (Colombo, 1980; Balasubramania, 1994; and van Onselen, 1997). In Colombo (1980), a global vertical datum is defined by using the combination of geometric and geophysical data. For the connection of the vertical datums between continents, ~50 cm accuracy is attained by using three-dimensional geocentric coordinates and geoid undulations obtained from a high degree geopotential model which are defined for at least one point in each vertical datum aimed to be connected. According to Balasubramania, the accuracy for connecting the datums changes from ± 5 cm to ± 23 cm (Balasubramania, 1994). In van Onselen (1997), more advanced satellite and terrestrial data are included. The error in the connections is estimated around 80 cm when only the satellite-only geoid models are used, and this is improved to be 20 cm by including the terrestrial data (van Onselen, 1997). In spite of these early studies the unification of the regional vertical datums is not accomplished yet due to accuracy requirements. In general, the cm accurate datum is not applicable for some locals yet accordingly neither for a global scale (Klees and van Gelderen, 1997).

Recent studies suggest determining or adopting a W_0 value globally and provide links between the regional vertical datum origins (fundamental tide-gauge stations) to the W_0 surface. For example, Sánchez (2009) determined a W_0 value ($6263685.4 \text{ m}^2 \text{ s}^{-2}$) by using satellite altimetry measurements in the region of 60° N and 60° S , GGMs, and conventional constants. This geopotential value defines a reference surface which is used

in the unification of the South American heights systems. In this research, the reference surface and the individual height datums in South America are related.

Burša et al. (2004) worked on the realization of a global vertical reference frame by means of several regional and local vertical datums. The origin of four heights datums, North American Vertical Datum 1988 (NAVD88), Australian Height Datum 1971 (AHD71), local vertical datum of France Institut Geographique National 1969 (IGN69) and Brazilian Height Datum 1957 (BHD), are related with the adopted reference geopotential value W_0 ($62636856.0 \pm 0.5 \text{ m}^2 \text{ s}^{-2}$) and they have been determined at the 5 cm level. His methodology does not require a certain geopotential value; therefore, any arbitrary value can be chosen. Numerical evaluations of the recent studies can be found in Sánchez (2009), Ihde and Sánchez (2005) and Burša et al. (2004).

According to Heck and Rummel (1990) and Lehmann (2000), the four strategies listed below can be used to solve the global vertical datum problem.

a) Pure oceanographic approach: This method is done by ocean leveling which is based on the hydrodynamic equation of motion for the infinitesimal water particle (Rummel and Ilk, 1995). SST is the main problem when linking the regional vertical datums between continents that are separated by the ocean. SST is a dynamic surface that is difficult to model due to the complex variety of the salinity, temperature, density, current, wind stress, and air pressure. Differences of the gravity potential of the sea surface are modeled by oceanographers by geostrophic and steric leveling measurement techniques. Geostrophic leveling provides the geopotential differences by integrating along certain direction on the water surface of measured current velocities. Therefore it is applicable in shelf areas. Steric leveling performs integration along the plumb line between the water level and the reference surface (which is called level of no motion), where the isobaric and the equipotential surfaces coincide. Salinity, temperature and depth information are needed to be known for the steric leveling and it is applied in deep ocean areas. As it is the case with altimetry, in shallow regions and coastal areas, the reliability of these techniques decreases too.

Since the connections are made along coastal boundaries, this strategy is not adequate by itself.

- b) Satellite altimetry combined with geostrophic leveling:** Traditional oceanographic techniques, like geostrophic (dynamic) leveling used to derive the SST from measurements observed at sea, are combined with modern ones, such as satellite altimetry. Satellite altimetry can be used to derive global geopotential models and mean sea surface observations which help to determine the marine geoid. For the definition of the global vertical datum, the MSL must be known as a two-dimensional surface all over the oceans. Altimetry provides this information along satellite altimeter's tracks on discrete points. Interpolation from these point values can be used to obtain the information where it is desired. However, since the satellite altimetry has poor temporal resolution, geostrophic leveling is still required to extrapolate the SST at the tide gauges. Also, altimetry data covers 20 years of observations whereas some of the tide gauges have over 100-year records.
- c) Geodetic boundary-value problem (GBVP):** A geodetic boundary value problem (Moritz, 1980) is another approach to solve the vertical datum problem (Rummel and Teunissen, 1988; Heck and Rummel, 1990; Rummel and Ilk, 1995; Sanso and Venuti, 2002; Ihde and Sánchez, 2005; Sánchez, 2007; Sánchez, 2009; Ardan et al., 2009). This approach includes the usage of terrestrial data and global geopotential model combination where the available data change cross coastlines. The altimetry gravimetry boundary value problem (AGBVP) can also help to analyze the datum issues (van Gelderen, 1991; Lehmann, 1999; Grebenitcharsky, 2004). One should note that the GBVP approach is theoretically defined and the equations for its solutions have been derived. Due to the lack of unified data coverage for the whole Earth, this approach could not be applied until recently. However, the gravity field satellite missions GRACE and GOCE, new high resolution DEMs and terrestrial gravity data make this approach feasible. This approach is the one planned to be used in the realization of the North American and World Height Systems. More details are given in section 2.5.

d) Satellite positioning combined with gravimetry: This approach makes use of the GNSS obtained geometric heights and leveled heights referred to a certain local vertical datum connection (Heck and Rummel, 1990; Lehmann, 2000). Only New Zealand has adopted a gravimetric geoid in 2009 as an official vertical datum regionally (Amos, 2009). The accuracy depends on the accuracy of the ellipsoidal heights and the internal precision of the gravimetric geoid model. It is a very promising approach and many studies have been conducted in Canada (Véronneau, et al., 2006; Véronneau and Huang, 2007) as well as in the rest of the world at regional and continental scales.

In Balasubramania (1994), two options to establish a global vertical datum were investigated based on the adjustment of heterogeneous data (given in option d). For option one, four types of data uniformly distributed over the Earth are required. These are free-air gravity anomalies, precise orthometric heights or heights of the benchmarks above the regional vertical datum, an accurate global geopotential model, and accurate ellipsoidal heights of stations collocated with the leveling benchmarks stations. There are two important factors: distribution and accuracy. Since the datasets were not uniformly distributed and collected with enough accuracy, this approach had limited application. Thus, due to the lack of information on most parts of the Earth, this approach was ran only a single iteration. According to the first results provided, a global vertical datum could be realized by ± 5 cm accuracy (Fotopoulos, 2003).

The second option was created based on a more practical realization of a global vertical datum by making use of GPS/DORIS tracking networks and accurate geoid models. The orthometric heights derived from the GPS and leveling measurements are corrected with a corrector surface model and referred to a geoid which is independent from any specific MSL information. This approach requires a precise global geoid model in order to be actualized (Fotopoulos, 2003).

2.3.3. Regional vertical datum

As stated in the introductory part of this section, there are many leveling-based regional vertical datums realized by different approaches. There are five main approaches defined in Vaniček (1991) for the realization of a regional vertical datum. They are reviewed in Fotopoulos (2003), and summarized in the following.

- a) A tide gauge network is defined on the coasts of the country, and the geoid surface is defined by the MSL measurements obtained from tide gauge records. The datum is fixed to zero at these stations. Distorted heights will be the result of this approach due to the disparity between the MSLs at the selected tide gauge stations and the geoid. As mentioned before, the MSL is not an equipotential surface. Moreover, by fixing the datum to zero at these tide-gauges, it is also assumed that the tide gauge records do not include any error, or the error is acceptable. Additionally, in some cases, such as in Canada due to the post-glacial rebound, land movement is another factor that needs to be taken into account.
- b) The vertical datum is defined by performing a free-network adjustment where only one point is held fixed. Resulting heights from the adjustment are shifted so that the mean height of all tide gauges equals zero. This approach is a modified version of approach (a), and it ignores all other MSL observations made at the other tide gauges and relies on just one tide gauge records.
- c) The best available model is used to estimate the mean sea surface topography (MSST) at the tide gauge stations from satellite altimetry and hydrostatic models. Then, the network is adjusted by forcing MSL-MSST to zero for all tide gauge stations. Most of the drawbacks in approaches (a) and (b) are eliminated with this approach, but some practical limitations in accuracy exist. Satellite altimetry performs poorer in coastal areas where tide gauge stations are located. In shallow areas, global ocean circulation models derived from altimetry and hydrostatic models can cause decimeters uncertainties whereas they give 2-3 cm accuracy in open ocean (Shum et al., 1997).

- d) The vertical datum is defined as in approach (c); however, the reference tide gauges are allowed to float in the adjustment by error estimates. All MSL and SST information at the reference tide gauges can be incorporated in this approach. Accuracy estimates of the observations can be made with the improved satellite altimetry derived models and better comprehension of the tide gauge observations such as stability of the benchmarks or location change.
- e) In this approach, the vertical datum is defined as in option (d), but orthometric heights are estimated from the satellite-based ellipsoidal heights and gravimetric geoid heights. Since the satellite-derived heights are referred to a global reference ellipsoid, the regional datum is linked to the global vertical reference surface. This approach helps to realize an international World Height System (WHS) or a global vertical datum (Colombo, 1980; Balasubramania, 1994).

The regional vertical datums used in North America are given in the following section.

2.4. Current Vertical Datums in North America

In this section, several vertical reference datums used in North America are discussed. They are the Canadian Geodetic Vertical Datum of 1928, CGVD28, the North American Vertical Datum of 1988, NAVD88, and the International Great Lakes Datum of 1955 and 1985, IGLD55 and IGLD85, respectively.

2.4.1. The Canadian Geodetic Vertical Datum of 1928 (CGVD28)

The current vertical datum in Canada is the Canadian Geodetic Vertical Datum of 1928 (CGVD28) which was realized by leveling measurements (Cannon, 1929). The current published normal-orthometric heights used in Canada refer to CGVD28. A leveling network created from over 80,000 benchmark points were used to establish CGVD28. CGVD was determined by using the MSL values at five tide gauges, two of them located on the Pacific Ocean coast, two on the Atlantic Ocean coast and one on the St. Lawrence River, namely Vancouver, Prince-Rupert, Yarmouth, Halifax, and Pointe-au-Père (Véronneau et al., 2006).

CGVD28 is not compatible with the geoid since the MSLs observed at the five gauges are not on the same equipotential surface, and processing of the leveling data includes only normal geopotential numbers.

The CGVD28 normal-orthometric heights (approximation to the orthometric heights),

H_{CGVD28}^* were computed by:

$$H_{CGVD28}^* = \frac{C_{CGVD28}}{\bar{\gamma}}, \quad (2.15)$$

where C_{CGVD28} is the CGVD geopotential number and $\bar{\gamma}$ is the mean normal gravity.

To relate the CGVD28 with a geoid model, GPS observations should be collected at benchmarks. A representation of CGVD28 and its relation with the equipotential surfaces that the tide gauges are referred to is given in Figure 2.6.

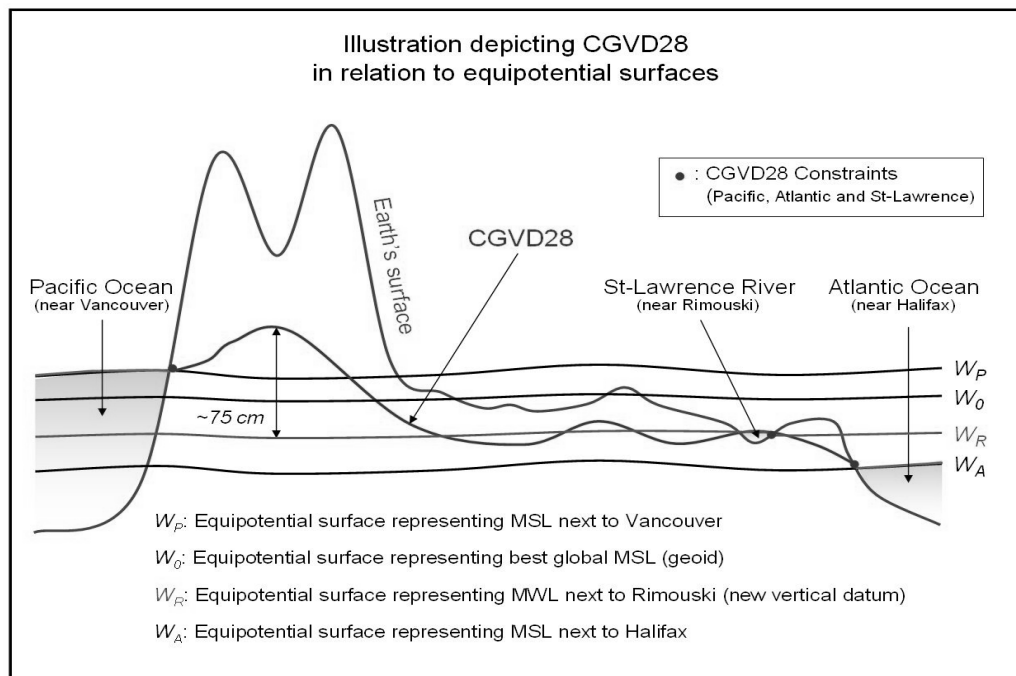


Figure 2.6: Depiction of the Canadian Geodetic Vertical Datum of 1928, CGVD28 and its relation with the equipotential surfaces representing the MSLs at the tide gauges that the datum is constrained to (NRCan, 2011).

Existing Problems and Solutions:

Evidently, CGVD28 does not meet the requirements of modern GNSS-based height determination. Its coverage is limited by 80,000 benchmarks located mostly in the southern part of Canada (Véronneau, NRCan report). Only a small percentage of them (3%) is associated with GPS measurements. In other words, CGVD28 is only known at benchmarks; therefore, by doing interpolation of the known geoid heights between the points, a continuous vertical reference surface cannot be determined homogeneously and accurately. The network can only be extended by performing spirit leveling and GNSS measurements. Since the Natural Resources Canada does not continue spirit leveling measurements at a national level, the usage of the CGVD28 will last for only as long as the benchmarks exist.

Moreover, CGVD28 is not directly compatible with GPS (Véronneau and Héroux, 2007). Even though it is an acceptable accurate model regionally, at the national level it does not meet today's required accuracy mainly due to the distortion introduced by local sea surface topographies at the defining tide gauges. Also, CGVD28 has known systematic errors at both regional and national scale (Véronneau, 2001; Véronneau et al., 2006).

Due to the problems with CGVD28 given above, it is evident that there is a need to develop a new vertical datum in Canada. The new realization approach, i.e., a geoid-based vertical datum along with the new terrestrial datasets and the new satellite models are expected to overcome these problems.

2.4.2. The North American Vertical Datum of 1988 (NAVD88)

NAVD88 was created in collaboration of Canada, USA and Mexico and it was realized as a traditional datum based on leveling. The mean water level measured at the point Pointe-au-Père/Rimouski tide gauge station in 1988 was adopted as the only reference point. NAVD88 provides Helmert-orthometric heights defined by eq. (2.7), namely

$$H_{NAVD88} = \frac{C_{NAVD88}}{g + 0.0424H}, \quad (2.16)$$

where C_{NAVD88} is the geopotential number in NAVD88 and g is the gravity measured at point P .

It is found that the NAVD88 has an east-west systematic error accumulating to over one metre from the east to the west coasts of Canada. Therefore, Canada did not adopt NAVD88. Most of the benchmarks located in Canada have a NAVD88 referred Helmert-orthometric height. Since both datums are realized by leveling, the conversion between NAVD88 and CGVD28 is possible on the benchmarks published in two height systems (Véronneau, NRCan report).

Existing Problems and Solutions

Because of the known errors in NAVD88, this datum does not meet the accuracy requirements of the GNSS height observations. Dedicated satellite missions (GRACE and GOCE) are supposed to provide cm-accurate global gravimetric geoid models in the scale of 100 km. Previous studies showed that the residuals of the GRACE/GPS obtained orthometric heights and NAVD88 leveled heights differ at a meter level across the country after a 500 km low-pass filter is applied (Véronneau, NRCan report). In this procedure the low-pass filtering helps to eliminate the features that GRACE is not sensitive to. This difference shows the long wavelength disagreement between the GRACE geoid and the NAVD88 zero elevation reference surface. Besides the error coming from the observations, crustal motion is another error source that needs to be considered.

2.4.3. Great Lakes Vertical Datums

International Great Lakes Datum of 1955 (IGLD55)

The International Great Lakes Datum of 1955 was developed under the authority of a Coordinating Committee which was established in 1953 under the International Joint Commission of Canada and the United States. The Great Lakes and St. Lawrence River System has been considered as one unit with datum and reference surfaces based on mean water level (MWL) at the outlet of the system in the Gulf of St. Lawrence.

The reference zero point was assigned to Pointe-au-Père (Father’s point), Quebec. There are four reasons of this choice:

- 1) This point was located at the outlet part of the system.
- 2) The tide gauge at the location had long and reliable records.
- 3) The mean water level at the point had values approximate to the mean sea level of the Atlantic Ocean.
- 4) This point was connected to the rest of the system through first order leveling.

Upon the analysis and completion of the first-order leveling and tide gauge records, the new datum was adopted in 1955 and was based on dynamic heights. More information about the establishment of IGLD55 can be found in the report “Establishment of IGLD55, Second Edition” prepared by the Coordinating Committee (IGLD, 1979; IGLD (1991).

International Great Lakes Datum of 1985 (IGLD85)

The IGLD85 was established based on the same idea as IGLD55. The Coordinating Committee consisting of Canadian and American representatives worked under the aim of developing a new common international vertical datum for Canada, US, and Mexico. National Oceanic and Atmospheric Administration (NOAA)/National Ocean Service (NOS) and National Geodetic Survey (NGS) made the elevations of the common benchmarks available on both NAVD88 and IGLD85. The geopotential numbers for individual benchmarks were assigned to the same value in both NAVD88 and IGLD85. IGLD85 values are given in dynamic heights (see equation 2.17) whereas the NAVD88 values are given in Helmert-orthometric heights.

$$H_{IGLD85}^{dyn} = \frac{C_{NAVD88}}{\gamma_{45}^{\circ}}, \quad (2.17)$$

where C_{NAVD88} is the geopotential number of the NAVD88 and γ_{45}° is the normal value determined at latitude of 45 degrees. A representation of the dynamic and orthometric heights of a lake is shown in Figure 2.7. As shown in the figure, dynamic heights

measured at tide-gauge points around the same lake are supposed to give the same value whereas the orthometric heights change depending on the gravity value measured at the points.

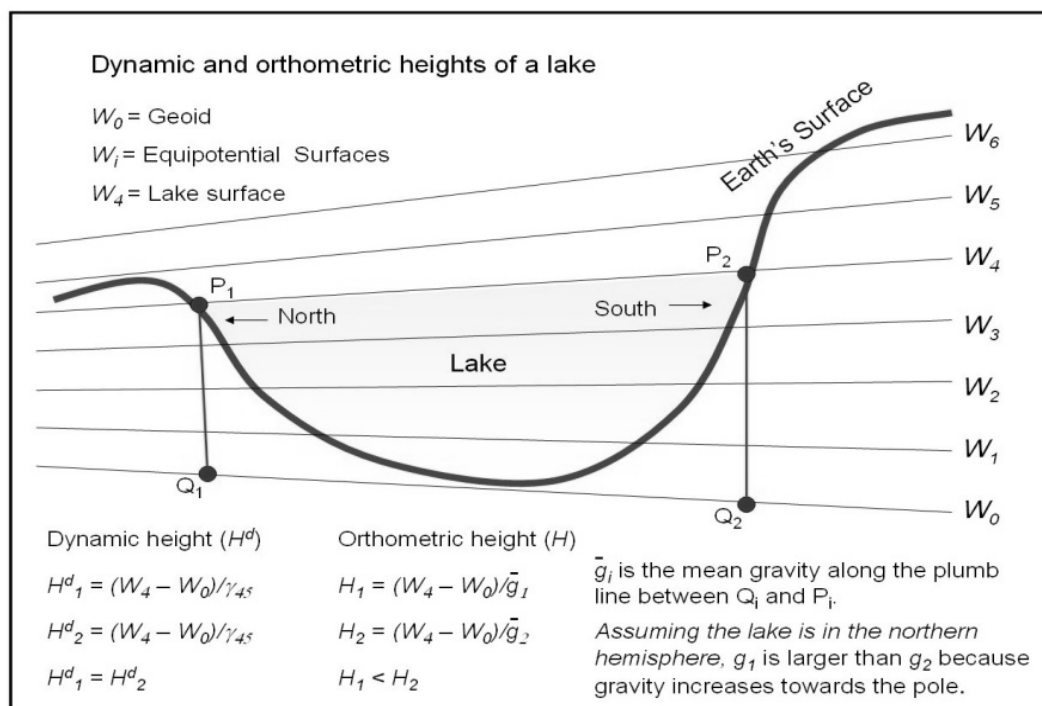


Figure 2.7: A representation of dynamic and orthometric heights of a lake (NRCan, 2011).

The dynamic height of the same point from IGLD85 and IGLD55 can differ from 1 to 40 cm. The development of IGLD85 and NAVD88 had been processed during the same time period and their establishments coincided. Vertical control networks of three countries, Canada, U.S. and Mexico, have been included in IGLD85.

It is well-known that the Great Lakes and St. Lawrence River region are subject to post glacial rebound or glacial isostatic adjustment effect (Zilkoski, 1991; Rangelova, 2007). This effect basically causes a gradual uplift of the crust. Accordingly, the vertical datum defined for the Great Lakes should be renewed every 25-30 years period. In Zilkoski,

(1991), it was also shown that the magnitude of crustal movement on the tide gauge stations differ from each other. As a result of these local changes, the benchmarks are shifted not only with respect to the initial reference point but also with respect to each other (IGLD, 1995).

Existing Problems and Solutions

In the Great Lakes area there is a need for a new vertical datum due to the two main reasons given below:

- 1- As discussed before, the elevations of the benchmarks change with respect to the reference point as well as with respect to each other due to the vertical crustal movement and unstable markers.
- 2- Like in NAVD88, there exist systematic errors in IGLD85, which are greater than half a meter across the Great Lakes region (IGLD, 1995).

Development of an accurate, consistent, and commonly accessible vertical datum is necessary for the Canadian and US agencies working in the Great Lakes and St. Lawrence River region. More details can be found in IGLD (1995). The upcoming vertical datum for the Great Lakes region expected by 2015 should serve both countries and all agencies' necessities in this region.

2.5. A Geoid-based Height System

As expressed in the previous section, the geoid surface is defined by the W_0 value. Traditionally, W_0 is associated with the equipotential surface of the Earth's gravity field passing through the selected tide gauge point in the region. This approach has been used in the realization of regional height systems and therefore incompatibilities exist with the rest of height systems around the world. Thus, this kind of application does not allow us to combine the geometrical and physical heights in a global sense (Sánchez, 2007).

As expressed in section 2.3.2, approach (c), a global vertical datum can be realized via choosing a geopotential value, W_0 and the corresponding equipotential surface. Choosing this W_0 can be achieved either by adopting a geopotential value for some regional vertical datum, or just by adopting some arbitrary value. Changes in the geopotential values will

be based on the local data used. Some estimations are given in de Bruijne et al. (1997) and Grafarend and Ardalan (1997).

According to the Gauss-Listing definition, a globally defined reference level W_0 can be estimated by the geopotential averaged over the undisturbed ocean surface. In other words, the W_0 value should represent the mean sea level equipotential surface where the sea surface topography is zero (Mather, 1978; Sánchez, 2007 and 2009). Following the Gauss-Listing definition, the W_0 values should satisfy the condition given below:

$$\int_{S_0} (W - W_0) dS_0 = \min \quad (2.18)$$

where S_0 represents the global ocean surface.

Nowadays, the W_0 value can be computed by making use of GGMs, mean sea surface models and altimetry measurements. Burša et al. (2004) proposed a definition of the global vertical datum by using an adopted W_0 value that is averaged over the oceans. Recently, this value can be obtained from satellite altimetry observations (using Topex/Poseidon, Jason, or a combination of data from different missions) and global gravity models, in particular models from the GRACE and GOCE gravity satellite missions with an accuracy of 5 cm. Besides altimetry data, GPS/leveling heights (referring to a specified regional vertical datum), a global geopotential model, the geocentric gravitational constant, the angular velocity of the Earth's rotation and the second zonal harmonic coefficients are the other required datasets and parameters needed for the solution.

The determination of W_0 requires caution with respect to the dependence on the seasonal changes that occur in the oceans and also the latitudinal limits which the observations are subjected to. According to Sánchez (2007), the W_0 can be calculated by use of a GGM derived from satellite data from CHAMP, GRACE, and GOCE. Satellite observations provide the highest accuracy in the determination of the lower and medium frequency part of the Earth's gravity field. Moreover, it is also indicated that the dependence of the W_0 value on the spherical harmonics above 120 is negligible (Sánchez, 2007). The terrestrial gravity data are excluded due to the possible vertical datum inconsistencies.

According to Sánchez (2007), the calculated W_0 values are almost independent from the GGM, slightly dependent on the MSS model and strongly dependent on the region extension. The variation of W_0 with time is almost negligible (until now); however, since the sea surface changes constantly after some years it can reach a significant change. For this reason, it is necessary to define a reference epoch that the W_0 value is referred to (Burša et al., 2007; Ihde et al., 2007; Ihde and Sánchez, 2005; Sánchez, 2007 and 2009).

Canada will start using a geoid-based vertical datum by 2013 with the most accurate regional geoid model developed thus far. NRCan has already prepared a prototype of a geoid-based height system in Canada. The latest official Canadian gravimetric geoid model of 2010, CGG2010 (Véronneau and Huang, 2011), is explored as a prototype of a geoid-based height system in Canada (Huang et al., 2011).

For the definition and realization of a geoid-base height system the following parameters are needed (Huang et al., 2011):

- a conventional geopotential value, W_0
- the conventional constants GM and ω (adopted to the GGM's parameters used in the development of the geoid model),
- a well-defined reference ellipsoid by the U_0 , GM_e , J_2 and ω_e where the parameters correspond to normal gravity potential, gravitational constants of the Earth, dynamic form factor of the Earth and the angular velocity of the ellipsoid, respectively,
- a tide reference system (e.g. mean, zero, tide-free),
- an accurate global gravity model,
- epoch information of the datasets,
- ITRS and conventional geocenter.

The geopotential value, W_0 chosen defines which equipotential surface is selected as the geoid among many others. The W_0 value used in the development of EGM2008 and USGG2009 (United States Gravimetric Geoid of 2009) is used in the latest geoid model

of Canada, CGG2010. For the new vertical datum, it is to be determined from the sea level observations of North American tide-gauge records.

The geocentric gravitational constant of the real Earth GM is to compute the zero-degree geoid component and it is different from the GM_e adopted by GRS80 ellipsoid. GRS80 defines the reference ellipsoid for the geoid.

The angular velocities of the Earth ω and the ellipsoid ω_e (GRS80) adopted can be considered identical. The effect of the change of ω in time on geoid is too small to be considered. The value used in GRS80 can be used as a ‘true’ constant.

There are some uncertainties in the determination of the above mentioned parameters (Huang et al., 2011). More specifically:

- Significant differences exist between the calculated W_0 values depending on the methods and data used.
- There are still studies ongoing to develop and evaluate the global gravity models of the Earth and there is no consensus as a conventional model. The choice of the GGMs used (e.g. satellite-only or combined models) may change depending on the application and the region applied. Recently, EGM2008 has been widely used. With the contribution of the GOCE and new GRACE models, new future EGMXX may serve as an actual conventional model as EGM96 used to be in the past.
- The tide-free system has been adopted as a convention in Canada for GPS and gravity data. It is to be decided which tide system will be used in the realization of the vertical datum.
- Adoption of an epoch to the geoid model is questionable due to multi-epochs of the terrestrial gravity data collected. Terrestrial data cannot be reduced to a specific epoch; however, satellite-only solutions are expected to provide time-tagging. The geoid model with some epoch information will allow us to monitor the geoid change in time and update the vertical datum continuously.

- Lastly, there is a need for the exact relation with respect to a geometric reference frame. In other words, the relation between the geometric reference frame for GNSS and the reference frame for the geoid model are meant to be defined exactly.

Overview

With a careful consideration of these uncertainties, a prototype of a geoid-based height reference surface has been investigated for Canada by GSD. The latest Canadian gravimetric geoid model, CGG2010 (Véronneau and Huang, 2011), was computed based on the followings:

- The W_0 value ($62636855.69 \text{ m}^2 \text{ s}^{-2}$) which was used in the development of EGM2008 and USGG2009 was adopted to ensure consistency with the US and global geoids. This surface is 11 cm higher than the CGVD28-implied surface.
- Conventional values $GM = 3986004.415 \times 10^8 \text{ m}^3 \text{ s}^{-2}$ and $\omega = 7292115 \times 10^{-11} \text{ rad s}^{-1}$ were used in the model computation.
- The geoid model refers to GRS80 ellipsoid.
- The geoid was computed in the tide-free system and can be transformed to the other tide systems.
- EGM2008 and the first generation GRACE and GOCE combined satellite only solution (GOCO01S) were included in the model computation.
- Because of the mixed epochs in the included datasets, the epoch is undefined but 2005.0 was adopted based on the used satellite information.

The latest Canadian gravimetric geoid model, CGG2010 is to be upgraded by 2013 with the new datasets collected.

CHAPTER 3

3. GRAVIMETRIC GEOID DETERMINATION

3.1. Introduction

In this chapter, the methodologies for the computation of the gravimetric geoid are described. This includes the basics of the gravity field, the global gravitational modeling and the regional geoid modeling in Helmert's space. The remove-compute-restore technique applied in combining satellite models with regional terrestrial gravity data and the methodology of the necessary data treatment are given in this section. Moreover, the Stokes integration and the modified Stokes kernel applied in the development of the regional geoid models are described. Lastly, methodologies used in the evaluation of a gravimetric geoid model are given.

The shape of the geoid is determined by the mass distribution inside the Earth and the centrifugal force existing as an effect of the rotation of the Earth and the attraction from the other celestial bodies. The potential of the gravity, W , is defined as the sum of the gravitational potential of the Earth, V , and the centrifugal force potential, Φ , (Hofmann-Wellenhof and Moritz, 2005) and it can be expressed by

$$W = V + \Phi. \quad (3.1)$$

According to the Newton's law of gravitation, the gravitational potential is (Hofmann-Wellenhof and Moritz, 2005):

$$V = G \iiint_v \frac{\rho dv}{r}, \quad (3.2)$$

where G is the gravitational constant ($\approx 6.6742 \times 10^{-11} \text{ m}^3 \text{ kg}^{-1} \text{ s}^{-2}$) (Torge, 2001), ρ is the density function of the Earth, dv is an element of volume inside the Earth, and r is the distance between the mass element and the computational point.

Outside the Earth's masses, V is harmonic and satisfies the Laplace differential equation

$$\Delta V = 0. \quad (3.3)$$

Inside the Earth masses, where the density changes discontinuously, the Poisson differential equation holds

$$\Delta V = -4\pi G\rho, \quad (3.4)$$

where Δ represents the Laplacian operator and is defined by $\Delta = \frac{\partial^2}{\partial x^2} + \frac{\partial^2}{\partial y^2} + \frac{\partial^2}{\partial z^2}$.

The centrifugal potential in equation (3.1) is expressed as

$$\Phi = \frac{1}{2}\omega^2(x^2 + y^2), \quad (3.5)$$

where ω is the angular velocity of the Earth's rotation, x , y are the coordinates of a point defined in a geocentric rectangular coordinate system, and the z axis coincides with the mean rotation axis of the Earth. By substituting equations (3.2) and (3.5) into (3.1), the gravity potential now can be expressed as

$$W = V + \Phi = G \iiint_v \frac{\rho dv}{r} + \frac{1}{2}\omega^2(x^2 + y^2). \quad (3.6)$$

As indicated in chapter 2, the level or equipotential surfaces have a constant gravity potential. The surface of the geoid is also defined as an equipotential surface with a constant gravity potential value, W_0 . Therefore, the geoid cannot be defined mathematically and the solution of it is not analytical (Hofmann-Wellenhof and Moritz, 2005). To linearize the problem, an ellipsoid is used as an approximation to the geoid. The value of the normal potential of the Earth, which is the potential of the ellipsoid, U , is used to approximate the actual gravity potential value (Hofmann-Wellenhof and Moritz, 2005). The normal potential of the Earth can be written as:

$$U = V_e + \Phi_e, \quad (3.7)$$

where V_e is the gravitational potential and Φ_e is the centrifugal potential of the ellipsoid.

The centrifugal potentials of the Earth and the adopted ellipsoid are assumed to be the same. The small difference remaining between the actual gravity potential and the normal gravity potential at a point P_0 is the disturbing potential T :

$$T_{P_0} = W_{P_0} - U_{P_0}, \quad (3.8)$$

where U_{P_0} can be approximated as:

$$U_{P_0} = U_Q + \left(\frac{\partial U}{\partial n'} \right)_Q N = U_Q - \gamma N, \quad (3.9)$$

where the point P_0 is located on the geoid and point Q is located on the ellipsoid (see Figure 3.1).

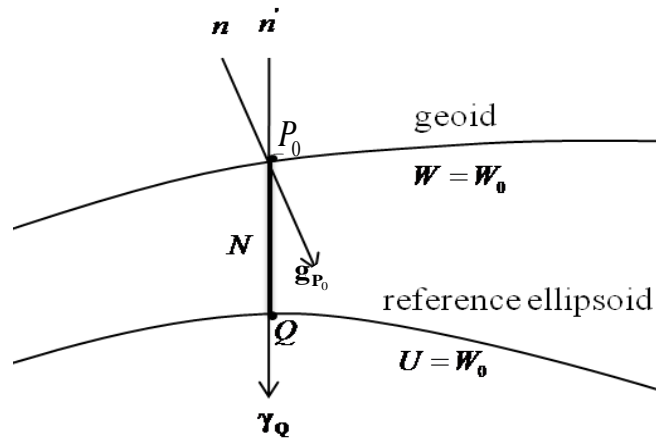


Figure 3.1: Illustration of the geoid, reference ellipsoid, and the vectors of the gravity and normal gravity (Hofmann-Wellenhof and Moritz, 2005).

It can be chosen that $W_{P_0} = U_Q = W_0$ constant, and thus T can be rewritten as:

$$T_{P_0} = \gamma N, \quad (3.10)$$

thus the determination of W is reduced to the problem of computing T .

At this point, it is necessary to introduce the difference between the gravity vector \mathbf{g} at the point P_0 on the geoidal surface and the normal gravity vector γ computed at the point Q on the ellipsoidal surface. The difference of these two vectors is called gravity anomaly vector and defined as follows:

$$\Delta\mathbf{g} = \mathbf{g}_{P_0} - \gamma_Q, \quad (3.11)$$

where the difference in magnitude is gravity anomaly. The two vectors can be compared at the same point P_0 . Then the difference between two vectors gives the gravity disturbance vector

$$\delta\mathbf{g} = \mathbf{g}_{P_0} - \gamma_{P_0}, \quad (3.12)$$

whereas the difference in magnitude is gravity disturbance.

The relation between the gravity anomaly and the unknown disturbing potential T is

$$\Delta g = -\frac{\partial T}{\partial n} + \frac{1}{\gamma_Q} \frac{\partial \gamma}{\partial n'} T, \quad (3.13)$$

where \mathbf{n} is the normal of the geoidal surface and \mathbf{n}' is the normal to the ellipsoidal surface. It is the fundamental equation of the physical geodesy as it relates T to the observations of gravity. In spherical approximation, where $\gamma = \frac{GM}{r^2}$ (Hofmann-Wellenhof and Moritz, 2005) is only applicable for small quantities of the disturbing potential functionals, the fundamental boundary condition can be written as:

$$\Delta g = -\frac{\partial T}{\partial r} - \frac{2T}{r}. \quad (3.14)$$

The gravimetric geoid can be obtained by solving the boundary value problem (BVP) for the disturbing potential T (Moritz, 1980) which is defined by $\Delta T = 0$ and eq (3.14). There are different types of boundary value problems depending on the boundary conditions and the boundary surfaces (Hofmann-Wellenhof and Moritz, 2005; Grebenitcharsky, 2004). Dirichlet's, Neumann's and Robin's problems are the main three

BVPs in potential theory (Martensen and Ritter, 1997). In physical geodesy, depending on the boundary surface chosen, two types of solutions are formulated (Moritz, 1980): The Stokes solution for the determination of the geoid, and the Molodensky solution for the determination of the quasi-geoid. Here the Stokes BVP is solved, i.e., the disturbing potential is obtained as a solution of the Stokes problem; and then the geoid undulation, N is obtained from the Bruns's formula (Hofmann-Wellenhof and Moritz, 2005):

$$N = \frac{T_{P_0}}{\gamma}. \quad (3.15)$$

On the geoid where $r=R$, the solution of Stokes's BVP is

$$T = \frac{R}{4\pi} \iint_{\sigma} \Delta g S(\psi) d\sigma, \quad (3.16)$$

where

$$S(\psi) = \frac{1}{\sin(\psi/2)} - 6 \sin \frac{\psi}{2} + 1 - 5 \cos \psi - 3 \cos \psi \ln \left(\sin \frac{\psi}{2} + \sin^2 \frac{\psi}{2} \right), \quad (3.17)$$

is the standard Stokes kernel, expressed in terms of Legendre polynomials as

$$S(\psi) = \sum_{n=2}^{\infty} \frac{2n+1}{n-1} P_n \cos(\psi), \quad (3.18)$$

where $S(\psi)$ is the Stokes function, ψ is the spherical distance between the computation point and the running point, R is the mean radius of the sphere and $d\sigma$ is the surface integration element (Hofmann-Wellenhof and Moritz, 2005).

By applying the Bruns's formula to equation (3.16), equation (3.15) can be rewritten as:

$$N = \frac{R}{4\pi\gamma} \iint_{\sigma} \Delta g S(\psi) d\sigma, \quad (3.19)$$

where $\iint_{\sigma} = \int_{\alpha=0}^{2\pi} \int_{\psi=0}^{\pi}$, and $d\sigma = \sin \psi d\psi d\alpha$, where the α is the azimuth angle.

To evaluate the Stokes integral, the following assumptions are made:

- The gravity anomalies are distributed all over the Earth on the geoid.
 - In practice, gravity anomalies are not available globally. Due to this fact the integral cannot be evaluated globally; a global gravity model is needed to account for the far-zone contribution of the Stokes integral.
- No masses exist outside of the geoid (to ensure the disturbing potential is harmonic outside the Earth).
 - In practice, the masses above the geoid are mathematically removed by using different reduction methods. Then a topography restoring process is applied afterwards. This remove-restore procedure introduces errors because the topographic density effect cannot be modeled exactly.

More details regarding the application of Stokes's integral is given in section 3.3.3 of this chapter.

3.2. Global Gravity Field Modeling

As stated in the previous section, a global gravity model should be included in the geoid computations since the terrestrial gravity anomalies are not available globally. More importantly, recently obtained satellite-based gravity field solutions provide more accurate information for the lower degree components of the gravity field than the regional terrestrial data. The GGMs are used in applications, such as the determination of satellite orbits, inertial navigation, development of geophysical and geodynamic models (Torge, 2001). A GGM consists of the coefficients of the solutions of Stokes's BVP as a series of spherical harmonics. With $n_{\max} = \infty$, it is an exact solution equivalent to Stokes's integral. The Earth's gravitational geopotential was computed from the surface gravity data with 2500 km resolution in 1950's (Rapp, 1997). Today, with the Earth Gravitational Model of 2008 (EGM2008) (Pavlis et al., 2008), the resolution has been improved to 9 km, which corresponds to a spherical harmonic degree 2190.

A global model should be developed in a way that any function of the gravity field is available at any point on the Earth's surface or above it (Pavlis, 1997; 2006). In this thesis, the main focus is on the determination of a high resolution regional geoid model

from global geopotential models. For an accurate estimation, variety of datasets such as satellite, land, marine and airborne gravity observations are combined in an optimal way to develop a high-resolution GGM such as EGM2008. Depending on the resolving power of the data used, the summation is truncated at a certain degree which also indicates the resolution of the GGM. To develop high-degree global gravitational models, four types of gravity information are currently available:

- 1) *Information obtained from satellite orbit perturbation analyses:* This type of information is obtained through satellite tracking data and it is used to construct the low degree components of the model. The improvement of the satellite-only models from the 1950's to present has been achieved due to the more accurate tracking data available from the tracking information of optic, Doppler and radio interferometric observations, Satellite Laser Ranging (SLR), DORIS and satellite-to-satellite tracking (SST-I or SST-II) data from GPS and Tracking and Data Relay Satellite System (TDRSS) constellations to low Earth orbiters. However, since the gravitational signal attenuates with increasing height, even the most improved satellites are not capable to solve the detailed features of the gravity field alone (Pavlis, 1997; 2006).
- 2) *Surface gravimetric data:* This type of data consists of land, marine and airborne gravity data which provide short and medium wavelength information of the gravity field features. However, this can be accomplished only if the datasets have a uniform, global distribution and accuracy. The accuracy and the density of the gravity measurements mostly depend on the geographic region. Moreover, gravity anomaly data are subject to different systematic errors (Heck, 1990). Hence, with the conjunction of the limited uniform coverage, long-wavelength gravitational information available from the surface data is weakened. Therefore, even though the new satellite-missions can be used to obtain the medium wavelength gravity information, the surface and airborne gravity data are the ones representing the short wavelength gravity features of the land (Pavlis, 1997; 2006).
- 3) *Satellite altimeter data:* Satellite altimetry enables a unique mapping over the oceans both in terms of accuracy and resolution. Topex/Poseidon (T/P) (Fu et al., 1994)

provided sea surface topography information for the first time without a significant radial orbit error. However, altimetry measurements are affected by the inclination of the satellites and the dynamic ocean topography (DOT) existing in the ocean surface measurements. An appropriate DOT model is necessary to be applied to the altimetry measurements that are used in the determination of the long wavelength gravitational field (Pavlis, 1997; 2006).

- 4) *The combination of altimeter data from multiple missions:* Multiple altimeter missions, where some of them have followed very closely spaced ground tracks, have provided dense sampling rate for most of the ocean's surface. The sea surface height (SSH) or SSH slope datasets obtained from these missions can be used to deliver an ocean-wide gravity anomaly data set with a resolution of 2° by 2° . Grid averages derived from these datasets can be combined with the corresponding land and airborne gravity anomalies for the same area. By doing this, the development of global equi-angular grid of gravity anomalies has become possible. Very efficient harmonic analysis and synthesis methods have been developed that take advantage of the geometry of such grids (Rizos, 1979; Colombo, 1981) to make the very high-degree spherical harmonic expansions possible. With the knowledge of DOT, the incorporation of altimetry into the GGMs can be made properly (Pavlis, 2006).

These datasets complement each other in both the spectral and the spatial domain. By combining them, the determination of the gravity field is possible over a wider spectral band and with improved accuracy compared to the one obtained using any of the datasets alone. Nowadays, the GGMs can be obtained from satellite-only observations, as well as from a combination of the aforementioned data types. The recently developed GOCE and GRACE satellite-only models, which will be used in this thesis, are examples of the satellite-only GGMs. On the other hand, the latest Earth global geopotential model EGM2008 (Pavlis et al., 2008) is an example of a GGM that combines satellite, terrestrial and altimetry data. The solution strategy for combining these datasets can be found in Pavlis (1997; 2006).

In our computations gravity field functionals are predicted by the spherical harmonic expansion. The global gravitational potential can be represented as follows:

$$V(r_p, \theta_p, \lambda_p) = \frac{GM}{r_p} \left[1 + \sum_{n=2}^{\infty} \left(\frac{a}{r_p} \right)^n \sum_{m=-n}^n \bar{C}_{nm} \bar{Y}_{nm}(\theta_p, \lambda_p) \right], \quad (3.20)$$

where r_p is the geocentric distance of the point P , θ_p and λ_p are geocentric co-latitude and longitude, respectively, GM is the geocentric gravitational constant and a is a scaling factor which is generally equal to the equatorial radius of an adopted mean-Earth ellipsoid. \bar{C}_{nm} is the fully-normalized, unitless spherical harmonic coefficient of degree n and order m and \bar{Y}_{nm} are fully-normalized surface spherical harmonic functions expressed as follows:

$$\bar{Y}_{nm}(\theta_p, \lambda_p) = \bar{P}_{n|m|}(\cos\theta_p) \cdot \begin{cases} \cos m\lambda_p & \text{if } m \geq 0 \\ \sin |m|\lambda_p & \text{if } m < 0 \end{cases}, \quad (3.21)$$

where $\bar{P}_{n|m|}(\cos\theta_p)$ is the fully-normalized associated Legendre function of the first kind, of the degree n and order m (Pavlis, 1997; 2006). Substituting eq. (3.21) into (3.20), the global gravitational potential can be rewritten as follows:

$$V(r_p, \theta_p, \lambda_p) = \frac{GM}{r_p} \left[1 + \sum_{n=2}^{n_{max}} \left(\frac{a}{r_p} \right)^n \sum_{m=0}^n (\bar{C}_{nm} \cos m\lambda_p + \bar{S}_{nm} \sin m\lambda_p) \bar{P}_{nm}(\cos\theta_p) \right]. \quad (3.22)$$

The spherical harmonic expansion of the disturbing potential T , geoid undulation N and gravity anomaly Δg are expressed in spherical approximation as follows, respectively:

$$T(r_p, \theta_p, \lambda_p) = \frac{GM}{r_p} \sum_{n=2}^{\infty} \left(\frac{a}{r_p} \right)^n \sum_{m=-n}^n (\bar{C}_{nm} \cos m\lambda_p + \bar{S}_{nm} \sin m\lambda_p) \bar{P}_{nm}(\cos\theta_p), \quad (3.23)$$

and

$$N(r_p, \theta_p, \lambda_p) = \frac{GM}{r_p \gamma_p} \sum_{n=2}^{\infty} \left(\frac{a}{r_p} \right)^n \sum_{m=-n}^n (\bar{C}_{nm} \cos m\lambda_p + \bar{S}_{nm} \sin m\lambda_p) \bar{P}_{nm}(\cos\theta_p), \quad (3.24)$$

and

$$\Delta g(r_p, \theta_p, \lambda_p) = \frac{GM}{r_p^2} \sum_{n=2}^{\infty} \left(\frac{a}{r_p} \right)^n (n-1) \sum_{m=-n}^n \left(\bar{C}_{nm} \cos m \lambda_p + \bar{S}_{nm} \sin m \lambda_p \right) \bar{P}_{nm}(\cos \theta_p). \quad (3.25)$$

The potential coefficients \bar{C}_{nm} and \bar{S}_{nm} used here are the remainders after subtraction of the even degree zonal coefficients of the normal gravitational potential (see Hofmann-Wellenhof and Moritz, 2005, Torge, 2001; Barthelmes, 2009). Thus, in practice these formulations are expanded up to n_{\max} degree. Geoid undulations obtained from a global gravity model up to spherical harmonic degree n_{\max} can be expressed:

$$N_{GM} = \frac{GM}{r\gamma} \sum_{n=2}^{n_{\max}} \left(\frac{a}{r} \right)^n \sum_{m=-n}^n \left(\bar{C}_{nm} \cos m \lambda + \bar{S}_{nm} \sin m \lambda \right) \bar{P}_{nm}(\cos \theta). \quad (3.26)$$

Similarly, the gravity anomaly predicted from a global gravity field model up to spherical harmonic degree n_{\max} is expressed

$$\Delta g_{GM} = \frac{GM}{r^2} \sum_{n=2}^{n_{\max}} \left(\frac{a}{r} \right)^n (n-1) \sum_{m=-n}^n \left(\bar{C}_{nm} \cos m \lambda + \bar{S}_{nm} \sin m \lambda \right) \bar{P}_{nm}(\cos \theta). \quad (3.27)$$

3.3. Regional Geoid Modeling in Helmert's Space

3.3.1. Remove-compute-restore technique

In general, the gravity field can be decomposed into three parts. Low-frequencies of the gravity spectrum are obtained from satellite-based global geopotential models. The medium frequencies are obtained from regional terrestrial gravity observations whereas the short wavelength component comes from topography data. Satellite-only solutions provide homogeneous long-wavelength components; however, with no local details. On the other hand, the terrestrial data provide the local details but with biased long-wavelength components caused by limited regional distribution and datum errors. Therefore, an optimum regional geoid solution can be obtained from the combination of the satellite solutions with the terrestrial data.

In this thesis, the remove-compute-restore technique, depicted in Figure 3.2, is applied in combining GGMs with the regional terrestrial gravity datasets and topography (Rapp and Rummel, 1975; Mainville et al., 1992; Sideris et al., 1992). The basic steps of the applied remove-compute-restore technique can be summarized as follows:

- 1) The Earth surface gravity observations are reduced on to the geoid (boundary surface) to remove the effect of the topography above the boundary surface and satisfy the boundary conditions. To achieve this, Helmert's second condensation method (Martinec et al., 1993) described in section 3.3.2.1 is applied.
- 2) The long-wavelength part of the gravity signal predicted from the geopotential model up to a chosen spherical harmonic degree (see eq. 3.27) is removed from the terrain-reduced gravity anomalies (see eq. 3.28). This is to remove the biased low-frequency part of the terrestrial gravity data and make use of the more accurate global geopotential model based information instead. The residual gravity anomaly can be expressed by

$$\Delta g_{res} = \Delta g_h - \Delta g_{GM}, \quad (3.28)$$

where Δg_h is the topography-reduced Helmert gravity anomaly on the geoid (see eq. 3.43), and Δg_{GM} is the model predicted gravity anomaly expanded to spherical harmonic degree n_{max} .

- 3) The residual geoid (to be exact, the co-geoid) undulations are obtained from the residual gravity anomalies by applying Stokes's integral. In this thesis, a degree-banded modified Stokes kernel (see section 3.3.3) is applied to provide the optimum combination of the satellite models with the terrestrial data. The residual co-geoid undulations are obtained by

$$N_{res} = \frac{R}{4\pi\gamma} \iint_{\sigma} \Delta g_{res} S_M(\psi) \cos\varphi d\sigma, \quad (3.29)$$

where $S_M(\psi)$ is the modified degree-banded Stokes kernel.

- 4) At this point, the geoid undulations predicted from the GGM expanded to a spherical harmonic degree n_{\max} , N_{GM} computed from equation (3.26) are restored.
- 5) Lastly, the indirect effect of the topography (see section 3.3.4) removed is restored to obtain the complete geoid model. Therefore, a complete gravimetric geoid can be expressed as

$$N_{grav} = N_{GM} + N_{res} + N_{ind}, \quad (3.30)$$

where N_{GM} is the model predicted geoid undulations, N_{res} is the residual co-geoid undulation obtained from the residual gravity anomalies and N_{ind} is the indirect topography effect obtained from the digital elevation data. A detailed flowchart of the remove-compute-restore process can be found in Figure 3.3.

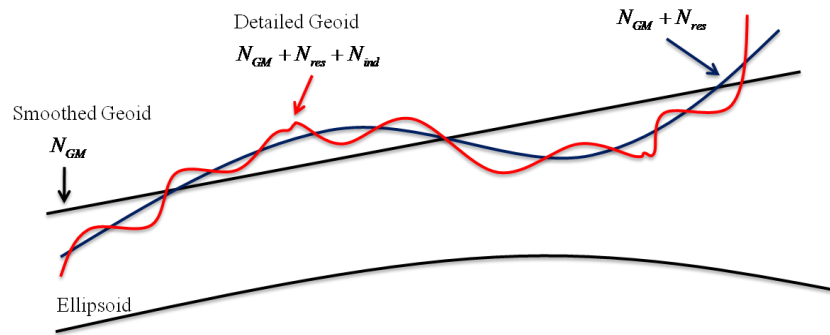
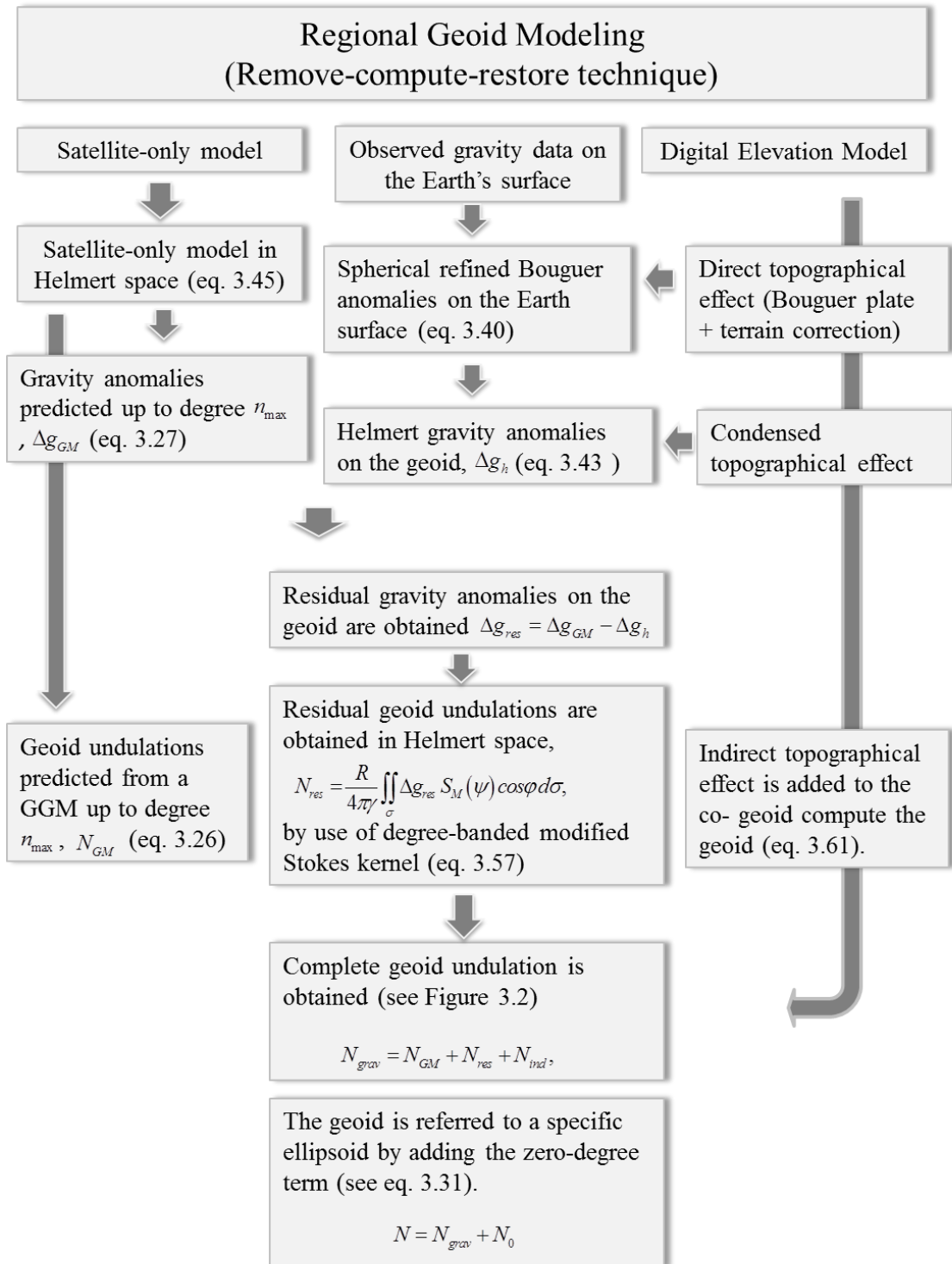


Figure 3.2: Computation of the local gravimetric geoid model using heterogeneous data (after Schwarz et al., 1987).

- 6) In case the reference ellipsoid's mass M_0 and gravity potential U_0 are different than these of the geoid (M , W) then the zero-degree term geoid,

$$N_0 = \frac{GM - GM_0}{R\gamma} - \frac{W_0 - U_0}{\gamma}, \quad (3.31)$$

is added to the solutions.



3.3.2. Helmert's Method

As explained in the previous section, to ensure Stokes's boundary conditions, there must be no topography above the geoid surface. There are different ways of reducing or shifting the topography. Each reduction method treats the topography in a different way to yield the boundary conditions. In this thesis, the topography is removed by applying Helmert's second condensation method (Martinec et al., 1993) where the restored topography is applied as a condensed layer right on the geoid after the downward continuation. Therefore, in order to create a harmonicity of the disturbing potential above the geoid, atmospheric masses also need to be considered.

The reduction process creates a new model Earth which is called Helmert's space and is distinguished from the actual Earth space by the difference of the potential of the topographic and atmospheric masses removed and condensed on the geoid later. The Helmert's gravity field can be represented by the following equation where the superscript h indicates Helmert's space:

$$W^h = W - \delta V^t - \delta V^a, \quad (3.32)$$

where δV^t and δV^a are the differences in the potential of the gravity field due to the condensed topographical and atmospheric masses, respectively (Ellmann and Vaníček, 2007). These differences are expressed as follow:

$$\delta V^t = V^t - V^{ct}, \quad (3.33)$$

and

$$\delta V^a = V^a - V^{ca}, \quad (3.34)$$

where V^t is the gravitational potential of the topography removed above the geoid and V^{ct} is the gravitational potential of the condensed layer, V^a and V^{ca} are the gravitational potentials of the atmospheric masses removed and condensed later.

The disturbing potential in Helmert's space can be expressed as:

$$T^h = W^h - U, \quad (3.35)$$

or

$$T^h = T - \delta V^t - \delta V^a, \quad (3.36)$$

and $\Delta T^h = 0$ holds everywhere above the geoid which is the boundary surface.

The gravitational potential of the topography -here the spherical bouguer shell and the topography deviating from the Bouguer shell- (Ellmann and Vaníček, 2007; Martinec, 1998) can be expressed as:

$$\begin{aligned} V^t = 4\pi G \rho_0 H \frac{R^2}{r_i} \left(1 + \frac{H}{R} + \frac{H^2}{3R^2} \right) + G \rho_0 \iint_{\sigma} \int_{r'=R+H}^{R+H'} l^{-1}(r_i, \psi, r') r'^2 dr' d\sigma \\ + G \iint_{\sigma} \delta \rho \int_{r'=R}^{R+H'} l^{-1}(r_i, \psi, r') r'^2 dr' d\sigma. \end{aligned} \quad (3.37)$$

The first element on the right-hand side of the equation represents the gravitational potential of the spherical Bouguer shell with a mean density ρ_0 and thickness as the orthometric height of the computation point, H (see Figure 3.4). The second part of the right-hand side of the equation derives the gravitational potential of the topography deviating from the Bouguer shell, where G is the gravitational constant, R is the mean radius of the Earth, H and H' are the orthometric heights of the computation and integration points with the geocentric radius of r_i and r' , $l(r_i, \psi, r')$ and ψ are spatial distance and geocentric angle between the computation and integration points, and $d\sigma$ is the area of the integration element. The last terms represents the gravitational potential effect of the anomalous density where $\delta\rho$ is the anomalous density (Ellmann and Vaníček, 2007).

Similarly, the gravitational potential of the condensed topography is

$$\begin{aligned}
V^a = 4\pi G\rho_0 H \frac{R^2}{r_i} \left(1 + \frac{H}{R} + \frac{H^2}{3R^2}\right) + G\rho_0 \iint_{\sigma} \frac{r_i^3 - r_i^3}{3} l^{-1}(r_i, \psi, R) d\sigma \\
+ G \iint_{\sigma} \delta\rho \frac{r_i^3 - R^3}{3} l^{-1}(r_i, \psi, R) d\sigma .
\end{aligned} \tag{3.38}$$

The first part of the right hand side of the equation represents the gravity potential of the condensed Bouguer shell layer and the second part derives the gravitational potential of the condensed terrain deviating from the spherical Bouguer shell. The third term represents the gravitational potential effect of the condensed topography caused by the anomalous density (Ellmann and Vaníček, 2007; Martinec, 1998).

The spatial distance between the computation and the integration points is calculated as follows:

$$l(r_i, \psi, r') = (r_i^2 - 2r_i r' \cos\psi + r'^2)^{1/2} . \tag{3.39}$$

The datasets used in the combination need to be considered in the same settings, Helmert's Earth.

3.3.2.1. Terrestrial data

Gravity anomalies measured on the Earth's surface must be reduced to the boundary surface, (the geoid) and there must be no masses above the geoid (Hofmann-Wellenhof and Moritz, 2005). In Vaníček et al. (1999), the masses above the geoid are transformed directly to a condensed layer onto the geoid. In this study an intermediate Bouguer Earth is applied. The topography is removed, downward continuation is applied and the topography is restored as a condensed layer (Véronneau and Huang, 2007).

The computation steps of the Helmert second condensation method are summarized below (see Figure 3.4):

- The gravity anomaly is measured at a point P on the Earth's surface.
- All masses between the geoid and the observation point are removed.

- Downward continuation is applied to move the gravity observation at point P on the topography to point P_0 on the geoid and spherical refined Bouguer anomalies on the geoid are created.
- The removed topography is restored as a condensed layer onto the geoid and Helmert gravity anomalies are evaluated on the geoid.

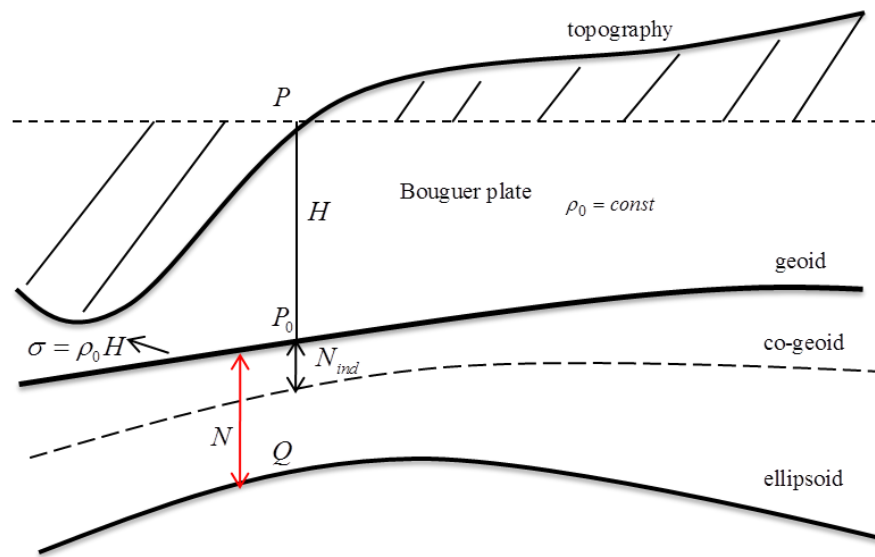


Figure 3.4: Helmert's second condensation method.

In the process of obtaining Helmert's gravity anomalies on the geoid, the downward continuation is executed cautiously. There are two approaches that have been investigated in the region of Western Canada by Huang and Véronneau (2005). The first approach is based on the evaluation of Helmert's anomalies on the topography, downward-continuing them to the geoid where the masses above the geoid are removed and added as a condensed layer on the geoid before the downward continuation performed. The second approach downward-continues refined Bouguer anomalies from the Earth's surface to the geoid and transforms them to Helmert gravity anomalies by adding the effect of the condensed topographical layer where the mass condensation is performed after the downward continuation (Huang and Véronneau, 2005). The Helmert anomalies used in this thesis are created based on the second approach, where the refined Bouguer

anomalies are evaluated first on the surface of the Earth and then downward continued to the geoid. The second approach is less sensitive to the downward continuation because of the smoothness of the refined Bouguer gravity field.

The spherical Bouguer anomalies on the Earth's surface can be expressed as:

$$\Delta g_{SRB}(r_t) = \Delta g_F + \frac{2}{r} H \Delta g_B + \frac{\partial V^t}{\partial r} + \Delta g_{SITE} + \Delta g_a, \quad (3.40)$$

where Δg_F is free-air gravity anomaly, the second term is a correction for the separation between the geoid and the quasi-geoid where Δg_B is simple Bouguer gravity anomaly, the third term is the attraction of the topographical masses (Bouguer shell and terrain correction) on the gravity computed on the Earth's surface, the fourth term is the secondary indirect topographical effect on gravity which is reckoned on the Earth surface and the last term is the direct atmospheric effect.

The attraction of the topographical masses is

$$\begin{aligned} \frac{\partial V^t}{\partial r} \Big|_{r=r_t} = & -4\pi G \rho_0 \frac{R^2}{r_t^2} H \left(1 + \frac{H}{R} + \frac{H^2}{3R^2} \right) + G \rho_0 \iint_{\sigma} \int_{r'=R+H}^{R+H'} \frac{\partial l^{-1}(r, \psi, r')}{\partial r} \Big|_{r=r_t} r'^2 dr' d\sigma \\ & + G \iint_{\sigma} \delta \rho \int_{r'=R}^{R+H'} \frac{\partial l^{-1}(r, \psi, r')}{\partial r} \Big|_{r=r_t} r'^2 dr' d\sigma . \quad (3.41) \end{aligned}$$

The first term on the right-hand side is the negative gravitational attraction of the spherical Bouguer shell, where the second term represents the gravitational attraction of the terrain deviating from the spherical Bouguer shell and the third term expresses the effect of the anomalous topographical density on the gravitational attraction (Ellmann and Vaníček, 2007). Thus, the spherical refined Bouguer anomalies are created on the Earth's surface. Afterwards, the refined Bouguer anomalies are downward continued to the geoid.

$$\Delta g_{SRB}(r_g) \doteq \Delta g_{SRB}(r_t) + f_{DC}, \quad (3.42)$$

where r_g represents the geocentric radius of the point on the geoid, r_i is the geocentric radius of the point at the Earth's surface and f_{DC} represents the downward continuation.

Finally, Helmert gravity anomalies on the geoid can be expressed as

$$\Delta g_h \doteq \Delta g_{SRB}(r_g) - \frac{\partial V^c}{\partial r}, \quad (3.43)$$

where condensed topographical effect on the geoid is

$$\begin{aligned} \frac{\partial V^{ct}}{\partial r} \Big|_{r=r_i} = & -4\pi G \rho_0 \frac{R^2}{r_i^2} \left(1 + \frac{H}{R} + \frac{H^2}{3R^2} \right) + G \rho_0 \iint_{\sigma} \frac{r_i^3 - r_i^3}{3} \frac{\partial l^{-1}(r, \psi, R)}{\partial r} \Big|_{r=r_i} d\sigma \\ & + G \iint_{\sigma} \delta \rho \frac{r_i^3 - R^3}{3} \frac{\partial l^{-1}(r, \psi, R)}{\partial r} \Big|_{r=r_i} d\sigma. \end{aligned} \quad (3.44)$$

where the first term on the right-hand side again accounts for the gravitational attraction of the condensed spherical Bouguer shell, the second term represents the gravitational attraction of the terrain deviating from the Bouguer shell and the last term expresses the effect of the anomalous condensed topographical density distribution on the gravitational attraction (Ellmann and Vaniček, 2007).

In Huang and Véronneau (2005), firstly, refined Bouguer anomalies are determined at each gravity station by using 1" x 1" gridded Digital Elevation Model. Terrain corrections (topography deviating from the Bouguer shell) are evaluated for only near-zone area within a radius of 50 km. The refined Bouguer anomalies are interpolated on 40" x 40" grid by least-squares collocation and averaged on to 2" x 2" grid. Data over oceans are filled with satellite altimetry-derived gravity data. After, the far-zone contribution (effect of the gravity outside the 50 km radius) is added to the refined Bouguer anomalies to produce the spherical refined Bouguer anomalies. After the downward continuation of the spherical Bouguer anomalies, the attraction of the removed topographical masses is restored and the gridded Helmert gravity anomalies are obtained on the geoid.

According to Huang and Véronneau (2005), the downward continuation effect on the geoid that is obtained from the second approach is smaller than 0.5 m in the region of Rocky Mountains and taken into account computations (Huang and Véronneau, 2005; Sideris, 1994; Omang and Forsberg, 2000).

More details of obtaining Helmert gravity anomalies in Canada can be found in Véronneau (1994) and Huang and Véronneau (2005). For the other reduction methods the reader is referred to Hofmann-Wellenhof and Moritz (2005), Forsberg (1994) and Bajracharya (2003).

3.3.2.2. Global Gravitational Model

The use of Helmert gravity anomalies requires the other components included in the regional geoid computations to be in the same model setting. Therefore, the GGMs also need to be transformed to Helmert's space. The Helmertization of the GGM can be processed in two ways. The gravitational potential can be corrected by taking the residual gravitational potential into account first and then modified potential coefficients representing the corrected gravitational potential can be used in the computations. The other way is to add the corrections to the gravity field functionals later. Here the first method is applied.

Firstly, the gravitational potential of the topographical masses is determined at the satellite altitude and the masses are removed according to the Helmert method. Thus, the exterior series of the topographical potential is valid from satellite altitude to sea-level. The direct effect of the Helmert condensation to the gravitational potential at the geoid to the maximum M degree is expressed as follows:

$$\delta V_{GM}^h = -2\pi G\rho \sum_{n=0}^M \sum_{m=-n}^n \left(\frac{n+2}{2n+1} \right) (H^2)_{nm} Y_{nm}(P), \quad (3.45)$$

where

$$(H^2)_{nm} = \frac{1}{4\pi} \iint_{\sigma} H_p^2 Y_{nm} d\sigma. \quad (3.46)$$

are the harmonic coefficients of the squared topography. The detailed derivations of the formulations can be found in Nahavandchi and Sjöberg (1997). Different applications on the same topic (e.g., mass conserved or mass-center conserved Helmertization) can be found in Vaníček et al. (1995), Novak (2000), and Heck (2003).

3.3.3. Stokes's integration

Stokes's integral (Stokes, 1849) can be used to compute the geoid undulations. A global integration of the gravity anomalies over the whole Earth is required for the evaluation of the Stokes integral. However, the gravity anomalies do not have a worldwide coverage dense and accurate as required, and generally the integration area is limited to a spherical cap around the computation point. The effect of the neglected area is obtained from global models. This kind of integration causes a truncation error, and by using a suitable Stokes kernel modification this error can be reduced (Véronneau and Huang, 2007).

An optimum combination of a global satellite model and regional terrestrial gravity data can be performed through the modification of the Stokes's kernel (Vaníček and Featherstone, 1998; Wong and Gore, 1969; and Huang and Véronneau, 2011). There exist many modifications to the Stokes kernel such based on different optimality criteria; see, e.g., as Vaníček and Kleusberg (1987), Meissl (1971), Sjöberg (1984, 1986, and 1991), Heck and Gruninger (1987), Vaníček and Sjöberg (1991), and Featherstone et al. (1998).

Before the gravity field dedicated missions, CHAMP, GRACE and GOCE, satellite gravity models were determined less accurately. The main reason for the kernel modification was to minimize the far-zone contribution of Stokes's integral (also called the truncation error) which was mostly determined from satellite models (Huang and Véronneau, 2011). Based on the fact that the satellite models obtained from the new gravity missions are more accurate than the terrestrial gravity data in the long-wavelength part of the gravity spectrum, the existing modification methods need to be revised to account for this (Huang and Véronneau, 2011).

The degree-banded Stokes kernel formulation based on deterministic methods is applied in this thesis. In the deterministic methods, the error information from GGMs and terrestrial datasets is not used in the geoid computation. Stochastic modification methods such as the least-square modification by Sjöberg (1984) require error information which is inadequately known for the terrestrial data.

The degree-banded Stokes kernel can be expressed as

$$S_{DB}(\psi) = \sum_{n=l+1}^{m_{TG}} \frac{2n+1}{n-1} P_n(\cos \psi), \quad (3.47)$$

where l is the maximum degree of the GGM used, $m_{TG} = \pi / \Delta$, and Δ is the sampling interval of the terrestrial gravity data. Accordingly, the spectral components higher than the data sampling frequency are removed by the modification (Huang and Véronneau, 2005; Huang and Véronneau, 2011). In this type of kernel, the geoid components of degree $l+1$ to m_{TG} are completely determined from the Stokes integration.

Since the computation is performed in a limited capsize, the Stokes kernel can be written as a discontinuous function in the areas within and outside the cap:

$$\overline{S}_{DB}(\psi, \psi_0) = \begin{cases} S_{DB}(\psi) & \text{for } 0 \leq \psi \leq \psi_0 \\ 0 & \text{for } \psi_0 \leq \psi \leq \pi \end{cases}, \quad (3.48)$$

and this can be expressed as the sum of an infinite series of Legendre polynomials:

$$\overline{S}_{DB}(\psi, \psi_0) = \sum_{n=2}^{\infty} \beta_n(\psi_0) \frac{2n+1}{n-1} P_n(\cos \psi), \quad (3.49)$$

where $\beta_n(\psi_0)$ are the coefficients associated with this Stokes kernel:

$$\beta_n(\psi_0) = \begin{cases} -\frac{n-1}{2} Q_n^{DB}(\psi_0) & n \leq l \\ 1 - \frac{n-1}{2} Q_n^{DB}(\psi_0) & \text{for } l+1 \leq n \leq m_{TG} \\ -\frac{n-1}{2} Q_n^{DB}(\psi_0) & m_{TG} + 1 \leq n \end{cases}, \quad (3.50)$$

and the truncation coefficients for the degree banded Stokes function are

$$Q_n^{DB}(\psi_0) = \int_{\psi_0}^{\pi} S_{DB}(\psi) P_n(\cos \psi) \sin \psi d\psi . \quad (3.51)$$

In Figure 3.5, an illustration of the $\beta_n(\psi_0)$ coefficients computed for different cap sizes are shown against to spherical harmonic degree expansion. The β_n coefficients are affected by the increase of the integration area. As it can be seen from Figure 3.5 the more ideal coefficient values are obtained as the cap size increases.

In this figure it is also possible to observe the oscillations around the spherical harmonic degree $l=90$ and $m_{TG}=5400$. These oscillations are tried to be minimized by modifying the degree-banded Stokes kernel band around the degrees l and m_{TG} .

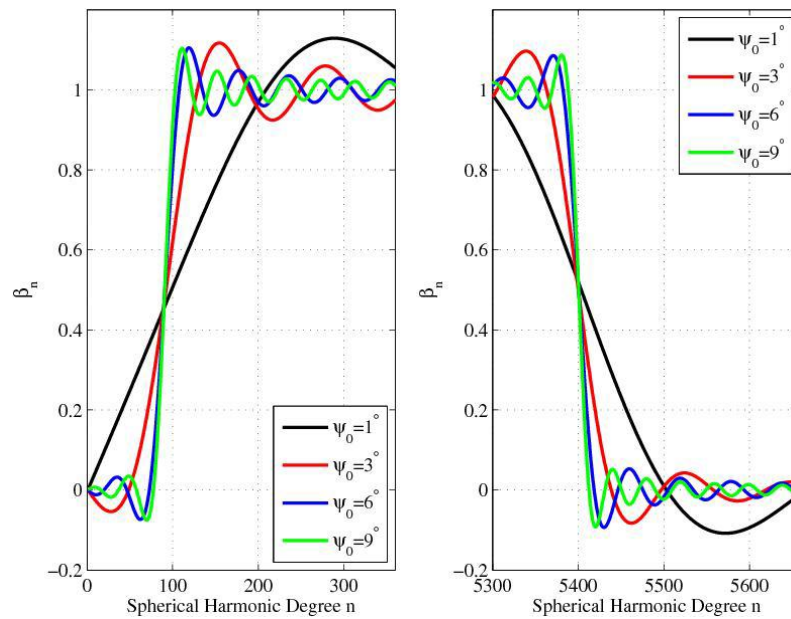


Figure 3.5: The $\beta_n(\psi_0)$ coefficients determined for different integration cap size vs to spherical harmonic degree of expansion (Huang and Véronneau, 2010).

In order to provide a smooth transition in these band intervals, a general form of the modified degree-banded Stokes kernel can be written as

$$S_M(\psi, \psi_0) = \sum_{n=l-u}^{m_{TG}+v} \alpha_n(\psi_0) \frac{2n+1}{n-1} P_n(\cos \psi), \quad (3.52)$$

where the $\alpha_n(\psi_0)$ are the weights introduced:

$$\alpha_n(\psi_0) = \begin{cases} 0 & n < l-u \\ s_n(\psi_0) & l-u \leq n \leq l \\ 1 & \text{for } l+1 \leq n \leq m_{TG} \\ t_n(\psi_0) & m_{TG}+1 \leq n \leq m_{TG}+v \\ 0 & n > m_{TG}+v \end{cases}, \quad (3.53)$$

where u and v are the transition band intervals and set to 60 and 120, respectively, and $s_n(\psi_0)$ and $t_n(\psi_0)$ can be computed with different approximations (see Huang and Véronneau, 2010; Vaníček and Kleusberg, 1987). These functions are basically introduced to make the change between 0 to 1 for the low degrees and 1 to 0 for the higher components smooth and stable. In this thesis cosine based functions are used to modify the $\beta_n(\psi_0)$ coefficients:

$$s_n(\psi_0) = 0.5 \left(\cos \left(\frac{\pi}{u} (n-l+u) + \pi \right) + 1 \right), \quad (3.54)$$

and

$$t_n(\psi_0) = 0.5 \left(\cos \left(\frac{\pi}{v} (n-m_{TG}) \right) + 1 \right). \quad (3.55)$$

Similarly, to equation (3.49),

$$\bar{S}_M(\psi, \psi_0) = \begin{cases} S_M(\psi) & \text{for } 0 \leq \psi \leq \psi_0 \\ 0 & \psi_0 \leq \psi \leq \pi \end{cases}, \quad (3.56)$$

and as an infinite series of the Legendre polynomials:

$$\overline{S_M}(\psi, \psi_0) = \sum_{n=2}^{\infty} \beta_n^M(\psi_0) \frac{2n+1}{n-1} P_n(\cos \psi), \quad (3.57)$$

where

$$\beta_n^M(\psi_0) = \alpha_n(\psi_0) - \frac{n-1}{2} Q_n^M(\psi_0), \quad (3.58)$$

and the truncation coefficients for the modified degree banded Stokes functions are expressed as follows:

$$Q_n^M(\psi_0) = \int_{\psi_0}^{\pi} S_M(\psi) P_n(\cos \psi) \sin \psi d\psi. \quad (3.59)$$

The modified $\beta_n(\psi_0)$ values, $\beta_n^M(\psi_0)$ are shown in Figure 3.6.

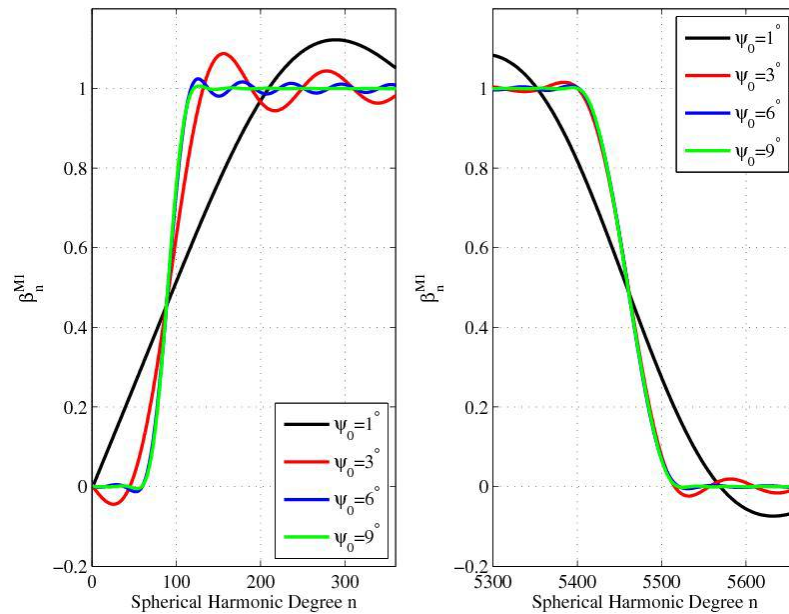


Figure 3.6: The modified transition coefficients $\beta_n^M(\psi_0)$ are shown vs to spherical harmonic degree of expansion (Huang and Véronneau, 2010).

The detailed derivation of these formulas and an example of application in Northwestern Canada and Alaska region can be found in Huang and Véronneau (2010).

3.3.4. Indirect effect of the topography

The distribution of the masses inside the geoid of Helmert's space is the same as inside the actual Earth. The model has no atmosphere, the condensation layer on the geoid is added to the mass distribution, and the topographical density distribution is subtracted. This reduction or shift of the masses above the geoid causes a change in the Earth's potential called direct topographical effect (Hofmann-Wellenhof and Moritz, 2005). The resulting potential change changes the geoid to a co-geoid. Accordingly, the Stokes integration provides the co-geoid surface rather than the geoid. A correction term is applied to the co-geoid to obtain the true geoid which is called the indirect effect of the gravity reduction on the geoid height and is obtained from

$$N_{ind} = \frac{\delta V^t}{\gamma} . \quad (3.60)$$

The change in the gravity potential is equal to the change in the gravitational potential since no change occurs in the centrifugal potential due to the condensation. The indirect effect of the gravity reduction on the geoid is called also as primary indirect topographical effect (PITE). In order to convert the co-geoid into the geoid PITE needs to be accounted for. PITE does not exceed 2 meters worldwide and can be represented as follows:

$$\begin{aligned} N_{PITE} = \frac{\delta V^t}{\gamma} = & \frac{G}{\gamma_0} 4\pi\rho_0 \left(RH - \frac{H^2}{2} - \frac{r_t^3 - R^3}{3R} \right) \\ & + \frac{G}{\gamma} \rho_0 \iint_{\Omega'} \int_{r=R+H}^{R+H'} l^{-1}(R, \psi, r') r'^2 dr' d\Omega' - \frac{G}{\gamma} \rho_0 \iint_{\Omega'} \frac{r_t'^3 - r_t^3}{3} l^{-1}(R, \psi, R) d\Omega' \\ & + \frac{G}{\gamma} \iint_{\Omega'} \delta\rho \int_{r=R}^{R+H'} l^{-1}(R, \psi, r') r'^2 dr' d\Omega' - \frac{G}{\gamma} \iint_{\Omega'} \delta\rho \frac{r_t'^3 - r_t^3}{3} l^{-1}(R, \psi, R) d\Omega' \quad (3.61) \end{aligned}$$

This correction (Ellmann and Vaníček, 2007) can be investigated in two separate regions, namely near-zone and far-zone regions. The effect of the near-zone area includes the contribution of the topographical masses within the spherical radius of the cap size

whereas the effect of the far-zone area accounts for the effect of the topographical masses outside of this radius (Huang and Véronneau, 2005, Véronneau and Huang, 2007).

The PITE has also an indirect effect on gravity, which is called the secondary indirect topographical effect (SITE) (see equation 3.40) (Huang and Véronneau, 2005, Véronneau and Huang, 2007) and can be computed from

$$\Delta g_{SITE} = \frac{2}{r} \gamma N_{PITE}, \quad (3.62)$$

which has a cm level contribution to the geoid.

3.3.5. Error of the combined gravimetric geoid model

The accuracy level of a gravimetric geoid model developed by using heterogeneous datasets depends on the accuracy of the components used in the remove-compute-restore technique. The main contribution to the long-wavelength error is associated with the spherical harmonic coefficients. Insufficient accuracy, density and coverage of the terrestrial data cause the medium wavelength errors (Heck, 1990). Lastly, improperly modeled topography and gaps in terrain data are the main reason of the errors in the short wavelengths (Schwarz et al., 1987, Sideris and Forsberg, 1991).

The errors coming from the GGMs used to be considered as the largest. According to Yang (1998), the errors coming from the terrestrial gravity and terrain data were smaller and could be reduced by using denser and more accurate gravity and terrain data. Also modeling the topographic effect could be improved. This was the situation before the GRACE and GOCE missions were launched. With the development of the GRACE- and GOCE-based models, the errors coming from the GGMs are reduced and the errors from terrestrial gravity and DEM data have become dominant.

3.3.5.1. Errors due to GGM

GGM based errors occur due to insufficient satellite tracking data, lack of terrestrial data and systematic errors existing in satellite altimetry. The errors can be categorized in two groups as omission and commission errors. The omission error occurs due to the truncation of the spherical harmonic series expansion at some degree. This truncation

causes the terms above the maximum degree to be omitted, thus causing the omission error (Jekeli, 1979; de Min, 1990). The other major error is the commission error which occurs due to the noise existing in the potential coefficients themselves. The commission error increases as the maximum degree, n_{max} , of the spherical harmonic expansion increases whereas the omission error decreases.

The error contribution coming from the satellite-only and satellite-combined models to the geoid model can be expressed (Huang et al., 2007), respectively as

$$V_{SG} = \frac{R}{2\gamma} \sum_{n=2}^l \left(\frac{2}{n-1} + Q_n^{DB} \right) \varepsilon_n^{SG}, \quad (3.63)$$

and

$$V_{CG} = \frac{R}{2\gamma} \sum_{n=l+1}^{m_{CG}} Q_n^{DB} \varepsilon_n^{CG}. \quad (3.64)$$

where

ε_n^{SG} and ε_n^{CG} are the gravity errors coming from the satellite-only and combined GGMs, respectively and are obtained based on the error coefficients of the GGMs.

3.3.5.2. Errors due to terrestrial gravity anomalies

The errors originating from the terrestrial gravity anomalies are due to the errors in the gravity measurements, topographic reduction applied, gridding and interpolation of gravity values, DEM and the actual topographical density distribution (Huang et al., 2007). The error coming from the terrestrial data can be expressed by:

$$V_{TG} = \frac{R}{4\pi\gamma} \sum_{n=l+1}^{m_{CG}} S_{DB}(\psi) \varepsilon_n^{TG} \Delta\sigma', \quad (3.65)$$

where ε_n^{TG} is the gravity error coming from the terrestrial gravity data. This error is also affected by DEM.

Accurate gravity anomalies distributed evenly and densely over the entire region can provide higher accuracy. However, there are some systematic errors affecting the quality

of the gravity anomalies, as well. According to Heck (1990), the major error sources influencing gravity anomalies that cause both systematic and random errors in the absolute and relative geoidal heights are the inconsistencies in the gravity datum(s), vertical datum(s), horizontal datum(s), type of heights, and the approximation error based on the use of a simplified free-air reduction formula. The datum inconsistencies can influence the medium to long wavelength spectral components of the gravity field as well as the geoid. More details about the topic can be found in Heck (1990).

3.4. Validation of a Gravimetric Geoid Model

There are different methods used in the validation of gravimetrically determined geoid models. In this thesis, GNSS/leveling-derived geoid undulations and the latest official global and regional geoid models are used in the validation of the satellite-only models and the combined regional gravimetric geoid models. The gravimetric geoid models are evaluated at GPS/leveling benchmark points and compared with the GPS/leveling-derived geoid undulations. The GPS/leveling-derived geoid undulations are considered as independent and external datasets that one can use for the validation of a gravimetric geoid model only if the GPS/leveling results are not included in the gravimetric geoid model solution (Fotopoulous, 2003).

3.4.1. Simple outlier detection

Outlier detection is required to obtain more realistic results in the geoid validation. The differences between the GPS/leveling-derived and gravimetric geoid values are tested on the benchmark points to detect any outliers by using the 3-sigma technique. Residuals larger than 3 times the standard deviation of the misclosures $l = h_{GNSS} - H - N_{grav}$ are detected and removed from the data.

$$|l_i - \bar{l}| > 3\sigma, \quad (3.66)$$

where l_i is the misclosure computed at each point, \bar{l} is the mean value of the misclosures and σ is the standard deviation of the misclosures. This method has been used in the

previous studies (Fotopoulos, 2003; Erol, 2007). There are other methods which can be used to detect the outliers for more precise investigations.

3.4.2. Validation by using GNSS/leveling-derived geoid undulations in absolute and relative sense

The gravimetric geoid is compared with the GNSS/leveling-derived geoid on benchmark points in two ways. Firstly, each geoid undulation value on each benchmark from the gravimetric geoid model is compared with the GNSS/leveling-derived undulation. This process is performed for every single benchmark included in the analysis after the removal of the outliers. This type of comparison is called an absolute comparison and the formulation is given as

$$l_i = h_{GNSS(i)} - H_{(i)} - N_{grav(i)}, \quad (3.67)$$

or

$$l_i = N_{GNSS/leveling(i)} - N_{grav(i)}. \quad (3.68)$$

This method is used when comparing the combined gravimetric geoid models. Both the GPS/leveling and the gravimetric geoid undulations of the same point cover the entire spectrum bandwidth.

In the case when a satellite-only gravimetric geoid is validated, the GPS/leveling-derived geoid undulations need to be reduced to the same spectral content of the gravimetric geoid model. This is performed by low-pass filtering, e.g., by removing the EGM2008-predicted higher frequency geoid component (e.g., above the maximum degree n_{max} of the satellite only models) from the GPS/leveling-derived geoid undulations (Gruber, 2009).

This can be expressed as:

$$l_i = (N_{GNSS/Leveling} - N_{n_{max}+1}^{2190}) - N_{grav(i)}^{n_{max}}, \quad (3.69)$$

where $N_{n_{max}+1}^{2190}$ is predicted from EGM2008.

The second method of testing the gravimetric models is the relative accuracy assessment using the following equation:

$$\Delta l_{ij} = (N_{GNSS/Leveling(j)} - N_{GNSS/Leveling(i)}) - (N_{grav(j)} - N_{grav(i)}), \quad (3.70)$$

where i and j are the benchmark points in the network.

The relative accuracy assessments for baseline distances S_{ij} are computed in parts per million (ppm) as follows by:

$$\Delta l_{ij}^{rel} (ppm) = \frac{\Delta l_{ij} (mm)}{[S_{ij}]_{km}}, \quad (3.71)$$

where

$$S_{ij} = \sqrt{(x_j - x_i)^2 + (y_j - y_i)^2 + (z_j - z_i)^2}. \quad (3.72)$$

This type of assessment provides the relative geoid accuracy which excludes the common errors for each pair of benchmarks.

3.4.3. Geoid fitting to the GPS/leveling benchmarks

In practice, the $h_{GNSS} - H - N_{grav}$ is not zero because it contains the errors in the geoid itself and also the errors in the GPS and leveling measurements. Gross, random, and systematic errors in the three different height types affect the difference in the geoid undulations from the two independent sources. According to Huang and Véronneau (2005), the internal accuracy of the geoid undulation in Canada is generally worse than the accuracy of the ellipsoidal and orthometric heights and it ranges from 2 to 5 cm when the systematic errors in the leveling network are omitted.

The systematic datum differences between the gravimetric geoid and the GPS/leveling data, and possible long-wavelength errors of the geoid, are removed by applying a correction model. This helps to make the gravimetric geoid model fit better the GPS/leveling data. According to Forsberg and Madsen (1990), the long-wavelength errors can be reduced by constraining the gravimetric geoid solution to the GPS/leveling-

derived undulations, which is sometimes called geoid fitting to the GPS/leveling benchmarks. The hybrid model approach by Roman and Smith (2000) is an example for this application.

The discrepancies between the GNSS/leveling-derived geoid heights and the gravimetric geoid can be expressed as:

$$l_i = h_i - H_i - N_i = \mathbf{A}_i \mathbf{x} - v_i, \quad (3.73)$$

or

$$\mathbf{A} \mathbf{x} = (N_{GNSS/leveling} - N_{grav}) + \mathbf{v}, \quad (3.74)$$

where \mathbf{A} is the design matrix, \mathbf{x} is the vector of unknown parameters and \mathbf{v} is vector of unknown random errors coming from GPS and leveling observations and geoid itself.

Even though the choice of the appropriate parametric model $\mathbf{A} \mathbf{x}$ depends on the distribution, density and the quality of the data used, in this thesis, a simplified 4-parameter version of the usual 7-parameter similarly datum shift transformation model is used to derive the corrector surface model (Hofmann-Wellenhof and Moritz, 2005). It has also been used in previous tests of the Canadian geoid (Kotsakis and Sideris, 1999; Fotopoulos, 2003).

The 4-parameter model can be expressed as

$$\mathbf{A}_i \mathbf{x} = x_1 + x_2 \cos \varphi_i \cos \lambda_i + x_3 \cos \varphi_i \sin \lambda_i + x_4 \sin \varphi_i, \quad (3.75)$$

where the φ_i , λ_i are the latitude and longitude of a GNSS/leveling point. The design matrix of the 4-parameter model can be expressed as

$$\mathbf{A}_{m \times 4} = \begin{pmatrix} 1 & \cos \varphi_1 \cos \lambda_1 & \cos \varphi_1 \sin \lambda_1 & \sin \varphi_1 \\ \cdot & \cdot & \cdot & \cdot \\ \cdot & \cdot & \cdot & \cdot \\ \cdot & \cdot & \cdot & \cdot \\ 1 & \cos \varphi_{m-1} \cos \lambda_{m-1} & \cos \varphi_{m-1} \sin \lambda_{m-1} & \sin \varphi_{m-1} \\ 1 & \cos \varphi_m \cos \lambda_m & \cos \varphi_m \sin \lambda_m & \sin \varphi_m \end{pmatrix}. \quad (3.76)$$

The coefficients of the model can be obtained by least-squares from

$$\hat{\mathbf{x}} = (\mathbf{A}^T \mathbf{A})^{-1} \mathbf{A}^T \mathbf{l}, \quad (3.77)$$

and the adjusted residuals are calculated by

$$\hat{\mathbf{v}} = \mathbf{A} \hat{\mathbf{x}} - \mathbf{l}. \quad (3.78)$$

This process is performed for errorless data where unit covariance matrix is considered. This method is the one applied in this thesis.

If the covariance matrices were known for ellipsoidal heights, \mathbf{C}_h , from the adjustments of the GPS measurements, orthometric heights, \mathbf{C}_H , from the adjustments of leveling and for gravimetric geoidal heights, \mathbf{C}_N , computed by error propagation then the coefficients of the model could be obtained from

$$\hat{\mathbf{x}} = \left[\mathbf{A}^T (\mathbf{C}_h + \mathbf{C}_H + \mathbf{C}_N) \mathbf{A} \right]^{-1} \mathbf{A}^T (\mathbf{C}_h + \mathbf{C}_H + \mathbf{C}_N) \mathbf{l}. \quad (3.79)$$

The reader is referred to Kotsakis and Sideris (1999) and Fotopoulos (2003) for more details.

After the calculation of the adjusted residuals, a grid form is created by using interpolation techniques. A corrector surface for the gravimetric geoid can be computed by using the combination of the gridded residual values and adjusted values for the parameters \mathbf{x} .

Some scientists describe this procedure either as a correction or corrector surface, or as a conversion (Featherstone et al., 2010). In fact this procedure distorts or modifies the model to fit a GNSS/leveling defined vertical datum which also introduces some errors. Although it has a practical usage, it does not improve the geoid model but it minimizes the datum discrepancies (Featherstone et al., 2010).

CHAPTER 4

4. EVALUATION OF THE SATELLITE-ONLY GEOID SOLUTIONS

4.1. Introduction

In this chapter, the geoids obtained from the global geopotential models (GGMs) are assessed. The geoid undulations derived from the first and the second generation GOCE-only and GRACE and GOCE combined satellite-only solutions (ESA, 2010) are investigated by performing comparisons with the GPS/leveling-derived geoid undulations in Canada (40-84 °N, 50-150 °W), in the Great Lakes area (40-50 °N, 65-95 °W) and in the Rocky Mountains region (48-54 °N, 114-124 °W) in absolute and relative sense. In absolute agreement comparisons GGMs are expanded up to different spherical harmonic degree expansions from 90 to 250 and compared on the benchmarks with GPS/leveling-derived geoid undulations reduced to the same spectral band of the gravity field as the GGM obtained geoid undulations. These tests will dictate the choice of the truncation degree of the GGM used in the combined regional geoid solution given in next chapter.

4.2. Overview of the satellite gravity missions

The dedicated gravity satellite missions CHAMP, GRACE, and GOCE have contributed to a significant improvement of the gravity field determination. CHAMP and GOCE are used in static gravity field determination whereas GRACE is typically used in the determination of both the time variable gravity change and the static field.

For the improvement of our knowledge about the Earth's gravity field, the following four items should be taken care of in the satellite dedicated missions concept (Rummel et al., 2002):

- 1- Uninterrupted satellite tracking in three spatial dimensions.
- 2- Measurement or compensation of the effect of non-gravitational forces.
- 3- Orbit altitude as low as possible.

4- Measurement of gravity gradient (Rummel et al., 2002; GOCE, 2008).

At present, there are three techniques available:

SST-hl – Satellite-to-satellite tracking between high and low orbiting satellites. The orbits of the high-orbiting satellites such as GPS and GLONASS are assumed to be known accurately so that they provide highly accurate 3D position information, velocity and acceleration determination of the low Earth orbiting satellites (LEO) by using satellite-to-satellite tracking between high and low orbits.

SST-l - Satellite-to-satellite tracking between low orbiting satellites. This kind of observation is based on the satellite-to-satellite tracking between two low orbiting satellites. The principle is based on the line-of-sight measurement of the range, range rate or acceleration difference between two low-orbit satellites.

SGG - Satellite Gravity Gradiometry. This type of observation is based on gravity acceleration measurements observed in 3-D over the short baselines of a gradiometer.

- CHAMP worked based on SST-hl and satisfied criteria 1 and 2.
- GRACE works based on SST-l coupled with SST-hl and satisfies criteria 1, 2 and partially 4.
- GOCE works based on SGG coupled with SST-hl and satisfies all criteria (GOCE, 2008).

Brief descriptions of the specifications of these missions are given in the following sections.

4.2.1. CHAMP

The CHAMP (CHALLENGING Minisatellite Payload) mission was designed to measure the gravity and magnetic fields of the Earth. Due to the influence of the gravity field disturbances on the satellite's orbit, the analysis of the orbit data could provide information about the structure of the gravity field. Therefore, the information of the satellite position is the main observation used in the determination of the gravity field. CHAMP is based on satellite-to-satellite tracking in high and low orbits (SST-hl), since

the low-flying CHAMP satellite's orbit is determined by the high-flying GPS satellites. Moreover, to account for the non-gravitational forces acting on the satellite and its orbit, such as atmospheric drag, solar radiation, albedo, etc., an on-board accelerometer was placed onboard CHAMP (Reigber et al., 2003). CHAMP was launched on July 15, 2000, and the end of the mission was on September 19, 2010 after more than 10 years of observations. The specifications of CHAMP are summarized in Table 4.1 and an illustration of its concept is depicted in Figure 4.1.

Table 4.1: Specifications of the CHAMP mission (Rummel et al., 2002; GOCE, 2008; Pavlis, 2006).

Launch date	15.07.2000
Status	End of mission 19.09.2010
Orbit	Near circular, inclination 87°
Altitude (s)	454 km
Mission objectives	Gravity and Magnetic fields Atmospheric Limb Sounding Ionosphere Sounding
Instrumentation and tracking	3-axis STAR accelerometer GPS and SLR Altitude decayed from 450 km to 300 km

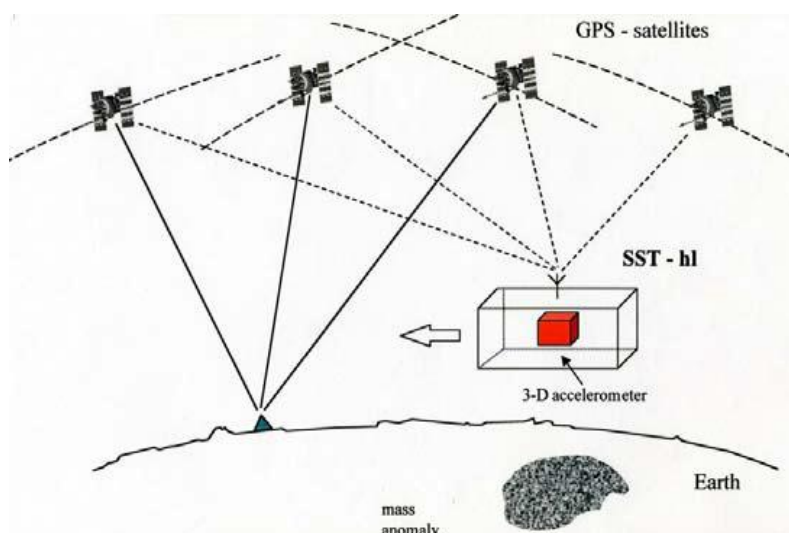


Figure 4.1: Concept of satellite-to-satellite tracking in high-low mode (SST-hl) for CHAMP (Rummel et al., 2002).

4.2.2. GRACE

GRACE (Gravity Recovery and Climate Experiment) has been designed as a twin satellite mission, which consists of two identical satellites following each other in the same orbit by a distance of about 200 km. The connection between the satellites to observe the relative motion (range, range-rate and range-acceleration) with high accuracy can be obtained via a microwave link by using the inter-satellite ranging systems installed in both satellites. The key measurement of GRACE is the K-band ranging system (Tapley and Reigbeir, 2004; Reigbeir et al., 2004); its purpose is to measure the dual one-way range between both satellites with a precision of about 1 μm . This principle of measuring gravity between satellites is known as low-low satellite-to-satellite tracking (SST-II). Both satellites carry a GPS receiver to measure their position and to enable observations between the high and low orbiting satellites (SST-hl). Moreover, the GRACE twin satellites are also equipped with an onboard accelerometer to account for non-gravitational forces (Rummel et al., 2002). GRACE was launched on March 17, 2002, and is still in service providing detailed measurements of the Earth's gravity field. These measurements are the temporal variations in the gravity field, such as seasonal and annual variations in groundwater and soil-moisture levels, and changes in the masses of the Arctic and Greenland ice sheets (Rummel et al., 2002). The specifications of GRACE are given in Table 4.2 and the principle of the GRACE mission is depicted in Figure 4.2.

Table 4.2: Specifications of the GRACE mission (Rummel et al., 2002; GOCE, 2008; Pavlis, 2006).

Launch date	17.03.2002
Status	Still in service
Orbit	Near circular, inclination 89°
Altitude (s)	485 km
Mission objectives	Gravity field and its temporal variation with a 400 km spatial and 10 days temporal resolution
Instrumentation, tracking	3-axis accelerometers GPS and SLR K-band inter-satellite ranging

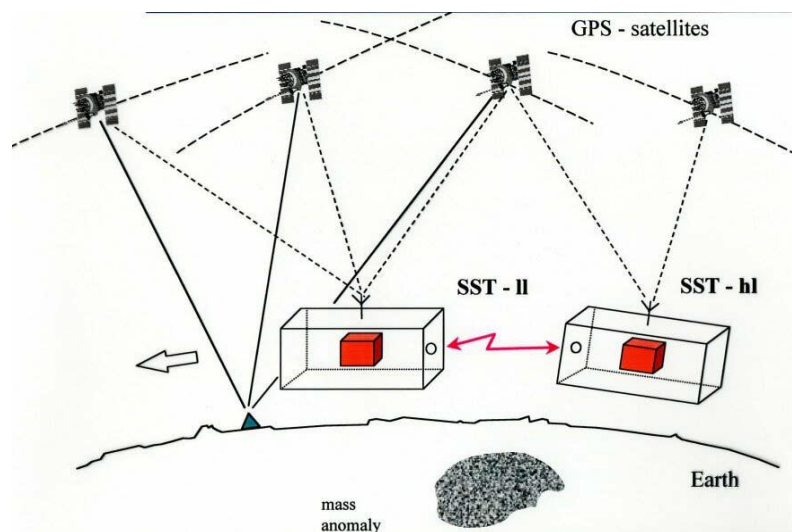


Figure 4.2: Concept of inter-satellite link (SST-II) coupled with SST-hl for GRACE (Rummel et al., 2002).

4.2.3. GOCE

GOCE (Gravity-field and steady-state Ocean Circulation Experiment) has been launched on March 17, 2009 for the purpose of developing high accuracy global models of the Earth's static gravity field. GOCE consists of an onboard gravity gradiometer and a GPS receiver. The Electrostatic Gravity Gradiometry (EGG or SGG) is included (Drinkwater et al., 2003) to derive the medium/short wavelength part of the gravity field whereas satellite-to-satellite tracking (SST) in high-low (hl) mode is used to determine the orbit and retrieve the long-wavelength part of the gravity field. In this sense, these techniques complement each other.

The three-axis EGG (see Figure 4.3) allows for measurements of the gravity gradients in all spatial directions. GOCE is the first gradiometric mission which was specifically designed for the determination of the stationary gravity field. The three gradiometers are located orthogonally to each other 50 cm apart; one aligned with the satellite's trajectory, one perpendicular to the trajectory and one pointing approximately towards the centre of the Earth. The precise position of the spacecraft obtained from the satellite-to-satellite tracking is used to derive the gravity information from orbit perturbation analysis. The

specifications of the GOCE are given in Table 4.3 and the concept of GOCE is illustrated in Figure 4.3.

Table 4.3: Specifications of the GOCE mission (Rummel et al., 2002; Drinkwater et al., 2003; GOCE, 2008).

Launch date	17.03.2009
Status	Still in service
Orbit	Sun synchronous orbit, inclination 96.7°
Altitude (s)	Initial altitude 270 km
Mission objectives	Determination of the gravity field (especially static) with an accuracy of 1 mGal and the geoid with an accuracy of 1cm, both with a spatial resolution of better than 100 km half-wavelength
Instrumentation, tracking	Six 3-axis accelerometers forming the gradiometer GPS/GLONASS and SLR

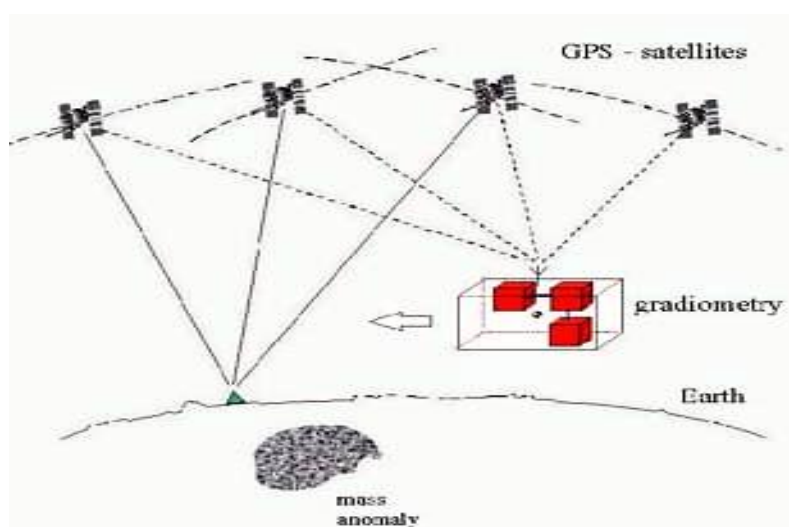


Figure 4.3: Schematic illustration of the combined electrostatic gravity gradiometer (EGG) and satellite-to-satellite (high-low) tracking (SST-hl) mission concepts (Rummel et al., 2002; GOCE, 2008).

The expected performances of the CHAMP, GRACE, and GOCE missions are illustrated in Figure 4.4 (Balmino et al., 1998). Representation of the error degree variance spectra of the gravity mission concepts SST-hl, SST-ll, and satellite gradiometry are depicted and

compared with one of the best currently available satellite gravity models (GMs) and with Kaula's degree variances of the gravity field (Rummel et al., 2002).

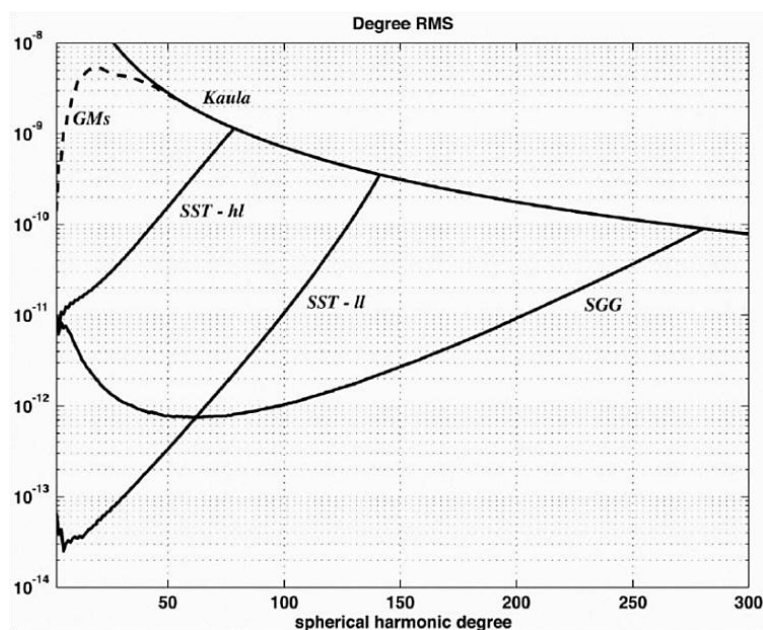


Figure 4.4: Expected performances of the satellite gravity missions (Rummel et al., 2002).

The high-slope of SST-II indicates that the any decrease or increase of the mission performance affects the spatial resolution very little where it has a large effect on its ability to resolve the temporal variations. The noise slope of SGG indicates that any increase in mission performance affects the temporal resolution very little but affects the ability to resolve the spatial resolution highly. In this sense GOCE and GRACE missions complement each other and CHAMP helps to make the current models more reliable (Rummel et al., 2002).

GOCE has been already used in many scientific applications, such as geodetic, sea level, ice, ocean, and solid Earth studies (see Figure 4.5) (Rummel et al., 2002; ESA, 2010). It is expected to improve our knowledge of the Earth's structure, ocean circulation, ice mass balance, and post glacial rebound. It is also expected to help in the development of a

unified height system (Drinkwater et al., 2003; ESA, 2010). A basic scheme which depicts the applications of GOCE in geosciences is given in Figure 4.5.

As discussed in section 2.5, a vertical datum can be defined by different methods but preferably, without using terrestrial gravity data in the computations. Instead, satellite-only models providing a global and unified coverage are recommended to compute a reference height surface. GOCE obtained models are expected to be used alone or combined with other satellite models (e.g., GRACE-based solutions) in the development of unified world height systems.

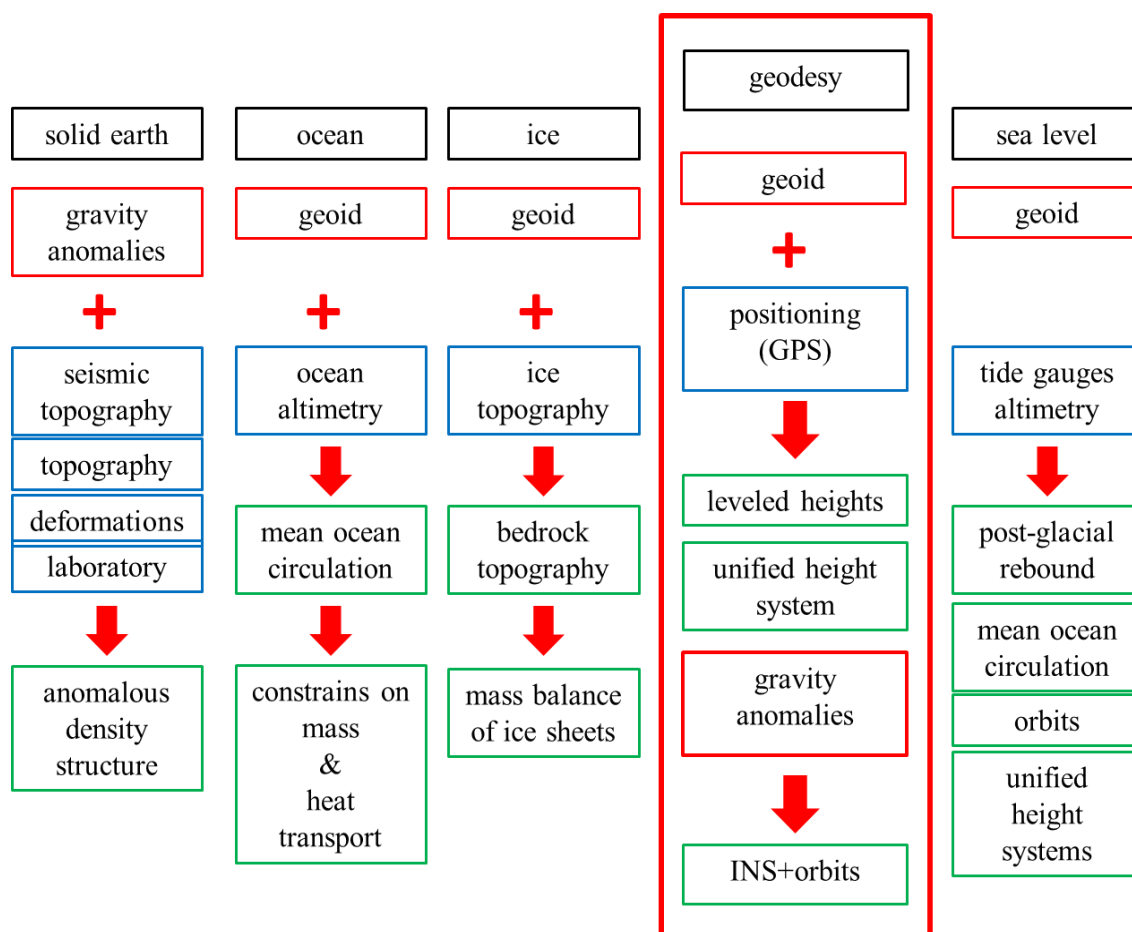


Figure 4.5: Overview of GOCE applications (ESA, 2010).

4.3. Investigations of the satellite-only global geopotential models

4.3.1. GOCE-based geopotential models

Since 2010, the first and the second generation GOCE global geopotential models have been released by the GOCE development team (ESA, 2010; 2011). They are shortly described in the following.

The first generation GOCE models were developed from the first two month observations cycle (November 2009 to January 2010) whereas the second generation GOCE models were created by using the first eight-month observations cycle (November 2009 to July 2010), (ESA, 2010; ICGEM, 2010). The three first generation GOCE-only models were developed by applying three different approaches: the direct-solution (Bruinsma et al., 2010), the time-wise (Pail et al., 2010a) and the space-wise (Migliaccio et al., 2010) approaches. The direct-solution approach requires starting with a background gravity field model and uses GOCE-reduced dynamic orbits and gradiometry as observation datasets. The time-wise approach starts with zero knowledge and uses only GOCE kinematic orbits and gradiometry as observation datasets. The space-wise approach starts with a priori knowledge for long-wavelengths and uses GOCE kinematic orbits and gradiometry as observation datasets. The second generation GOCE models were produced by the direct-solution and time-wise approaches only and space-wise solution is to be released later.

In this thesis, the first two letters of the names of the GOCE-only models are taken from the first letters of the applied approach and the last two digits denote the generation of the model. For example, the first generation direct solution GOCE model is named as DS01, whereas the second generation direct solution obtained model is called DS02. With the release of the first and the second generation GOCE-only models, ESA also made available the first and the second generation GRACE and GOCE combined satellite-only gravity models. These two models are named GOCO01S and GOCO02S.

DS01 represents the first generation GOCE-only gravity field model obtained by applying the direct-solution approach to spherical harmonic degree and order 240

(Bruinsma et al., 2010). DS01 is based on the hybrid GRACE and terrestrial data combined model EIGEN05-C (Förste et al., 2008). The EIGEN05-C was used as a background model for the polar gap stabilization (personal communication, Barthelmes, 2011) of the first generation GOCE direct solution model. DS01 has been proven to be a more accurate global gravity field model than the GRACE models for degrees 130-150 and up, but less accurate for the lower degrees (ESA, 2010; ICGEM, 2010).

The second first generation GOCE-only model TW01 was developed based on the time-wise approach up to spherical harmonic degree and order 224 (Pail et al., 2010a). No a-priori background model was applied to obtain this solution. Gradient, orbits, and altitude information are included as input data. The solution of TW01 is independent of any other gravity field data and can be combined with terrestrial data, satellite-only models or altimetry data (ESA, 2010; ICGEM, 2010).

The third first generation GOCE-only model, SW01 (Migliaccio et al., 2010) was developed by means of the space-wise approach up to degree and order 210 (ESA, 2010; ICGEM, 2010). For SW01, both satellite tracking data derived from the on-board GPS receiver and gravity gradients observed by the on-board electrostatic gradiometer were used. GOCE quick-look products (Pail et al., 2006) were used as a prior model to the SW01 (ESA, 2010; ICGEM, 2010).

The second generation GOCE-only models were created by using longer period satellite-observations. The direct and time-wise solution approaches were applied again to create the two second generation global gravity models. For DS02, the applied background model was the latest GRACE-only solution ITG-Grace2010s (Mayer-Guerr et al., 2010). This model was expanded up to maximum spherical harmonic degree 240, the same expansion degree as DS01.

TW02 (Pail et al., 2011) was developed as the second generation time-wise GOCE model and expanded up to spherical harmonic degree 250, which makes it a higher resolution model than the other GOCE-only models. TW02 was also created without applying any

background information. Moreover, like TW01, TW02 is also independent of any other gravity information.

In addition to the GOCE-only satellite models, the combined satellite-only gravity models from GRACE and GOCE, GOCO01S (Pail et al., 2010b) and GOCO02S (Goiginger et al., 2011) are also included in the study. In order to develop high accuracy and resolution static global gravity field models, the CHAMP, GRACE, GOCE, terrestrial gravity field, satellite altimetry and SLR data have been proposed to be combined.

GOCO01S is a first generation GRACE and GOCE combined satellite-only model. It was developed up to spherical harmonic degree 224 (Pail et al., 2010b) by using the first two-month GOCE observations with 7 years of GRACE GPS and K-band range rate data. Regularization was applied for the degrees between 170 and 224 by Kaula's rule (Kaula, 1966). According to Pail et al. (2010b), comparisons done with GPS/leveling data have shown that GRACE is the most important dataset to determine the low to medium degrees of the geoid whereas GOCE is a significant contributor for the degrees above 100, and even more effective beyond degree 150 in GOCO01S.

GOCO02S was developed from the eight-month GOCE observations cycle with 7 years of GRACE data, 8 years CHAMP data, and 12 months GOCE satellite-to-satellite tracking (SST-hl) data. Moreover, five years of SLR satellite data was included (Goiginger et al., 2011). The model was expanded up to spherical harmonic degree 250 and Kaula's rule was applied again for the regularization of the degrees between 180 and 250 (ESA, 2010; ICGEM, 2010).

Tables 4.4, 4.5, 4.6 and 4.7 summarize the specifications of the GOCE-only and GRACE and GOCE combined satellite-only models described above. The geopotential coefficients for each model can be downloaded from the ICGEM website (<http://icgem.gfz-potsdam.de/ICGEM>) freely. A sample of the geopotential coefficients and associated errors, \bar{C}_{nm} , \bar{S}_{nm} and $\sigma_{C_{nm}}$, $\sigma_{S_{nm}}$ can be found in Appendix A.

Table 4.4: First generation GOCE based models.

Model	Resolution in max. degree	Solution type	Data used	Reference
DS01	240	Direct solution, hybrid background model is applied	GOCE, (GRACE, CHAMP, G, A)	Bruinsma et al., 2010
TW01	224	Time-wise solution	GOCE	Pail et al., 2010a
SW01	210	Space-wise solution	GOCE EGM2008	Migliaccio et al., 2010
GOCO01S	224	Combined model	See Table 4.7	Pail et al, 2010b

Table 4.5: Second generation GOCE based models.

Model	Resolution in max. degree	Solution type	Data used	Reference
DS02	240	Direct solution, satellite-only background model is applied	GOCE GRACE	Bruinsma et al., 2010
TW02	250	Time-wise solution	GOCE	Pail et al., 2011
GOCO02S	250	Combined model	See Table 4.8	Goig. et al., 2011

Table 4.6: Specifications of the first generation GRACE and GOCE combined model, GOCO01S.

Data Type	Resolution in max. degree	Time span
ITG-Grace2010s	180	7 years
GOCE SGG	224	2 months
Kaula	170-224	-

Table 4.7: Specifications of the second generation GRACE and GOCE combined model, GOCO02S.

Data type	Resolution in max. degree	Time Span
ITG-Grace2010s	180	7 years
GOCE SST	11	12 months
GOCE SGG	250	8 months
CHAMP	120	8 years
SLR	5	5 years of 5 satellites
Kaula	180-250	-

The geoid signal and noise amplitudes of the first generation GOCE-only models and EGM2008, per degree and cumulatively are displayed in Figures 4.6 and 4.7, respectively.

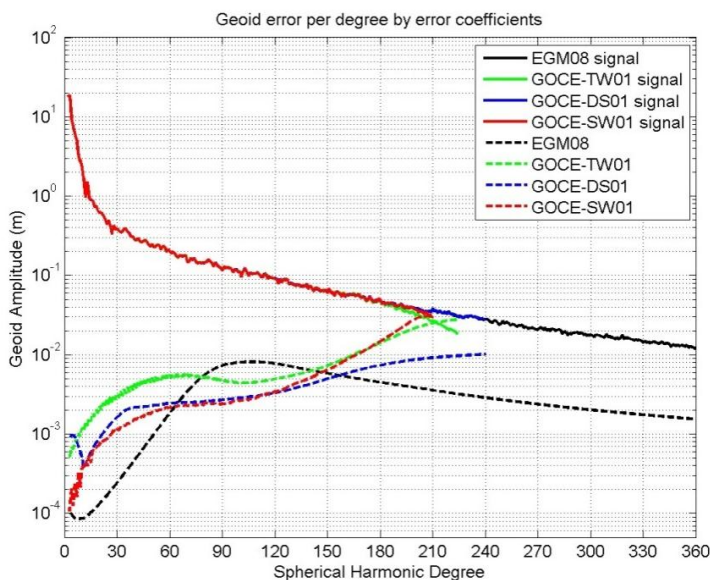


Figure 4.6: Geoid error per degree by error coefficients (Huang and Véronneau, 2010). The solid lines represent the geoid signal whereas the dashed lines illustrate the noise.

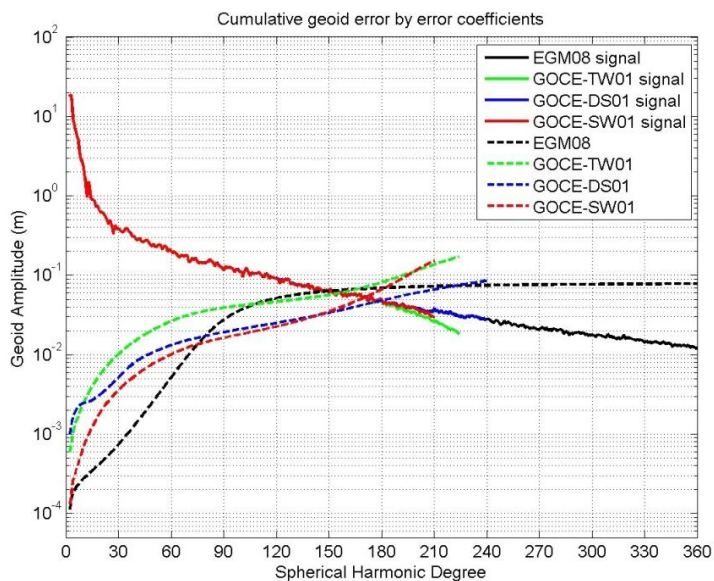


Figure 4.7: Cumulative geoid error by error coefficients (Huang and Véronneau, 2010). The solid lines represent the geoid signal whereas the dashed lines illustrate the noise.

The values are obtained from the potential coefficients and their associated errors thus Figures 4.6 and 4.7 represent the global behavior of the geopotential models and their errors. These refer to the internal accuracy of the global geoid models obtained from the associated error coefficients. Therefore, they may not represent the characteristics of the local study areas investigated in this thesis. Moreover, one needs to be cautious when doing comparisons of the geoid agreement with the independent datasets (e.g., GPS/leveling-derived geoid undulations) and internal accuracy assessments.

As one can easily notice, the amplitudes of the cumulative error and signal reach the same level and intersect at spherical harmonic degrees 160-180 as shown in Figure 4.7. The resolution of the model is determined by the intersection degree of the signal and noise spectral. Figure 4.7 shows that, EGM2008 has less noise for the lower degrees up to spherical harmonic degree around 70-80 because it was developed based on a GRACE solution. The three GOCE models follow similar behaviours with small deviations in the entire spectral band; in fact, for the degrees between 80 and 150-170 the GOCE models have lower level of noise than EGM2008. This can be used as an indicator that the GOCE models are capable of providing an improved solution globally compared to EGM2008 for degrees between 80 and 170.

GOCE's spatial resolution is approximately 80 km half wavelength. The overall predicted RMS of GOCE gravity field functionals (geoid undulations and gravity anomalies) for different corresponding resolutions (spherical harmonic degrees 20, 50, 100, 200 and 300) are given in Table 4.8. These are expected values predicted for the design of GOCE.

Table 4.8: Expected overall RMS errors of geoid heights and gravity anomalies at different resolutions for GOCE solutions (GOCE, 2008).

Spatial resolution (half-wavelength)	Maximum degree	Geoid height (mm)	Gravity anomaly (mGal)
1000 km	20	0.4	0.0006
400 km	50	0.5	0.001
200 km	100	0.6	0.03
100 km	200	2.5	0.08
65 km	300	~45	~2

In this thesis, most of the investigations on the satellite-only models are performed for different truncation degrees so that one can observe in which wavelength band GOCE improves the geoid in Canada and the two sub-regions. The RMS error in both the geoid height and gravity anomaly increases with the increase in the spherical harmonic degree due to the attenuation of the gravity signal by higher altitude. In other words, the satellite-only models provide accurate information only for the long and medium wavelength components of the gravity field and are not capable of providing accurate knowledge of the high-frequency components.

A first estimate of the commission error of one of the GOCE-derived models is obtained as follows. Geoid undulations are computed in grid form for two different expansions of the first generation time-wise GOCE model and compared with geoid model obtained from EGM2008 expanded up to the same two truncation degrees as the GOCE model. For example, the geoid undulations obtained from TW01 expanded up to spherical harmonic degree 150 is subtracted from the geoid obtained from EGM2008 expanded up to the same spherical harmonic degree 150. The same comparison is then performed up to degree 210. Figures 4.8 and 4.9 show the corresponding differences between these two models. As one can easily notice, the amplitude of the differences increases with the increasing truncation degree. In Figure 4.8, the range of the differences is from -0.205 m to 0.231 m with a mean value of 0.007 m. In Figure 4.9, the range is from -0.555 m to 0.611 m with a mean value of 0.002 m. These randomly distributed variations may not represent any meaningful geodetic or geophysical information but may indicate the increase of the commission error with degree.

In some areas, such as the Great Lakes area in Canada, higher resolution global models may not provide a better agreement with GPS/leveling-derived geoid undulations due to the increasing commission error. Accordingly, the selection of the appropriate truncation degree needs to be investigated. For example our previous investigations show that in the Great Lakes area EGM2008 derived geoid model expanded up to spherical harmonic degree 1440 shows the same level or better agreement with GPS/leveling-derived geoid undulations as EGM2008 geoid model expanded up to spherical harmonic degree 2190.

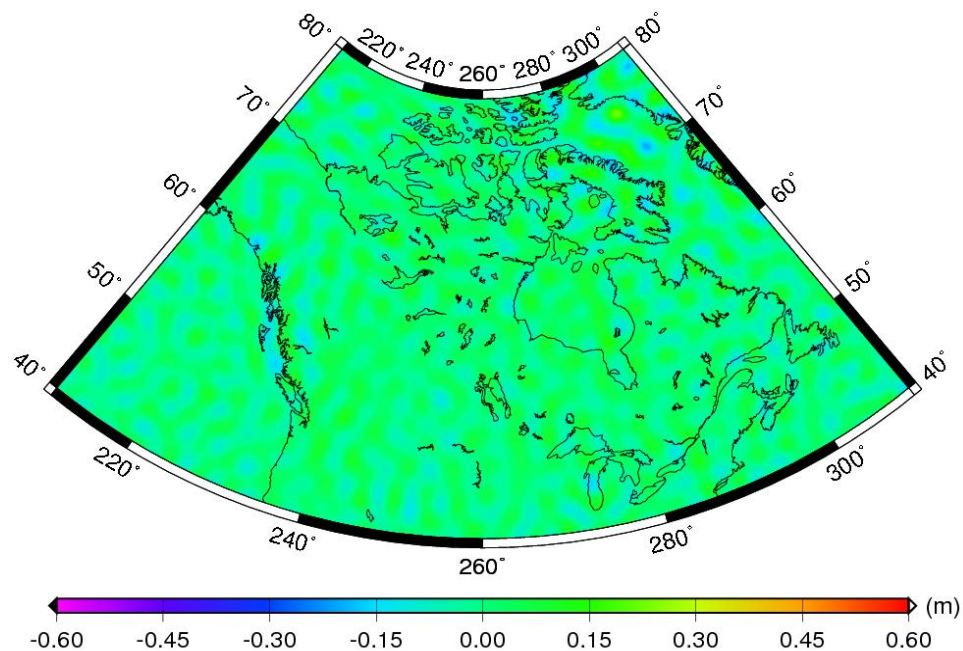


Figure 4.8: Differences, in m, in the geoid undulations obtained from EGM2008 and TW01 models both expanded up to spherical harmonic degree 150.

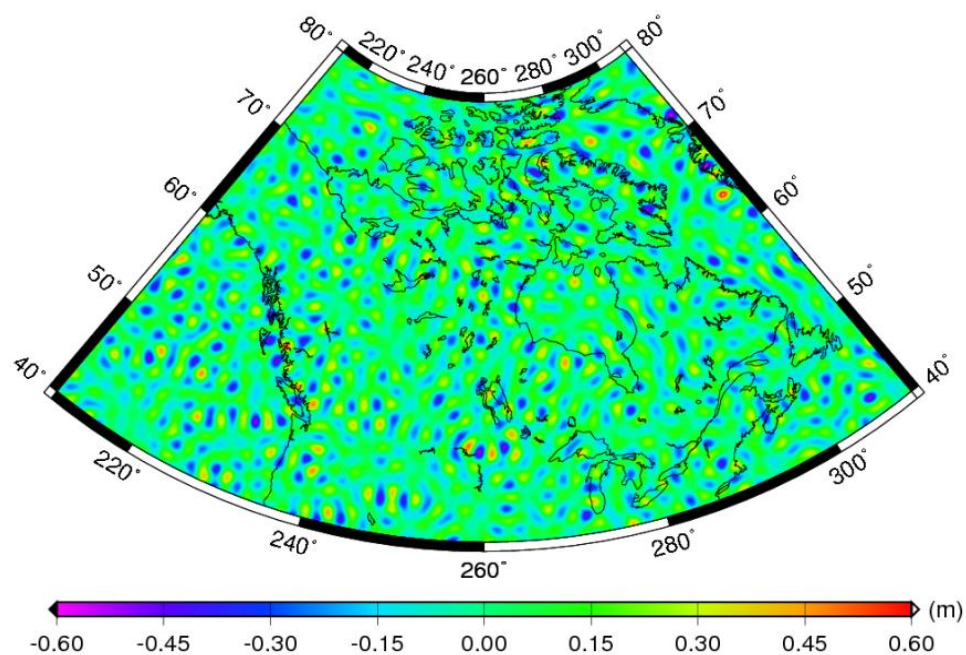


Figure 4.9: Differences, in m, in the geoid undulations obtained from EGM2008 and TW01 models both expanded up to spherical harmonic degree 210.

4.3.2. Assessment of the absolute agreement of the satellite-only geoid models

In this section, five GOCE-only and two GRACE and GOCE combined satellite-only solutions are investigated. These models are expanded up to different maximum spherical harmonic degrees, 90, 120, 150, 180, 210, 224, 240, and 250, in order to assess the behaviour of the GOCE solutions and any possible contribution of the GOCE models to the current geoids in Canada and the sub-regions at a certain spherical harmonic degree.

The geoids obtained from the seven different satellite-only solutions are assessed with the help of Canadian GPS/leveling-derived geoid undulations. In Canada, GPS/leveling measurements (see Figure 4.10) were collected over three decades (Huang and Véronneau, 2006). Besides the epoch differences among the measurements, different GPS equipment, such as single and double frequency receivers, the length of the observations, and the observing procedures cause the estimation accuracy of the ellipsoidal heights to vary (Véronneau and Huang, 2007). Their precision range varies from millimeters to 10 cm at 95% confidence level. In addition, there are some surveys where the accuracy is few decimeters, mainly due to the usage of single frequency receivers and mixed antenna types. Another error source is that the GPS observations have not been corrected for the effects of post glacial rebound. Overall in Canada, the accuracy of GPS measurements is stated around 4 cm (Véronneau and Huang, 2007).

In leveling data, there is an accumulation of systematic errors building up from the fundamental point in Rimouski ($48^{\circ} 28' N$, $68^{\circ} 29' W$), Québec, to the west coast of Canada. Moreover, Véronneau and Huang (2007) showed the accumulation of the systematic errors for different epochs as well. Precision of the height differences is generally better than a few mm and it increases systematically with the increasing distance from the fixed station in Rimouski. In national level the standard deviation of the leveling measurements is stated 8 cm (Véronneau and Huang, 2007). Besides these drawbacks, evidently most of the benchmarks are located in the southern part of the country and not accessible in the Northern part.

The investigations have been performed in entire country as well as in two sub-regions, the Great Lakes and Rocky Mountains areas outlined by red rectangles in Figure 4.10. These areas have a good coverage of GPS/leveling data compared to the rest of the country.

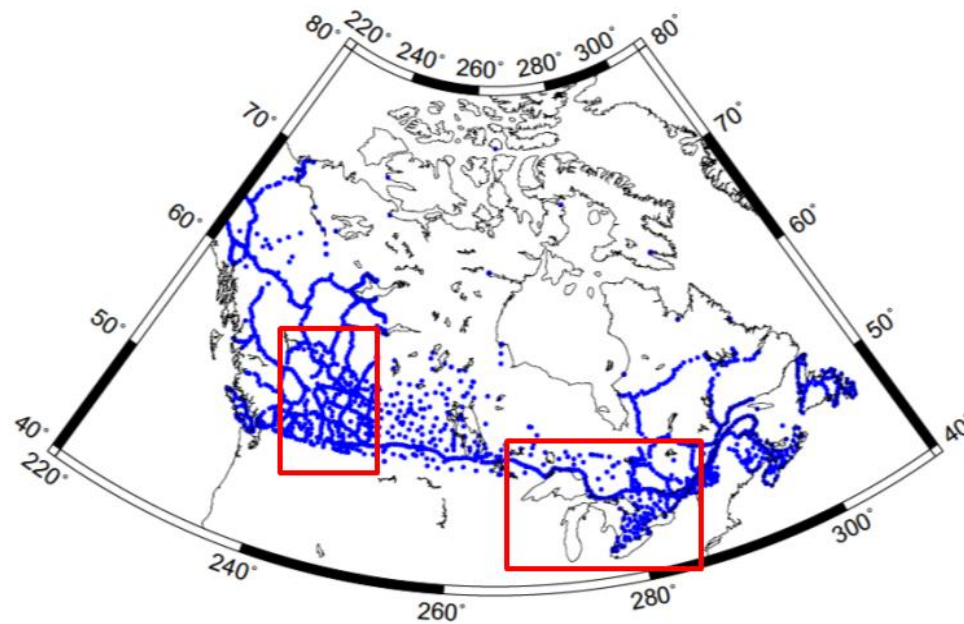


Figure 4.10: Distribution of the GPS/leveling benchmarks in Canada and the two sub-regions, the Great Lakes area and Rocky Mountains.

The first and the second generation GOCE-derived geoids are compared with the GPS/leveling-derived geoid undulations at the benchmark points. As mentioned, these comparisons are performed by expanding the GOCE solutions up to different spherical harmonic degrees. At this point, to perform a realistic and informative comparison, one needs to consider the omission error that is caused by the truncation of the global solutions. To ensure fair comparisons, the GPS/leveling-derived geoid undulations should also be reduced to the same spectral content of the gravimetric geoids. The description of the comparison methodology is given in Chapter 3.

According to this methodology, the gravimetric geoids truncated at different spherical harmonic degrees are compared with the GPS/leveling-derived geoid undulations that correspond to the same spectral interval of the gravity field. To achieve this, the contribution of the geoid undulation from spherical harmonic degree $n_{\max} + 1$ to 2190 is computed from EGM2008 and removed from the GPS/leveling-derived geoid heights.

The standard deviation (std) and root mean square (rms) values of the misclosures between the GPS/leveling-derived geoid undulations and the first generation GOCE geoid model undulations are depicted in Figures 4.11, 4.12 and 4.13 for Canada, the Great Lakes and the Rocky Mountains areas, respectively. The standard deviation of the misclosures is shown by solid colour-coded lines whereas the rms is shown with dashed lines.

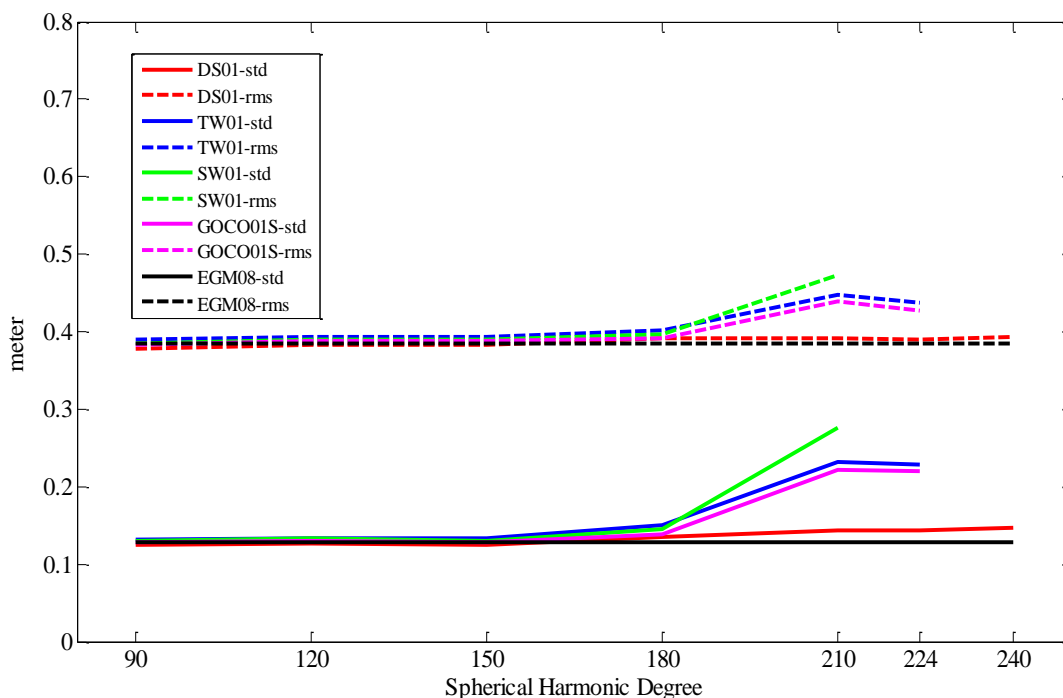


Figure 4.11: Standard deviations (std, solid) and root mean squares (rms, dashed) values of the differences in meter as functions of the spherical harmonic degree of the three first generation GOCE-only solutions (DS01, TW01, and SW01), the combined GRACE-GOCE model GOCO01S and EGM2008 with GPS/leveling-derived geoid undulations on 2579 benchmarks in Canada.

Although most of the GPS/leveling points are located in the southern part of the country, the models are investigated by making use of all 2579 GPS/leveling data points in Canada. In the Great Lakes and Rocky Mountains regions, 652 and 659 benchmark points are used, respectively.

Evidently, the statistics of the comparisons may change depending on the benchmarks chosen and the quality of the GPS/leveling datasets included in the evaluation. One may obtain better or worse agreement results by just changing the chosen GPS/leveling benchmarks included in the comparisons.

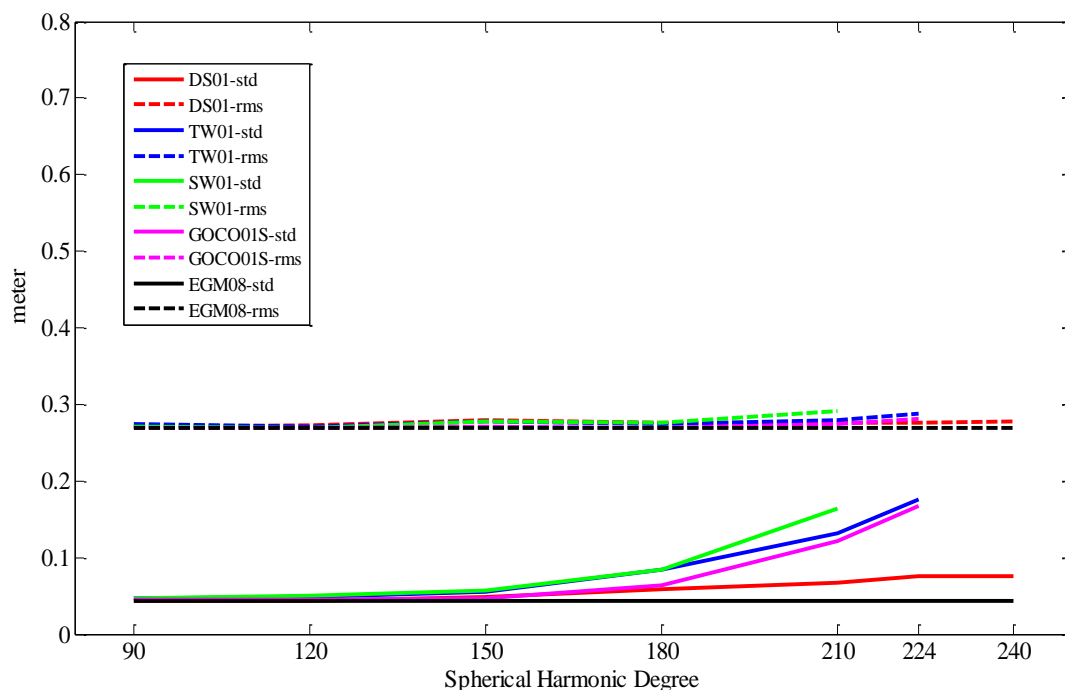


Figure 4.12: Standard deviations (std, solid) and root mean squares (rms, dashed) values of the differences in meter as functions of the spherical harmonic degree of the three first generation GOCE-only solutions (DS01, TW01, and SW01), the combined GRACE-GOCE model GOCO01S and EGM2008 with GPS/leveling-derived geoid undulations on 652 benchmarks in the Great Lakes area.

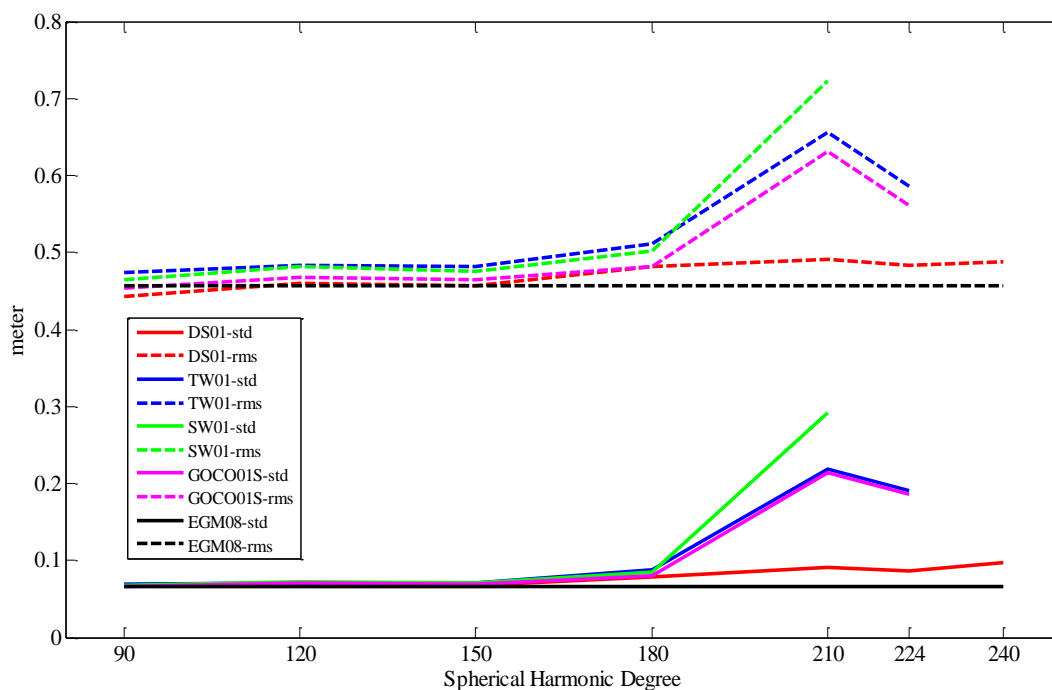


Figure 4.13: Standard deviations (std, solid) and root mean squares (rms, dashed) values of the differences in meter as functions of the spherical harmonic degree of the three first generation GOCE-only solutions (DS01, TW01, and SW01), the combined GRACE-GOCE model GOCO01S and EGM2008 with GPS/leveling-derived geoid undulations on 659 benchmarks in the Rocky Mountains.

In this thesis, the standard deviation is used as the main indicator of the agreement. As shown in the Figures 4.11 to 4.13 rms values are shifted from the standard deviations which mostly due to the bias resulting from the differences of the W_0 value adopted for the GOCE based geoid models and the geoid where the leveling measurements are referred to.

The statistics of the comparisons for the highest spherical harmonic degree expansions of the GOCE only, combined GRACE and GOCE satellite-only solutions and EGM2008 are given in Tables 4.9, 4.10 and 4.11 for Canada, the Great Lakes and Rocky Mountains areas, respectively. Since all the comparisons have been assessed under the same conditions to obtain quick interpretations of the model behaviours, outliers were not removed at this stage of the investigations.

Table 4.9: GPS/leveling differences, in m, of the highest expansions of GOCE solutions in Canada.

Model Degree	DS01 (240)	DS02 (240)	TW01 (224)	TW02 (250)	SW01 (210)	GOCO01S (224)	GOCO02S (250)	EGM08
max	-0.403	-0.140	-0.359	-0.304	-0.217	-0.365	-0.290	-0.423
min	-1.477	-1.824	-1.526	-1.974	-1.612	-1.524	-1.980	-1.433
mean	-0.910	-0.917	-0.939	-0.933	-0.965	-0.932	-0.930	-0.905
std	0.147	0.231	0.228	0.224	0.276	0.220	0.223	0.127
rms	0.922	0.946	0.967	0.959	1.003	0.958	0.956	0.914

Table 4.10: GPS/leveling differences, in m, of the highest expansions of GOCE solutions in the Great Lakes area.

Model Degree	DS01 (240)	DS02 (240)	TW01 (224)	TW02 (250)	SW01 (210)	GOCO01S (224)	GOCO02S (250)	EGM08
max	-0.495	-0.238	-0.390	-0.325	-0.217	-0.440	-0.353	-0.490
min	-1.015	-1.321	-1.239	-1.298	-1.302	-1.234	-1.288	-0.967
mean	-0.804	-0.785	-0.799	-0.804	-0.805	-0.794	-0.800	-0.799
std	0.076	0.192	0.175	0.163	0.164	0.167	0.159	0.044
rms	0.806	0.808	0.819	0.820	0.822	0.811	0.816	0.800

Table 4.11: GPS/leveling differences, in m, of the highest expansions of GOCE solutions in the Rocky Mountains.

Model Degree	DS01 (240)	DS02 (240)	TW01 (224)	TW02 (250)	SW01 (210)	GOCO01S (224)	GOCO02S (250)	EGM08
max	-0.590	-0.140	-0.509	-0.377	-0.454	-0.505	-0.348	-0.729
min	-1.300	-1.824	-1.497	-1.518	-1.612	-1.497	-1.520	-1.258
mean	-1.013	-1.014	-1.100	-1.058	-1.219	-1.074	-1.054	-0.985
std	0.097	0.190	0.191	0.175	0.291	0.186	0.178	0.066
rms	1.018	1.032	1.116	1.073	1.253	1.090	1.069	0.987

According to Figures 4.11, 4.12 and 4.13, and Tables 4.9 to 4.11, GPS/leveling comparisons suggest a geoid agreement of 14.7 cm to 27.6 cm for the highest expansions of GOCE-only models in Canada, and 7.6 cm to 17.5 cm and 9.7 cm to 29.1 cm for the

Great Lakes area and the Rockies, respectively (see Tables 4.9, 4.10 and 4.11 highlighted). One need to remember that these comparison results given in Tables 4.9, 4.10 and 4.11 contain both the GPS/leveling errors and the model commission errors. Statistics of the geoid height differences for each expansion degree (90, 120, 150, 180, 210, 224, 240, and 250) of the first and the second generation GOCE-only and GRACE and GOCE combined satellite-only solutions as well as one of the latest GRACE-only solutions are shown in Figures 4.14, 4.15 and 4.16 and given in Tables 4.12 to 4.14 for Canada, the Great Lakes area and the Rocky Mountains, respectively.

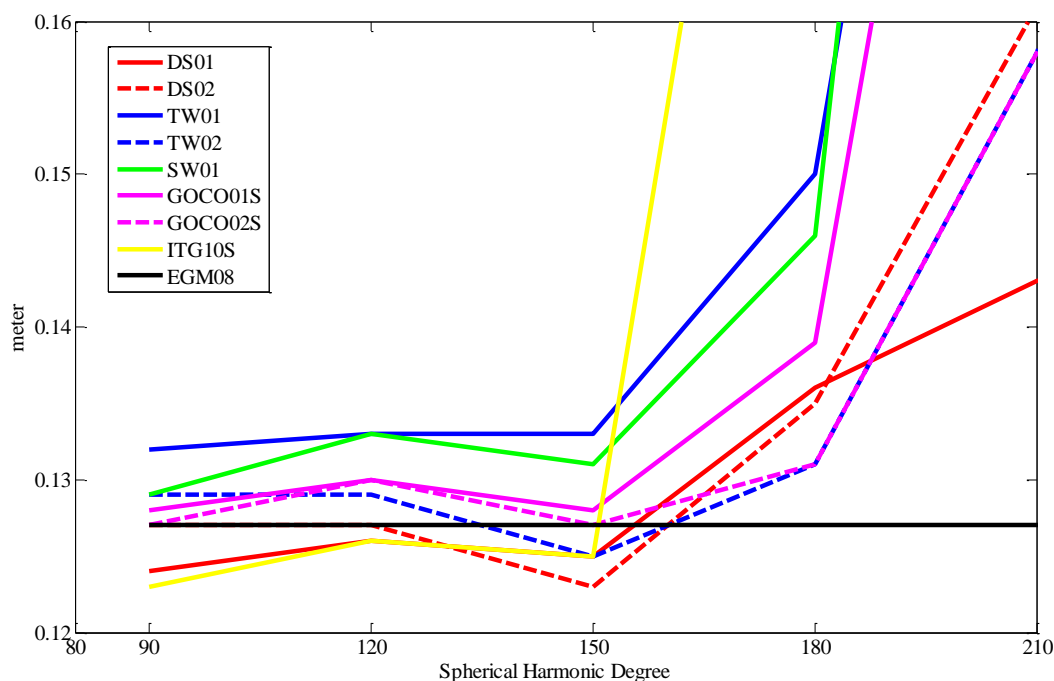


Figure 4.14: Standard deviations of the differences in meter as a function of the spherical harmonic degree of the three first, two second generation GOCE-only solutions (DS01, TW01, SW01, DS02, and TW02), the combined GRACE-GOCE models GOCO01S and GOCO02S, the latest GRACE-only model ITG10S and EGM2008 with the GPS/leveling-derived geoid undulations on 2579 benchmarks in Canada.

Figure 4.14 shows the comparison results in Canada for the first and the second generation GOCE-only and GOCE-GRACE combined satellite-only models, the latest GRACE-only model and the latest global gravity field model EGM2008. DS01 shows

better agreement than the other GOCE-only models up to spherical harmonic degree about 120 and follows ITG10S closely up to about degree 150. DS02 shows better agreement than any other model starting from degree about 130 to 160. TW02's agreement is much better than TW01's in any wavelength interval due to the longer GOCE observation cycles used in its development. It is also shown that the ITG10S's agreement with GPS/leveling-derived geoid undulations is better than the rest of the models starting from degree about 90 to 120. Moreover, GOCO02S is better than GOCO01S especially for the higher degree components where the components are obtained from GOCE-only data. SW01 also shows slightly better comparison results than TW01; therefore, its agreement with GPS/leveling-derived geoid undulations is worse than all the other models. According to these results, currently available and upcoming GOCE models are expected to improve EGM2008 geoid model in Canada.

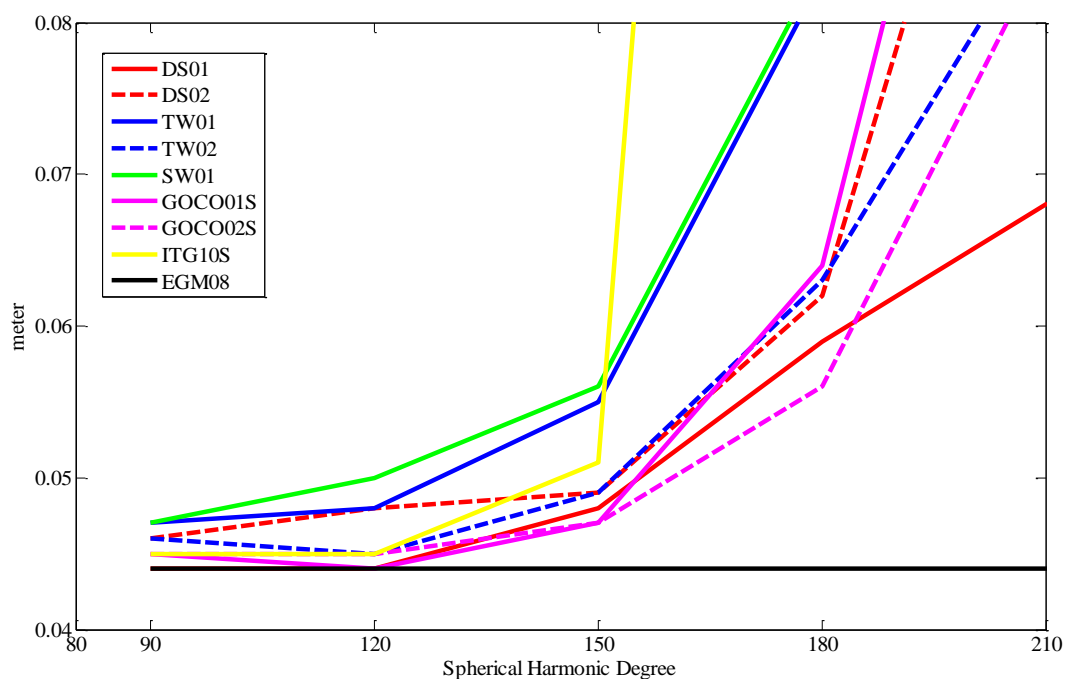


Figure 4.15: Standard deviations of the differences in meter as a function of the spherical harmonic degree of the three first, two second generation GOCE-only solutions (DS01, TW01, SW01, DS02, and TW02), the combined GRACE-GOCE models GOCO01S and GOCO02S, and the EGM08 geoid model.

GOCO02S, the latest GRACE-only model ITG10S and EGM2008 with the GPS/leveling-derived geoid undulations on 652 benchmarks in the Great Lakes area.

Figure 4.15 shows the similar results for the Great Lakes area. In this region EGM2008 shows the best agreement with GPS/leveling-derived geoid undulations in any wavelength interval. In general, the second generation GOCE-based models provide better agreement with the GPS/leveling-derived geoid undulations than the first generation ones (except direct solution models). It is also shown that the GRACE-GOCE combined models provide better agreement than the GOCE-only or GRACE-only models for the lower degree components and GOCO02S's agreement is better than all the other models above spherical harmonic degree about 150 to 180-190.

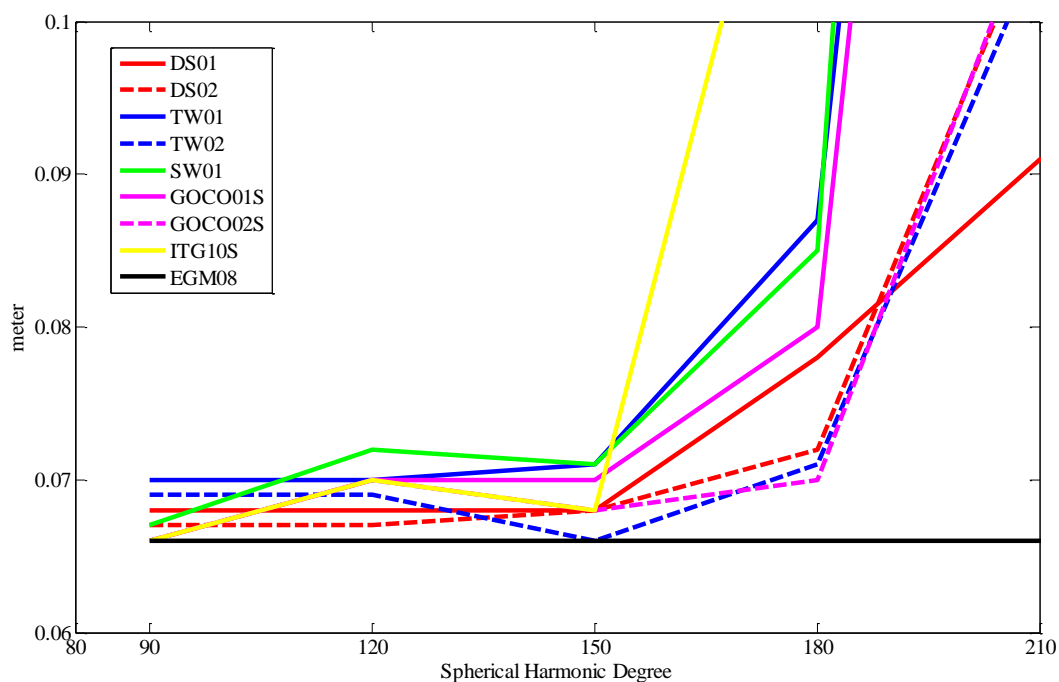


Figure 4.16: Standard deviations of the differences in meter as a function of the spherical harmonic degree of the three first, two second generation GOCE-only solutions (DS01, TW01, SW01, DS02, and TW01), the combined GRACE-GOCE models GOCO01S and GOCO02S, the latest GRACE-only model ITG10S and EGM2008 with the GPS/leveling-derived geoid undulations on 659 benchmarks in the Rocky Mountains.

Figure 4.16 shows the same comparison results for the Rocky Mountains region. EGM2008 shows the best agreement with the GPS/leveling-derived geoid undulations in any wavelength interval also in this region. Again, the second generation GOCE-based models provide better agreements than the first generation models. It is also shown that in the wavelength interval starting from around 135 to 170, TW02 shows better agreement than the GOCE-only, GRACE-only and as well as GRACE-GOCE combined satellite-only models. According to these results, GOCE models are not expected to contribute to the EGM2008 geoid model in this area significantly. The details of the statistics of the Figures 4.14, 4.15 and 4.16 can be found in Tables 4.12, 4.13, and 4.14, for Canada, the Great Lakes region and Rocky Mountains, respectively.

Table 4.12a shows the test results of the agreement of GOCE-only models with GPS/leveling-derived geoid undulations in Canada whereas Tables 4.13a and 4.14a show the statistics of the same test results for the Great Lakes and the Rocky Mountains areas, respectively. These results indicate that the GOCE models agree with each other closely up to spherical harmonic degree 150-180.

The results of the GRACE-GOCE combined models are given in Tables 4.12b, 4.13b and 4.14b for Canada, the Great Lakes area and the Rocky Mountains, respectively. These two models are compatible with each other and GOCE-only models up to spherical harmonic degree about 150 in the three areas. GOCO02S provides better agreement especially after spherical harmonic degree around 150.

Tables 4.12c, 4.13c and 4.14c show the results of the latest two of the GRACE-only models, GGM03S and ITG2010S. These two models are included to provide a good contrast to the GOCE-only and GRACE-GOCE combined satellite-only models. The GRACE-only models are compatible with each other in all expansion degrees and compatible with GOCE-only models up to degree about 150.

Finally, Tables 4.12d, 4.13d and 4.14d show the agreement of the EGM2008 model with GPS/leveling-derived geoid undulations in the three areas. Since the omission error removed from the GPS/leveling-derived geoid undulations is predicted by using

EGM2008 coefficients, EGM2008 comparisons with GPS/leveling-derived geoid undulations show a constant behaviour in all the three regions.

Table 4.12a: GPS/leveling differences, in m, of the different expansions of the GOCE-only solutions in Canada.

DS01	90	120	150	180	210	224	240	
max	-0.424	-0.427	-0.489	-0.465	-0.421	-0.432	-0.403	
min	-1.401	-1.389	-1.357	-1.460	-1.484	-1.463	-1.477	
mean	-0.899	-0.905	-0.905	-0.911	-0.911	-0.909	-0.910	
std	0.124	0.126	0.125	0.136	0.143	0.143	0.147	
rms	0.908	0.913	0.914	0.921	0.922	0.920	0.922	
DS02	90	120	150	180	210	224	240	
max	-0.435	-0.397	-0.440	-0.248	-0.343	-0.288	-0.140	
min	-1.423	-1.422	-1.380	-1.472	-1.447	-1.554	-1.824	
mean	-0.902	-0.903	-0.899	-0.902	-0.904	-0.896	-0.917	
std	0.127	0.127	0.123	0.135	0.161	0.181	0.231	
rms	0.911	0.912	0.907	0.912	0.918	0.914	0.946	
TW01	90	120	150	180	210	224		
max	-0.417	-0.417	-0.473	-0.411	-0.367	-0.359		
min	-1.429	-1.437	-1.376	-1.491	-1.577	-1.526		
mean	-0.910	-0.913	-0.914	-0.919	-0.950	-0.939		
std	0.132	0.133	0.133	0.150	0.232	0.228		
rms	0.920	0.923	0.924	0.931	0.978	0.967		
TW02	90	120	150	180	210	224	240	250
max	-0.431	-0.416	-0.444	-0.381	-0.359	-0.362	-0.307	-0.304
min	-1.441	-1.434	-1.394	-1.451	-1.458	-1.579	-1.806	-1.974
mean	-0.910	-0.911	-0.909	-0.911	-0.920	-0.910	-0.930	-0.933
std	0.129	0.129	0.125	0.131	0.158	0.174	0.216	0.224
rms	0.919	0.921	0.917	0.921	0.933	0.926	0.955	0.959
SW01	90	120	150	180	210			
max	-0.443	-0.437	-0.474	-0.468	-0.217			
min	-1.420	-1.408	-1.368	-1.444	-1.612			
mean	-0.905	-0.910	-0.910	-0.9142	-0.965			
std	0.129	0.133	0.131	0.146	0.276			
rms	0.914	0.919	0.919	0.926	1.003			

Table 4.13a: GPS/leveling differences, in m, of the different expansions of the GOCE-only solutions in the Great Lakes area.

DS01	90	120	150	180	210	224	240	
max	-0.511	-0.480	-0.501	-0.491	-0.492	-0.474	-0.495	
min	-0.966	-0.944	-0.944	-0.999	-1.017	-1.017	-1.015	
mean	-0.799	-0.801	-0.807	-0.804	-0.803	-0.803	-0.804	
std	0.044	0.044	0.048	0.059	0.068	0.076	0.076	
rms	0.801	0.802	0.809	0.806	0.806	0.807	0.808	
DS02	90	120	150	180	210	224	240	
max	-0.508	-0.499	-0.526	-0.543	-0.420	-0.288	-0.238	
min	-0.970	-0.949	-0.946	-1.012	-1.123	-1.258	-1.321	
mean	-0.797	-0.795	-0.798	-0.800	-0.789	-0.782	-0.785	
std	0.046	0.048	0.049	0.062	0.111	0.146	0.192	
rms	0.798	0.797	0.800	0.802	0.797	0.795	0.808	
TW01	90	120	150	180	210	224		
max	-0.532	-0.526	-0.568	-0.541	-0.472	-0.390		
min	-0.981	-0.967	-1.015	-1.060	-1.210	-1.239		
mean	-0.803	-0.800	-0.806	-0.801	-0.799	-0.800		
std	0.047	0.048	0.055	0.083	0.132	0.175		
rms	0.804	0.801	0.808	0.805	0.810	0.819		
TW02	90	120	150	180	210	224	240	250
max	-0.511	-0.502	-0.552	-0.554	-0.515	-0.411	-0.410	-0.325
min	-0.975	-0.949	-0.996	-1.042	-1.073	-1.115	-1.241	-1.298
mean	-0.802	-0.798	-0.803	-0.807	-0.801	-0.796	-0.794	-0.804
std	0.046	0.045	0.049	0.063	0.087	0.118	0.152	0.163
rms	0.803	0.800	0.805	0.810	0.806	0.804	0.808	0.820
SW01	90	120	150	180	210			
max	-0.523	-0.508	-0.548	-0.578	-0.217			
min	-0.979	-0.946	-0.990	-1.037	-1.302			
mean	-0.800	-0.798	-0.805	-0.802	-0.805			
std	0.047	0.050	0.056	0.084	0.164			
rms	0.801	0.800	0.807	0.806	0.822			

Table 4.14a: GPS/leveling differences, in m, of the different expansions of the GOCE-only solutions in the Rocky Mountains.

DS01	90	120	150	180	210	224	240	
max	-0.708	-0.720	-0.713	-0.659	-0.647	-0.655	-0.590	
min	-1.261	-1.250	-1.250	-1.262	-1.304	-1.297	-1.300	
mean	-0.970	-0.987	-0.984	-1.009	-1.017	-1.010	-1.013	
std	0.068	0.068	0.068	0.078	0.091	0.086	0.097	
rms	0.972	0.989	0.986	1.012	1.021	1.013	1.018	
DS02	90	120	150	180	210	224	240	
max	-0.712	-0.713	-0.670	-0.692	-0.630	-0.491	-0.140	
min	-1.267	-1.254	-1.267	-1.236	-1.355	-1.479	-1.824	
mean	-0.973	-0.976	-0.956	-0.972	-0.988	-0.954	-1.014	
std	0.067	0.067	0.068	0.072	0.107	0.137	0.190	
rms	0.976	0.978	0.958	0.974	0.994	0.964	1.032	
TW01	90	120	150	180	210	224		
max	-0.741	-0.743	-0.738	-0.699	-0.574	-0.509		
min	-1.298	-1.299	-1.311	-1.267	-1.471	-1.497		
mean	-1.001	-1.010	-1.009	-1.038	-1.166	-1.100		
std	0.070	0.070	0.071	0.087	0.218	0.191		
rms	1.003	1.013	1.012	1.041	1.186	1.116		
TW02	90	120	150	180	210	224	240	250
max	-0.739	-0.744	-0.702	-0.719	-0.703	-0.550	-0.428	-0.377
min	-1.293	-1.280	-1.286	-1.253	-1.334	-1.389	-1.490	-1.519
mean	-0.997	-1.003	-0.985	-0.994	-1.034	-0.986	-1.063	-1.058
std	0.069	0.069	0.066	0.071	0.105	0.126	0.172	0.175
rms	0.999	1.005	0.987	0.997	1.039	0.994	1.077	1.073
SW01	90	120	150	180	210			
max	-0.738	-0.743	-0.735	-0.701	-0.454			
min	-1.272	-1.283	-1.307	-1.255	-1.612			
mean	-0.993	-1.010	-1.003	-1.029	-1.219			
std	0.067	0.072	0.071	0.085	0.291			
rms	0.995	1.012	1.006	1.032	1.253			

The tests have shown good comparisons of the first and the second generation GOCE-only, GOCE and GRACE combined satellite-only models, two of the latest GRACE-only models and as well as EGM2008 global geoid model. The change with respect to EGM2008 by using a satellite model is caused by the replacement of the EGM2008 spectral components with the counterpart components of the satellite models. In principle, a higher-accuracy satellite-model reduces the EGM2008 commission error; this leads to a better agreement in the GPS/Leveling comparison and vice versa. EGM2008 was developed by using GRACE observations for the lower degrees and terrestrial data for the higher degree components. The GOCE geoid models obtained from their respective maximum degrees can be compared to EGM2008 expanded up to the same spherical harmonic degrees.

In general, DS01 follows EGM2008 closer due to the GRACE-combined hybrid background model that it is referred to. Even though this background model is applied only to fill the polar gaps, the comparisons performed with DS02 where the background model is satellite-only solution verifies that the datasets used for the polar areas affect not only the regions applied but the entire global model (Personal communication, Barthelmes, 2011).

TW01 and SW01 follow each other closely in all the wavelength intervals. In all the regions TW02 shows better agreement with GPS/leveling-derived geoid undulations than TW01. GOCO01S follows TW01 closely with a slight deviation and shows a slightly better agreement with GPS/leveling-derived geoid while GOCO02S shows better agreement than GOCO01S.

As expected, in the Rocky Mountains the standard deviation of the misclosures is larger than the other areas due to the rough topography. In general, the standard deviations of the misclosures show a stable behaviour up to degree 150, and after spherical harmonic degree 150 they start showing a rapid increase due to the increasing commission error.

None of these satellite models show any significant improvement over EGM2008 for each of the regions. Canadian terrestrial data have contributed to EGM2008 from

spherical harmonic degree 90 to 2190. Thus, this information may indicate that the GOCE models generally agree with the terrestrial data within the spectral band of 90 to 150, and beyond 150.

4.3.3. Assessment of the relative agreement of the geoid models

For the evaluation of the relative agreement of the gravimetric geoid models with the GPS/leveling data, relative differences are computed for the maximum spherical harmonic expansions of the first generation GOCE-only models and EGM2008 and plotted against baseline distances. The baseline distances are computed with an increment of 20 km among all GPS/leveling stations and the geoid height differences are computed for all baselines composed between the GPS/leveling points.

In Figures 4.17 to 4.19, the comparisons of the relative geoid undulation accuracy are plotted. It is obvious that EGM2008's relative accuracy is significantly better than the satellite-only models due to the contribution of the surface gravity data. As indicated in the previous paragraph, these investigations have been performed for the maximum available spherical harmonic expansions of the GOCE models. Our results show that the GOCE models show similar behavior with each other. However, relative agreements of the models are shifted with respect to each other which possibly are due to the different maximum spherical harmonic expansion degrees and existing systematic errors in the spherical harmonic coefficients representing the medium-wavelength part of the tested models. DS01 was expanded up to spherical harmonic degree 240 whereas TW01 and SW01 were expanded up to spherical harmonic degree 224 and 210, respectively. Accordingly, the omission error as well as the commission error need to be considered in these comparisons.

In Canada, the statistics are computed using all 2579 benchmarks. EGM2008 shows a relative geoid agreement of 0.1 to 2 ppm which corresponds to 2.9 to 10 cm over baselines of 20 to 800 km. The first generation GOCE-only models show a relative agreement of 0.4 to 20.3 ppm which corresponds to 25 to 81 cm in Canada. The relative errors of the GOCE models show a slowly increasing trend with decreasing baseline until

200 km where a very sharp increase starts. This disproportional increase indicates the fast deterioration of the GOCE models for baselines shorter than 200 km due to the limited satellite resolution.

For the Great Lakes area, EGM2008 shows a relative agreement of 0.06 to 2.02 ppm which corresponds to 3 to 5 cm for baselines of 20 to 800 km. The results change to 0.35 to 8.7 ppm corresponding to 11.5 to 49.5 cm relative agreement with the GOCE models for the same region. Although the GOCE relative errors show the same trend in the Great Lakes as for the entire Canada, the performance is generally better for short baselines because of the flat topography and the smoother gravity field.

For the Rockies, due to the rough topography, the relative agreement is poorer. EGM2008 shows 0.07 to 2 ppm relative agreement corresponding to 2.8 to 14 cm for the baselines from 20 to 800 km. GOCE-only models show 0.4 to 21 ppm corresponding to 29 to 125 cm relative agreement.

The results of the relative agreements are summarized in Table 4.15. These assessments have also been performed for the second generation GOCE-only models. However, since they do not provide any significant improvement over the first generation GOCE-only models in terms of the relative agreement of the geoid models they are not shown in the figures to avoid complication.

Table 4.15: The statistics of the relative agreement over baseline distances 20km to 800km.

Models	Canada		Great Lakes		Rocky Mountains	
	cm	ppm	cm	ppm	cm	ppm
EGM2008	2.9-10	0.1-2	3-5	0.06-2.02	2.8-14	0.07-2
GOCE-only	25-81	0.4-20.3	11.5-49.5	0.35-8.7	2-125	0.47-21

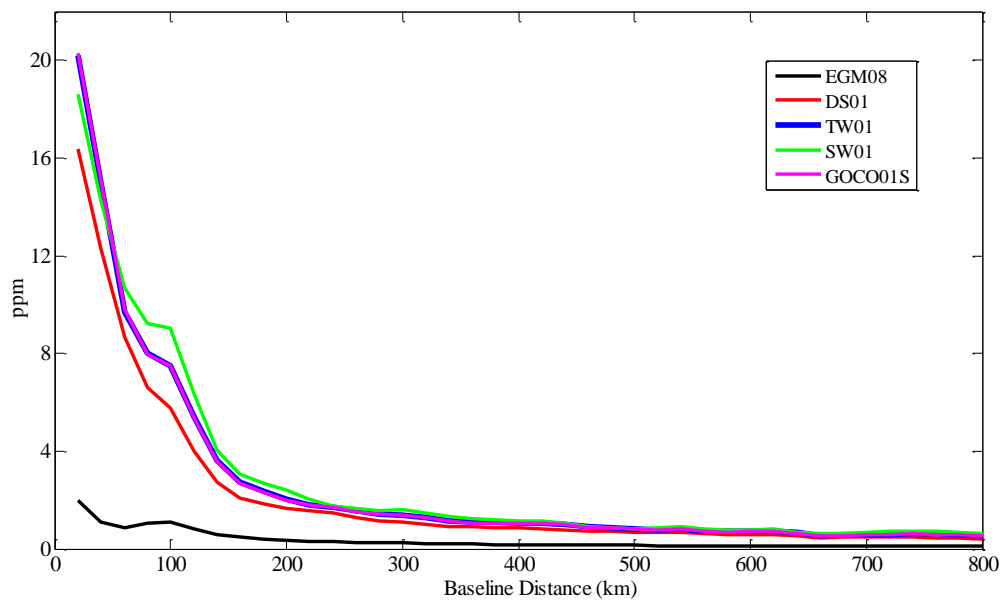


Figure 4.17: Relative undulation accuracy [ppm] as a function of baseline distance [km] for Canada from EGM2008, three first generation GOCE solutions (DS01, TW01, and SW01) and the GRACE-GOCE combined satellite-only model GOCO01S.

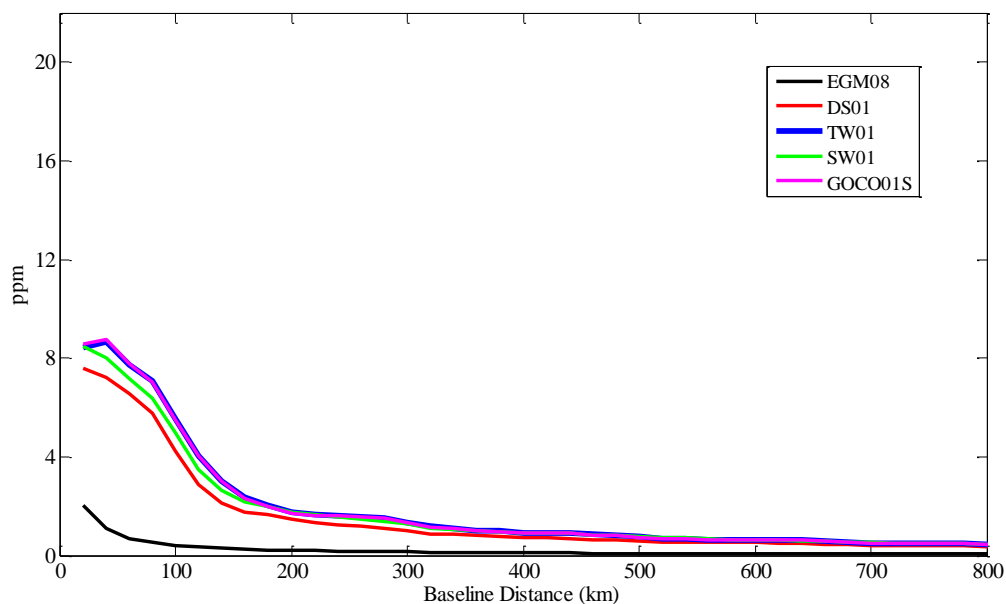


Figure 4.18: Relative undulation accuracy [ppm] as a function of baseline distance [km] for the Great Lakes area from EGM2008, three first generation GOCE solutions (DS01, TW01, and SW01) and the GRACE-GOCE combined satellite-only model GOCO01S.

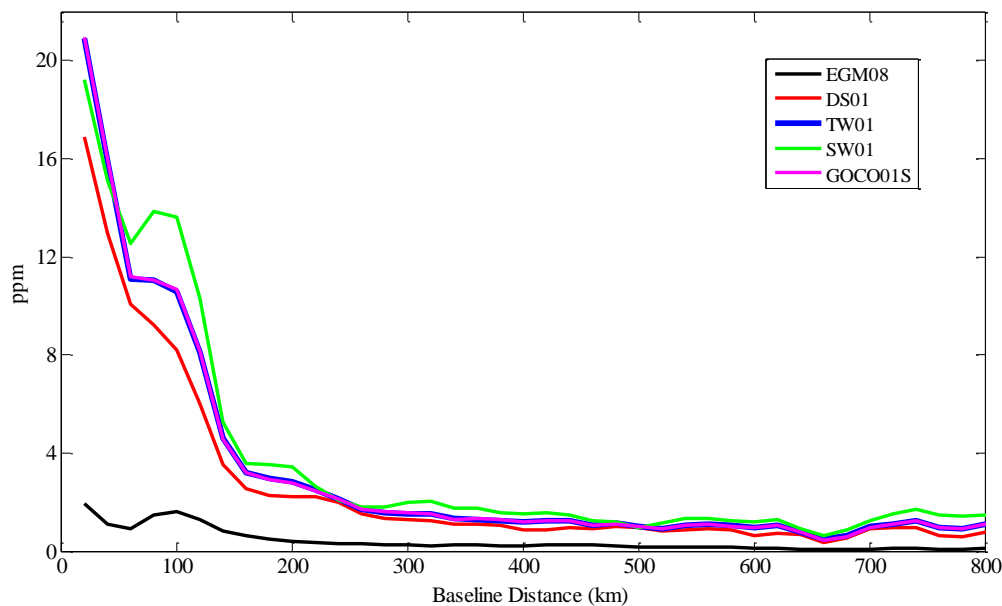


Figure 4.19: Relative undulation accuracy [ppm] as a function of baseline distance [km] for the Rocky Mountains from EGM2008, three first generation GOCE solutions (DS01, TW01, and SW01) and the GRACE-GOCE combined satellite-only model GOCO01S.

Evidently, in the Great Lakes area, the general relative agreements of the geoid models are better due to the flat land features. As in the absolute agreement case, factors such as rough topography, distribution of stations, noise in GPS and leveling data, and long wavelength errors contribute to the large deviations and worse precision in the Rockies.

In the Figures from 4.17 to 4.19, the peaks in the first 80 to 100 km of the baselines are assumed due to the limited satellite resolution. As mentioned before, the resolution of the GOCE satellite mission is approximately 80 km and the information belonging to the smaller baselines is not captured by GOCE models. The results for the Rocky Mountains may also suffer in this interval even more due to the different topographical pattern of the benchmark points.

As expected, satellite-only models provide poorer relative agreement than the combined model EGM2008, which can be attributed to the limited spherical harmonic expansion or the omission error. According to the previous studies GOCE models agreement shall also

be improved by including the local gravity or height data (Sideris et al., 1992; Sideris and She, 1995; Kotsakis et al., 2009).

4.4. Summary

In this chapter, the first and the second generation GOCE-only and GRACE-GOCE combined satellite-only models are evaluated by comparing them with GPS/leveling-derived geoid undulations. The comparisons are performed in absolute and relative sense. First, global gravity field satellite-only model predicted geoids are compared with the GPS/leveling-derived geoid undulations on the benchmarks. This test is repeated for different expansions of the gravity field. To perform fair comparisons between the two geoids, GPS/leveling geoid is also reduced to the same spectral interval of the gravity field component of the satellite-based geoid. This process can be defined as a low-pass filtering process and EGM2008 predicted geoid undulations are used to filter the low degree components of the GPS/leveling-derived geoid undulations.

According to the results obtained, GOCE models are proved to be compatible with EGM2008 and each other up to degree about 150-180. After degree 150, commission error causes GOCE models to agree with GPS/leveling geoid worse. In general, the second generation GOCE-only and GRACE-GOCE combined satellite-only solutions are better compared to the first generation models (except DS01 for the lower degree components). In addition, none of the GOCE-based satellite-only models (except DS01) show any significant improvement over EGM2008.

The second assessment is done based on the relative agreement of the geoid undulations obtained from the first and the second generation GOCE-models expanded up to their highest spherical harmonic degrees available and GPS/leveling-derived geoids. The results show that the GOCE models follow similar behaviour in the three regions with small shifts with respect to each other. Shifts occurred can be attributed with the different expansion degrees and systematic/commission error existing in the spherical harmonic coefficients representing the medium wavelength components. EGM2008 shows a much better agreement due to the terrestrial data included in its development.

It was expected that the relative agreement comparisons show smaller error in the Great Lakes area and larger error in the Rockies due to the flatness and roughness of the topography of the regions. Moreover, the second generation GOCE models do not show a significant improvement to the relative geoid agreement of the first generation ones. This might be used as an indicator that the first and the second generation GOCE models have the same level of relative geoid agreement compared to the GPS/leveling-derived geoid undulations.

CHAPTER 5

5. COMBINED GRAVIMETRIC GEOID MODELS FOR CANADA AND THEIR ASSESSMENT

5.1. Introduction

In this chapter, the GOCE-only solution TW01 obtained from the first two-month observations cycle is combined with the regional terrestrial data to investigate possible improvements coming from GOCE to the medium wavelength interval of the existing geoid models in Canada. This model has been chosen since it was developed based only on GOCE data. It includes only the information obtained from the GOCE kinematic orbits and gradiometry and no other information rather than GOCE and Canadian terrestrial data has been included in the combined models. Thus, it will be possible to see what exactly GOCE's contribution is to the new models developed here. The reader is referred to Chapter 3 for the methodology of the combination procedure.

The combined models are assessed with respect to the GPS/leveling-derived geoid heights and also by comparing them with the existing global and Canadian geoid models. In the first part of the chapter, the existing global and regional geoid models are shortly described and the agreements of these models with GPS/leveling-derived geoid undulations are given for Canada and the two sub-regions, the Great Lakes and Rocky Mountains.

In the second part, the GOCE-only solution TW01 is combined with the regional terrestrial data by applying the remove-compute-restore technique and the modified Stokes kernel. These combined models are investigated by again comparing them with the GPS/leveling-derived geoid undulations. In this section, in contrast to the previous investigations given in Chapter 4 which have been done to do quick investigations on GOCE models, the outliers existing in the misclosures are detected by a 3-sigma technique separately for each area and removed from the evaluation. Thus, this will help

to obtain more realistic and final conclusions on the contribution of the GOCE models. The detection of the outliers has been performed by comparing EGM2008-derived geoid undulations on the benchmarks with GPS/leveling-derived geoids. The outliers detected in Canada, in the Great Lakes and Rocky Mountains regions are shown with red markers in Figures 5.1, 5.2 and 5.3, respectively. There are 24 outliers detected in Canada whereas 9 and only 8 outliers are detected in the Rockies and Great Lakes regions, respectively.

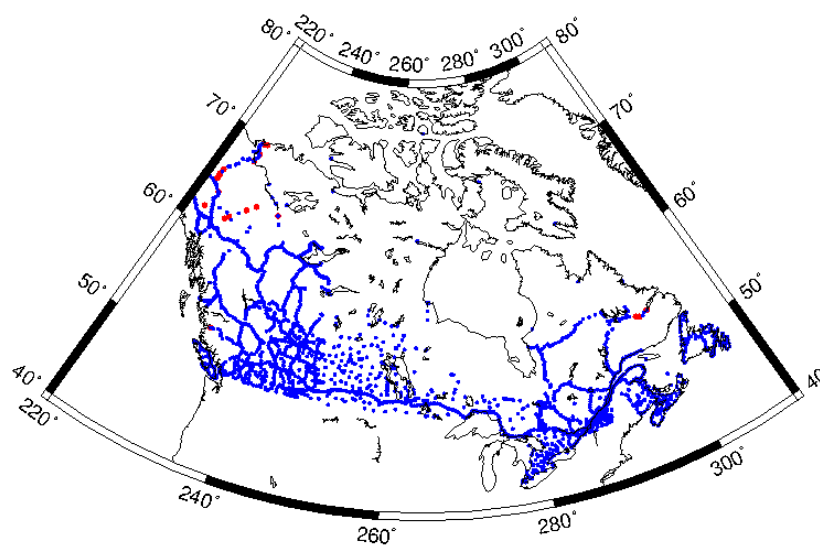


Figure 5.1: The GPS/leveling benchmarks in Canada and 24 outliers (shown with red markers) detected by a 3-sigma technique.

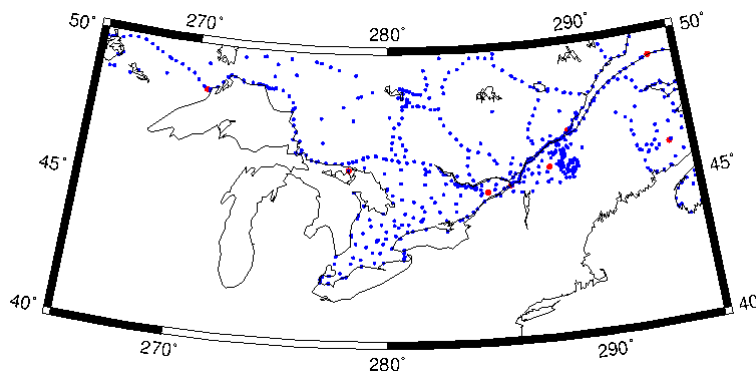


Figure 5.2: The GPS/leveling benchmarks in the Great Lakes area and 8 outliers (shown with red markers) detected by a 3-sigma technique.

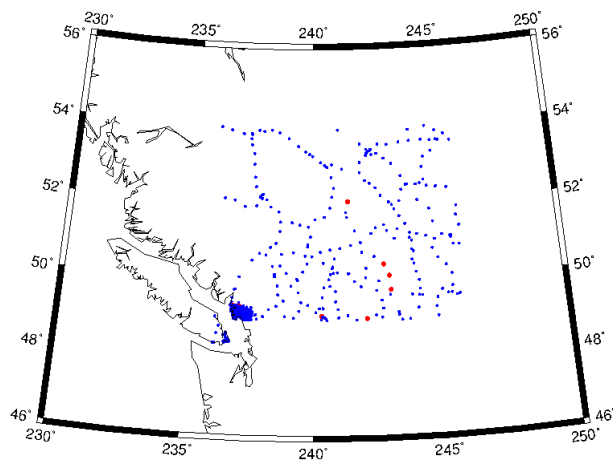


Figure 5.3: The GPS/leveling benchmarks in the Rocky Mountains region and 9 outliers (shown with red markers) detected by a 3-sigma technique.

Different from the previous investigations the 4-parameter corrector surface is applied to obtain an assessment on the GOCE combined geoid solutions where the long wavelength error of the gravimetric geoid model and the datum inconsistencies among the height types are minimized. Firstly the investigations on the existing geoid models before the removal of outliers are given in section 5.2.

5.2. Evaluation of the Existing Global and Regional Geoid Models

5.2.1. Earth Gravitational Model of 2008 (EGM2008)

EGM2008 was developed by making use of GRACE data and also a global set of terrestrial (land and marine) gravity anomalies. It was publicly released by the National Geospatial-Intelligence Agency (NGA) EGM Development Team in 2008 and is accessible freely from:

<http://earthinfo.nga.mil/GandG/wgs84/gravitymod/egm2008/index.html>.

It is the first global gravity field model which is expanded up to spherical harmonic degree 2190 and has a spatial resolution of 5 arc minutes (Pavlis et al., 2008). The model is complete to degree and order 2159; furthermore, additional coefficients are added which are used to convert the ellipsoidal harmonic coefficients to the spherical ones. The

agreement of EGM2008 with GPS/leveling-derived geoid undulations is given as 13 cm globally (Pavlis, 2010). In Canada, the evaluation of EGM2008 model was assessed by NRCan and can be found in Huang and Véronneau (2009). Here, EGM2008 is included to provide a comparison to the developed combined geoid models.

An illustration of EGM2008 geoid in Canada is given in Figure 5.4. The EGM2008 geoid ranges from about -50 to 50 m in Canada. The comparisons with the GPS/leveling-derived geoid undulations have been made on all available benchmarks points firstly without removing the outliers, 2579 in Canada and 652 and 659 points in the Great Lakes and Rocky Mountains areas, respectively. The comparisons of EGM2008 model up to the highest degree available can be found in Table 5.1 for Canada, the Great Lakes and the Rocky Mountains. It is stated in Huang and Véronneau (2009) that the agreement of the EGM2008 geoid model with the GPS/leveling geoid was a standard deviation of 13.3 cm in Canada tested on 2579 benchmark points. This supports our comparisons, where the agreement is 13.2 cm.

Table 5.1: The statistics of the agreement of EGM2008 geoid with the GPS/leveling-derived geoid undulations tested on 2579, 652 and 659 benchmarks in Canada, the Great Lakes and the Rocky Mountains regions, respectively. The values in paranthesis are obtained after the 4-parameter corrector surface is applied. The statistics are given in meter.

EGM2008	Canada	Great Lakes	Rockies
Max	0.065 (0.418)	-0.011 (0.120)	-0.133 (0.243)
Min	-0.918 (-0.341)	-0.438 (-0.137)	-0.775 (-0.199)
Mean	-0.387 (0)	-0.277 (0)	-0.468 (0)
Std	0.132 (0.078)	0.046 (0.037)	0.078 (0.066)
Rms	0.408 (0.078)	0.281 (0.037)	0.474 (0.066)

After the four-parameter fitting process is performed, the range of the misclosures decreases in all the three areas and the standard deviations are improved. The ranges of the miclosures are reduced from 98.3 cm to 75.9 cm in Canada, 44.9 cm to 25.7 cm in the Great Lakes area and 90.8 cm to 44.2 cm in the Rockies. Thus, the standard deviation of the misclosures is improved to 7.8 cm from 13.2 cm in Canada after the four-parameter

fitting process is performed. For the Great Lakes and the Rocky Mountains regions, the statistics show a 4.6 cm and 7.8 cm agreement with GPS/leveling-derived geoid undulations, and the results are improved to 3.7 cm and 6.6 cm, respectively after fitting.

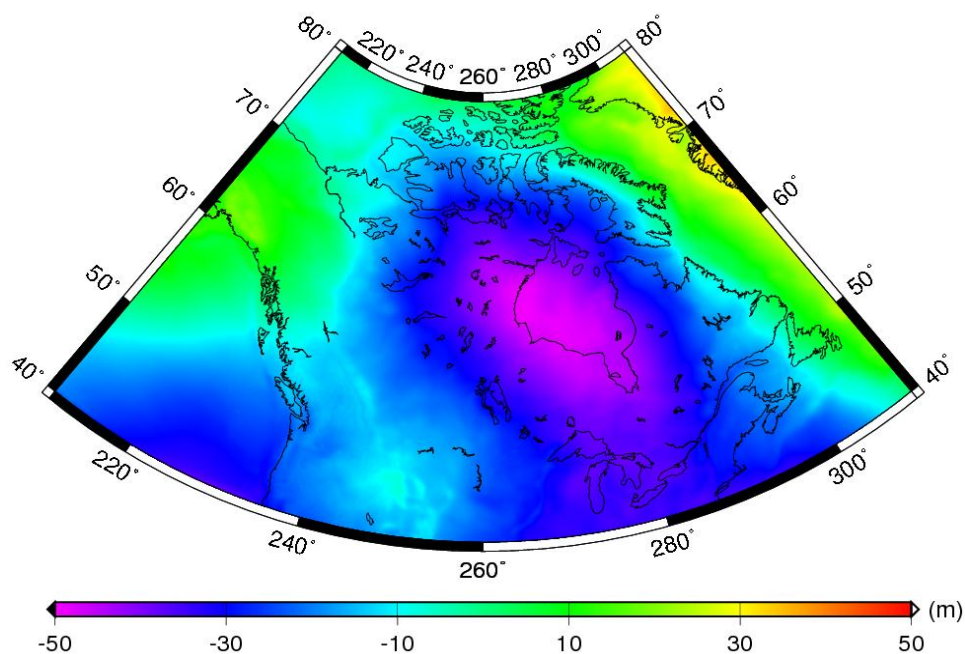


Figure 5.4: EGM2008 geoid in Canada.

The residuals (misclosures) obtained from the GPS/leveling-derived geoid undulations and the geoid heights obtained from EGM2008 (degree 2 to 2190) range from -90 cm to 10 cm, and are depicted by color-coded points in Figure 5.5. The apparent tilt existing from east to west is likely due to the accumulation of the systematic errors in the leveling (Huang et al., 2007). It is also possible to see large discrepancies in the north-west Canada and middle part of the Rockies. As mentioned in the previous section, some of these large misclosures are detected as outliers and filtered out for the following investigations.

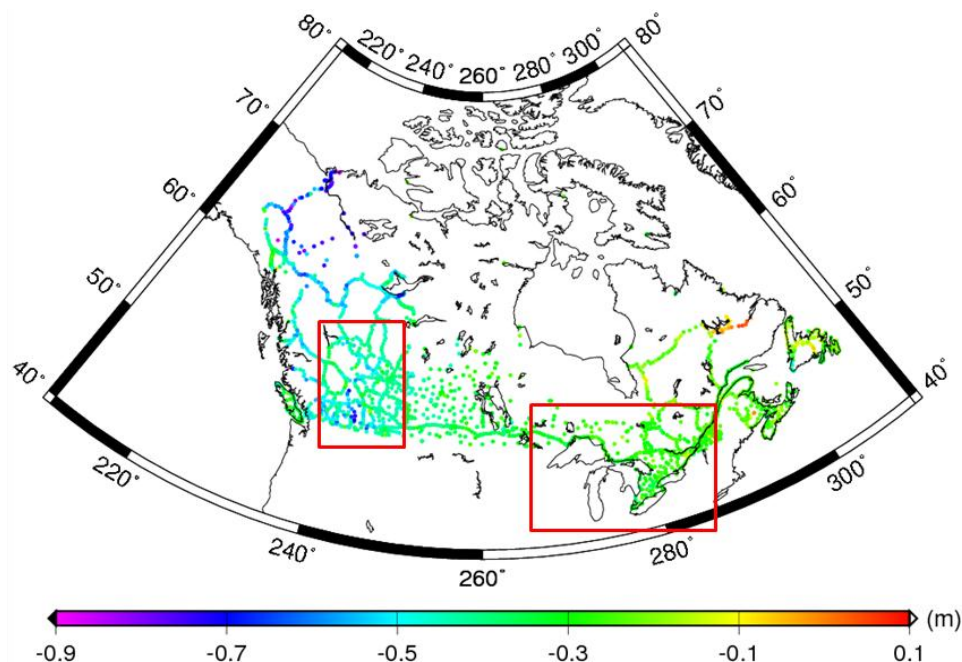


Figure 5.5: Differences between the geoid undulations derived from GPS/leveling and EGM2008 up to the maximum spherical harmonic degree 2190.

5.2.2. Canadian Gravimetric Geoid Model of 2005 (CGG2005)

The Canadian Gravimetric Geoid Model of 2005, CGG2005, is a purely gravimetric geoid model developed by NRCan using 2.2 million gravity measurements obtained from different international sources, such as NRCan, NGS, NIMA and KMS (Véronneau and Huang, 2007). CGG2005 covers the area within the geographical coordinates following: N20° to N80°; W10° and W170°, and it has a resolution of 2 arc minutes. The W_0 value used was estimated by Burša (1995), $62636856.88 \text{ m}^2/\text{s}^2$, and the model represents the separation between the W_0 defined surface and the GRS80 reference ellipsoid. CGG2005 is a geocentric model as it coincides with a realization of ITRF and assumed to be in ITRF00 for the approximate epoch 2003 (Véronneau and Huang, 2007).

Besides surface gravity anomalies, the GGM02-C combined model (UTEX CSR, 2004) (degree and order 200) up to degree 90 was also included in the development of CGG2005. EGM96 (Lemoine et al. 1998) was included to provide the spherical harmonic degrees from 201 to 360 that increase the resolution of the global gravity field. Therefore,

GGM02-C and EGM96 provided the long wavelength components of the geoid model whereas the surface gravity anomalies were used to complement the short wavelength information. The satellite model and terrestrial data have been combined by the degree banded Stokes kernel (Véronneau and Huang, 2007).

The Digital Elevation Model (DEM) used in CGG2005 was collected from federal sources. For British Columbia and Alberta, DEMs were obtained from 1:20k and 1:10k scaled maps, respectively and DEM for the rest of Canada was obtained from the Canadian Digital Elevation Data (CDED) set. For US, the Digital Terrain Elevation Data (DTED) set was used, which was created by using a similar approach as the one for CDED (Véronneau and Huang, 2007).

In general, CGG2005 can be defined as an enhanced version of the previous Canadian geoid model of 2000, CGG2000. The improvement is due to the Stokes kernel modification, which helps to filter out the long wavelength contribution from the surface gravity measurements containing systematic errors. The degree-banded Stokes kernel was modified to degree 90. GRACE-based model GGM02-C was used to complement the long wavelength components up to spherical harmonic degree 90. The kernel was truncated at degree 5400 representing the resolution of the 2'x 2' gridded terrestrial Helmert gravity anomalies used. Terrestrial data were integrated at 6-degree cap radius. These parameters were determined based on the test analysis performed.

A depiction of the difference between CGG2005 and the official Canadian vertical datum CGVD28 is given in Figure 5.6. The range of the difference changes from -35 cm to 75 cm. More details about the model can be found in the report of CGG2005 (Véronneau and Huang, 2007). The report is accessible on NRCan's website (<http://www.geod.nrcan.gc.ca/hm/pdf/cgg05v5.pdf>). The investigations of CGG2005 for Canada and the two sub-regions are summarized in Table 5.2. The comparisons with GPS/leveling-derived geoid suggest a 13.2 cm agreement in Canada, and 5.5 cm and 7.1 cm for the Great Lakes and the Rocky Mountains, respectively.

* Equipotential surface coincides with MWL in Rimouski

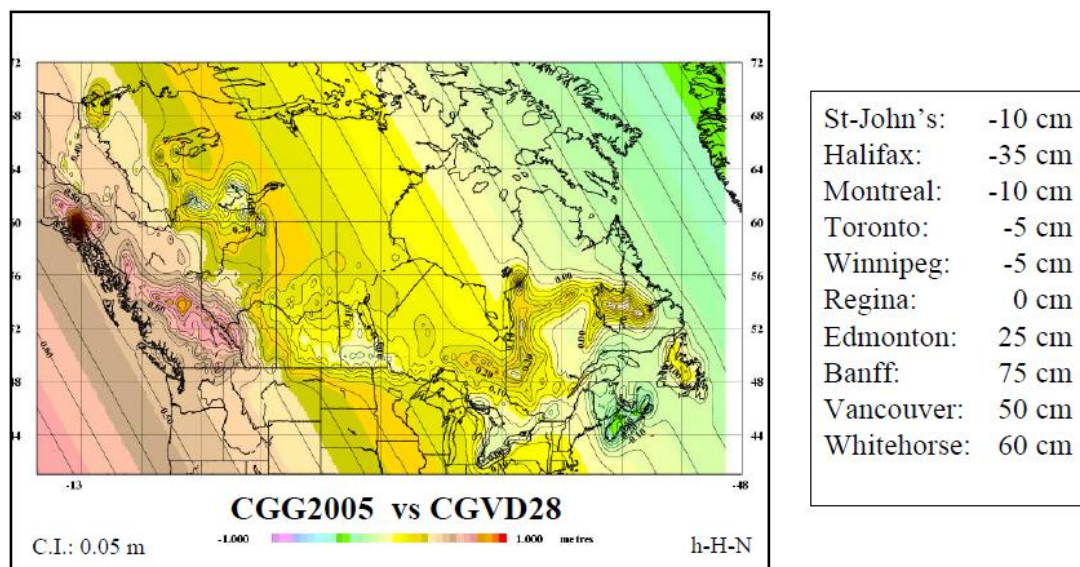


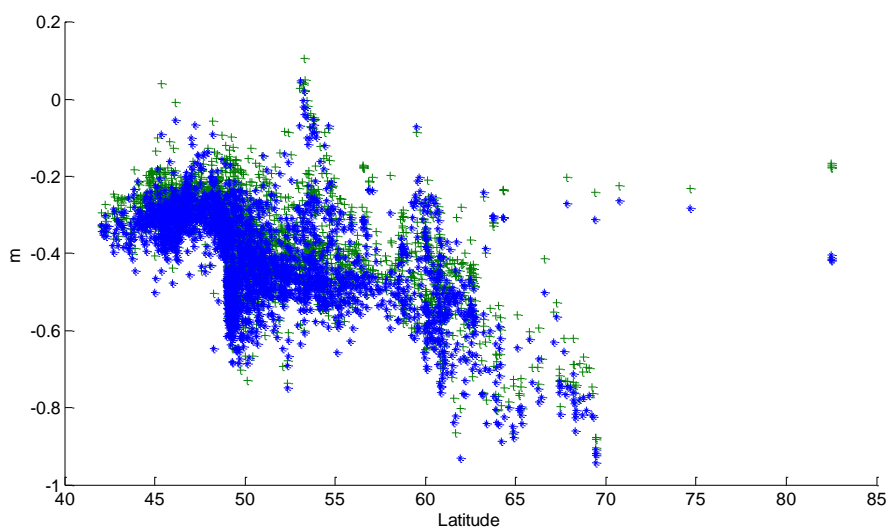
Figure 5.6: Differences between the official Canadian geoid, CGG2005, and the official Canadian vertical datum, CGVD28 (NRCan, 2010).

Table 5.2: The statistics of the agreement of CGG2005 geoid with the GPS/leveling-derived geoid undulations tested on 2579, 652 and 659 benchmarks in Canada, the Great Lakes and the Rocky Mountains regions, respectively. The values in paranthesis are obtained after the 4-parameter corrector surface is applied. The statistics are given in meter.

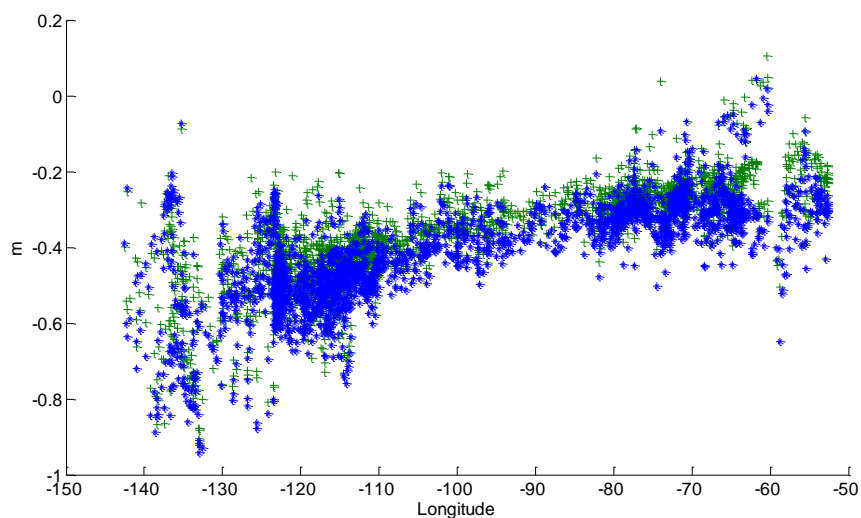
CGG2005	Canada	Great Lakes	Rockies
Max	0.048 (0.496)	-0.053 (0.146)	-0.246 (0.216)
Min	-0.742 (-0.360)	-0.501 (-0.166)	-0.686 (-0.187)
Mean	-0.423 (0)	-0.308 (0)	-0.504 (0)
Std	0.132 (0.081)	0.055 (0.045)	0.071 (0.058)
Rms	0.443 (0.081)	0.313 (0.045)	0.509 (0.058)

The misclosures dependencies on longitude and latitude obtained from EGM2008 and CGG2005 comparisons are illustrated separately in Figures 5.7(a) and (b). Figure 5.7 (a) shows the dependency on latitude, where there is an accumulation of the error from the south to the north. Figure 5.7(b) illustrates the dependency on longitude; the misclosures become larger in the west of the country due to the accumulation of systematic errors in

leveling with respect to the reference point, Father Point in Rimouski ($48^{\circ} 28' N$, $291^{\circ} 31' E$), located in the east of the country. CGG2005 shows a good agreement with EGM2008 in general. The misclosures follow similar behaviour as EGM2008.



(a)



(b)

Figure 5.7: The existing official geoid models, CGG2005 and EGM2008, are compared with undulations obtained from Canadian GPS/leveling. The residuals (CGG2005 shown with blue, EGM2008 shown with green) versus latitude and longitude are shown in Figures 5.7(a) and (b), respectively.

5.2.3. An Experimental Canadian Geoid Model of 2010 (ECG10)

An experimental Canadian Geoid Model was developed by NRCan. ECG10 is a test model created before the release of GOCE solutions and includes basically the same datasets as CGG2005. Additionally, EGM2008 has been included in ECG10 to fill in the areas lacking data. Furthermore, different from CGG2005, a later GRACE solution has been included in ECG10. The differences between EGM2008 and ECG10 are shown in Figure 5.8. The higher resolution, as well as the different datasets included in ECG10 such as GRACE new solutions and ship-borne data recently obtained in coastal areas, are the main reasons of the differences between these two models.

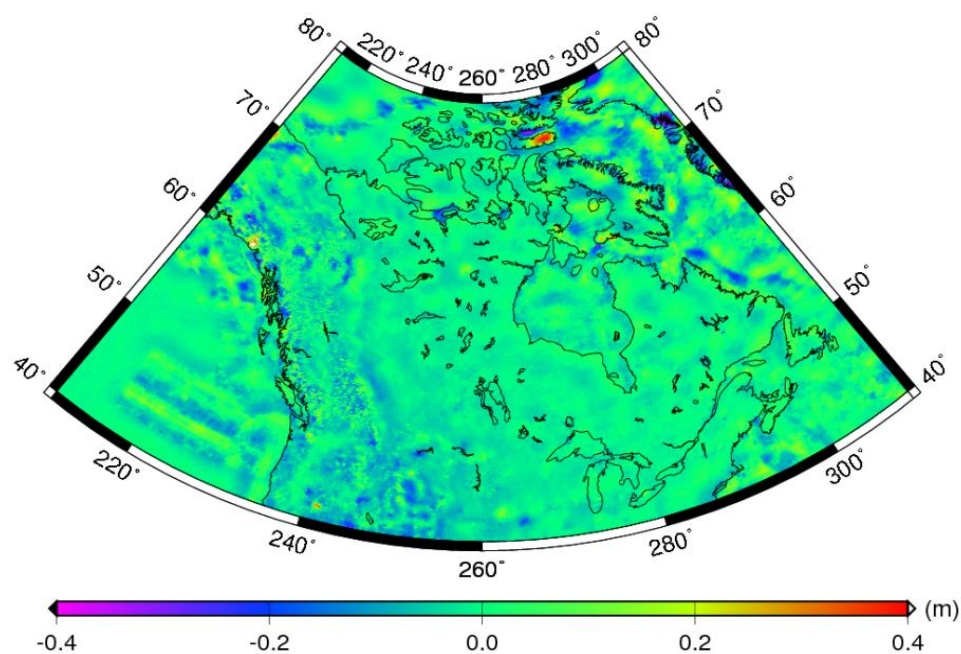


Figure 5.8: Differences between ECG10 and EGM2008. The differences occur due to the different and higher resolution of ECG10, as well as different data included in its development such as GRACE new solutions and the use of ship-borne data in coastal area.

The statistics of the agreements with the GPS/leveling comparisons are given in Table 5.3. ECG10 provides slightly improved agreement with the GPS/leveling-derived geoid undulations than EGM2008 and CGG2005. With the contribution of GOCE data, it is expected to be improved even more.

Table 5.3: The statistics of the agreement of ECG10 geoid with the GPS/leveling-derived geoid undulations tested on 2579, 652 and 659 benchmarks in Canada, the Great Lakes and the Rocky Mountains regions, respectively. The values in paranthesis are obtained after the 4-parameter corrector surface is applied. The statistics are given in meter.

ECG10	Canada	Great Lakes	Rockies
Max	0.101 (0.446)	-0.008 (0.116)	-0.199 (0.213)
Min	-0.895 (-0.348)	-0.435 (-0.118)	-0.601 (-0.171)
Mean	-0.365 (0)	-0.262 (0)	-0.442 (0)
Std	0.122 (0.074)	0.048 (0.038)	0.070 (0.058)
Rms	0.385 (0.074)	0.266 (0.038)	0.447 (0.058)

One should note that ECG10 is a not a publicly released model, and is given here just to show the status of the current developments.

5.3. Investigations of the GOCE and Terrestrial Data Combined Models

As explained before, the long wavelength components of the combined geoid models are obtained from the global geopotential models. In this thesis, the first generation GOCE-only solution TW01 is used to obtain the long wavelength part of the geoid model. As stated before, TW01 has been chosen to see the improvements coming from GOCE-only model without any effect of GRACE data (e.g., GOCO01S, GOCO02s) and any background model used (e.g., DS01). In order to choose the optimal maximum degree of the satellite models, different spherical harmonic degree truncations were tested in combined models by the help of the modified Stokes kernel and the results are presented in this section. Gridded Helmert gravity anomalies provided by NRCan are used as complementary datasets for the high frequency gravity information. These gridded values were obtained from point gravity measurements. The gravity measurements were collected on land, lakes, and oceans using relative and absolute gravimeters, satellite

altimetry and airborne gravimetry (Véronneau, and Huang 2007; Huang and Véronneau, 2009). The locations of the gravity measurements in Canada are displayed in Figure 5.9. Compared to most other countries, Canadian terrestrial gravity data are proven to be relatively more accurate and well-distributed.

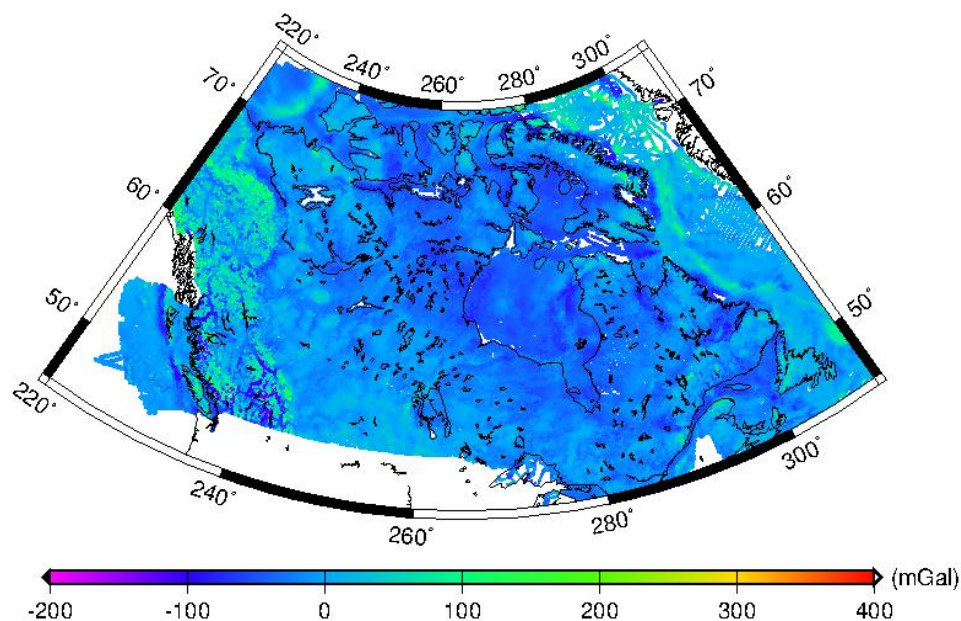


Figure 5.9: The point gravity measurements in Canada.

The Helmert gravity anomalies used in the combined models were created based on the methodology given in Chapter 3. An intermediate Bouguer Earth was created first and the Helmert gravity anomalies were evaluated on the geoid later. The 2' x 2' gridded Helmert gravity anomalies used in the computations are shown in Figure 5.10 and their statistics in Canada and the sub-regions are given in Table 5.4. The amplitude of the largest anomaly existing is around 524 mGal and the average of the anomalies are around -4.4 mGal, -7.3 mGal and 9.5 mGal for Canada, the Great Lakes and the Rocky Mountains, respectively.

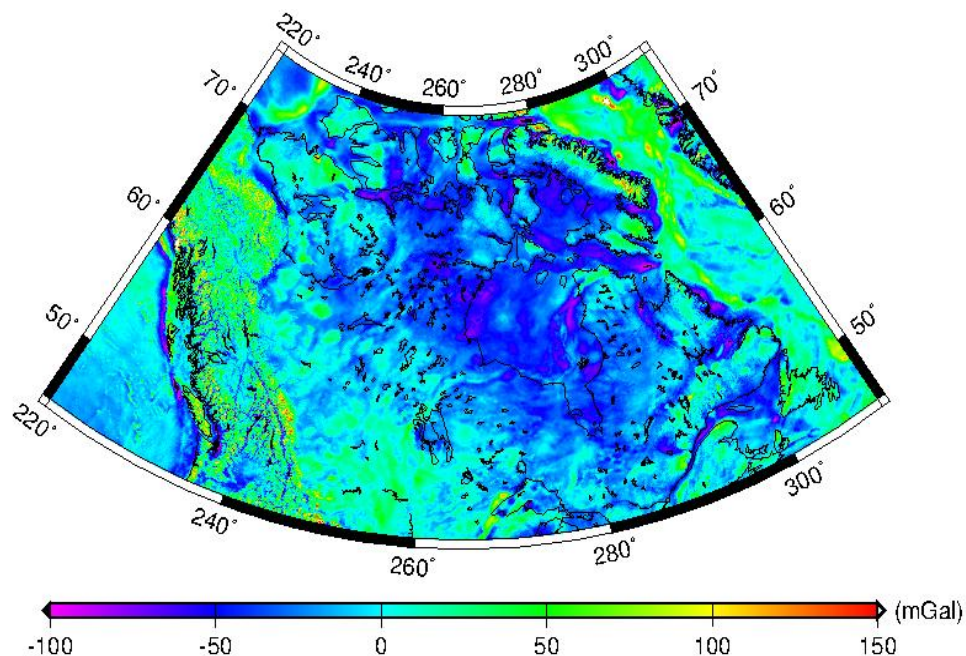


Figure 5.10: The 2'x 2' gridded Helmert gravity anomalies in Canada.

Table 5.4: Statistics of the gridded Helmert gravity anomalies in Canada, the Great Lakes and the Rocky Mountains given in mGal.

Area	Canada (40-84°N, 50-150°W)	Great Lakes (40-50°N, 65-95°W)	Rocky Mountains (48-54°N, 114-124°W)
Max	524.7	128.5	203.8
Min	-175.5	-84.1	-138.5
Mean	-4.4	-7.4	9.5
Std	33.7	22.4	43.8
Rms	34.0	23.6	44.9

Besides the aim of investigating the improvement coming from GOCE-only data, our tests assessed in the previous chapter have led us to use the first generation time-wise model in the combined solutions here. In the previous chapter it is discussed that DS01 was developed by using satellite and terrestrial data combined background model and affected by terrestrial gravity data; thus, SW01 made use of EGM2008 for the long wavelength gravity information.

In all the combined models developed in this thesis, basic steps given below are followed.

- The methodology given in Figure 3.3 is followed in the development of the combined models. This methodology basically develops a Helmert co-geoid model which differs from the geoid by the indirect effect of the topography.
- HTW01 (TW01 in Helmert's space) geoid developed up to different spherical harmonic degrees (see eq. 3.26) are created on 2'x 2' grid and complemented with 2'x 2' gridded terrestrial Helmert gravity anomalies by the remove-compute-restore technique.
- The degree banded modified Stokes kernel (see eq. 3.57) is applied to the residual gravity anomalies to provide an optimum combination of the satellite and terrestrial datasets and to reduce the truncation error.
- The indirect topographical effect is added to obtain the geoid from the Helmert co-geoid. The indirect effect of the near-zone (within 6° capsize) and the far-zone topography are computed from 2'x 2' and 1°x 1° gridded DEMs, respectively.
- Combined complete geoid models are developed in 2'x 2' grid.

The evaluation of the geoid undulations interpolated on the benchmark points from the gridded gravimetric geoid model are compared with the GPS/leveling-derived geoid undulations after the removal of the outliers. Finally, a 4-parameter corrector surface is applied to remove the datum inconsistencies between the combined geoid model developed from GOCE and terrestrial data and GPS/leveling geoid and the comparison statistics are reviewed.

The models investigated in the following part are named M1 to M11. Models M1 to M3 are based on the available GGM models only. The rest of the models are combined through the steps mentioned above for the different dataset combinations (GOCE, EGM2008 and terrestrial data) and different truncation degrees.

The far-zone contribution (truncation error) mentioned above occurs due to the integration over part of the Earth instead of the entire Earth. This basically causes an integration domain truncation error. The reason of this is the fact that the gravity data

outside of the Stokes cap-size still has an effect on the solutions and need to be taken into account. There are two ways to take the far-zone contribution into account in the combined models. The first approach is given in Vaníček and Featherstone (1998) where the global model expanded up to degree and order l is used in the remove-compute-restore technique and the far-zone contribution from $l+1$ to maximum degree of the global model is computed and added to the geoid solution separately.

In this thesis, the other approach is applied where the far-zone contribution is not evaluated separately but eliminated by using a higher degree global model in the remove-compute-restore process. According to Huang and Véronneau (2010), the GGM included in the combined model should be expanded up to spherical harmonic degree 200 and/or above to account for the far-zone contribution in the computation. If the model is expanded some degrees below spherical harmonic degree~200 the truncation error needs to be computed and added to the solution separately. In this methodology the global model predicted gravity anomalies up to degree M (above spherical harmonic degree 200) are removed from the terrestrial gravity data and restored. The use of the higher degree global models turns the far-zone contribution negligible. Then, the residual gravity anomalies are used to obtain the residual geoid undulations. Since the Stokes kernel is modified up to degree l , the geoid beyond degree l only depends on the terrestrial gravity data while the geoid components between the degree 2 and l are obtained from a combination of the global model and terrestrial gravity data. For this reason, in our calculations, TW01 is used up to its maximum degree (224) and the combination is realized by the degree banded modified Stokes kernel modification coefficients.

The geoid undulations for each of these models were obtained as dictated in Table 5.5 following.

Table 5.5: Summary of the GGM only and combined models investigated.

Models	HTW01	TW01	HEGM2008	EGM2008	Terrestrial data	Modified kernel	Specifications	Modification band
M1	-	-	-	360	-	-	EGM2008 only geoid model expanded up to s.h.d. 360.	-
M2	-	-	-	2190	-	-	EGM2008 only geoid model expanded up to its maximum s.h.d. 2190.	-
M3	-	224	-	-	-	-	TW01-only geoid model expanded up to s.h.d. 240.	-
M4	-	-	360	-	Yes	Yes	HEGM2008 co-geoid expanded up to s.h.d. 360 is complemented with terrestrial gravity anomalies. Degree-banded modified Stokes kernel is applied. Indirect effect is added to convert the Helmert co-geoid to geoid.	150
M5	224	-	225-360	-	Yes	Yes	Combined co-geoid model obtained from HTW01 expanded up to s.h.d 224 and HEGM2008 expanded up to s.h.d from 225 to 360 is complemented with terrestrial gravity anomalies. Modified Stokes kernel is applied. Indirect effect is added to convert the Helmert co-geoid to geoid.	150
M6	224	-	-	-	Yes	Yes	HTW01 co-geoid expanded up to s.h.d. 224 is complemented with terrestrial gravity anomalies. Degree-banded modified Stokes kernel is applied. Indirect effect is added to convert the Helmert co-geoid to geoid.	150

M7	150	-	151-2190	-	Yes	Yes	Combined co-geoid model obtained from HTW01 expanded up to s.h.d 150 and HEGM2008 expanded up to s.h.d from 151 to 2190 is complemented with terrestrial gravity anomalies. Modified Stokes kernel is applied. Indirect effect is added to convert the Helmert co-geoid to geoid.	150
M8	180	-	-	-	Yes	Yes	HTW01 co-geoid expanded up to s.h.d. 180 is complemented with terrestrial gravity anomalies. Degree-banded modified Stokes kernel is applied. Indirect effect is added to convert the Helmert co-geoid to geoid.	150
M9	224	-	-	-	Yes	Yes	HTW01 co-geoid expanded up to s.h.d. 224 is complemented with terrestrial gravity anomalies. Degree-banded modified Stokes kernel is applied. Indirect effect is added to convert the Helmert co-geoid to geoid.	120
M10	224	-	-	-	Yes	Yes	HTW01 co-geoid expanded up to s.h.d. 224 is complemented with terrestrial gravity anomalies. Degree-banded modified Stokes kernel is applied. Indirect effect is added to convert the Helmert co-geoid to geoid.	180
M11	224	-	-	-	Yes	Yes	HTW01 co-geoid expanded up to s.h.d. 224 is complemented with terrestrial gravity anomalies. Degree-banded modified Stokes kernel is applied. Indirect effect is added to convert the Helmert co-geoid to geoid.	90

s.h.d: spherical harmonic degree

HTW01: TW01 in Helmert's space

HEGM2008: EGM2008 in Helmert's space

The contributions of the GGM, residual gravity anomalies, and indirect effect of the topography in the combined model M6 are shown in Figures 5.11, 5.12 and 5.13, respectively and the statistics of the the contributions from each component are given in Table 5.6.

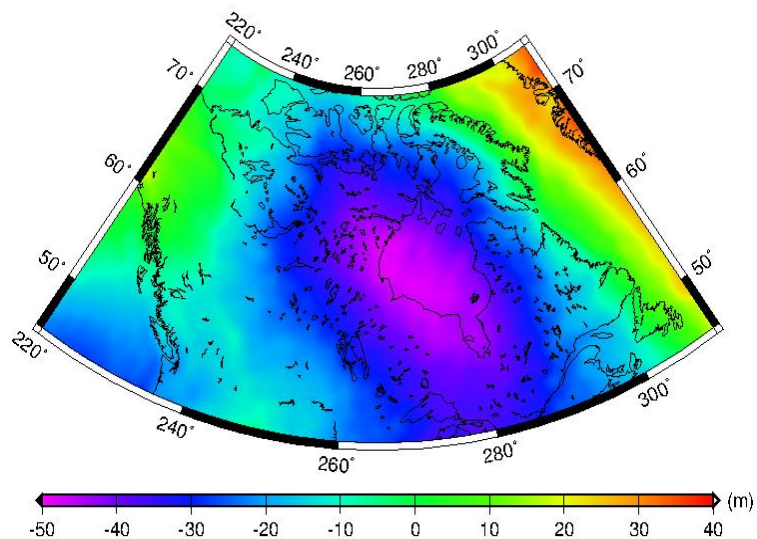


Figure 5.11: The geoid undulations predicted from HTW01 included in the combined solution.

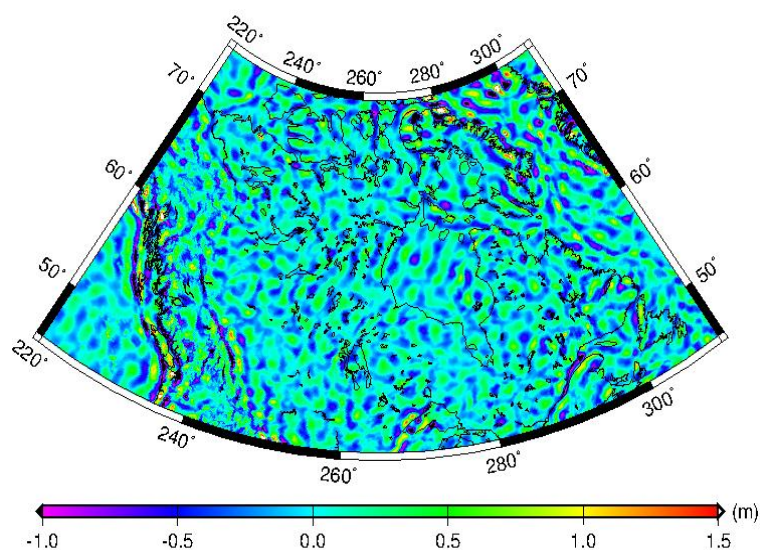


Figure 5.12: The residual geoid undulations obtained from residual gravity anomalies used in M6.

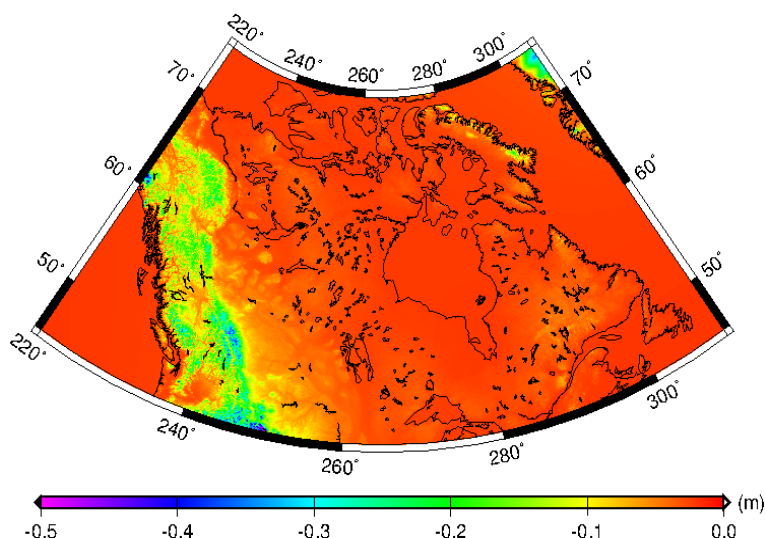


Figure 5.13: The indirect topographic effect on the geoid.

Table 5.6: The statistics of the components used in remove-compute-restore technique are given in meters.

Source	HTW01-only geoid	Residual geoid	Indirect effect	Complete model-M6
Max	36.262	3.271	-0.019	35.807
Min	-48.938	-2.140	-1.163	-49.072
Mean	-10.599	~0	-0.042	-10.640

As depicted in Table 5.6, the largest contribution comes from the GGM. The range changes from -50 m to 40 m and shows smooth changes. The residual geoid affects the geoid undulation amount of 3.271 m to -2.140 m. Even though the changes show a random distribution, it is possible to see shorter wavelength information in the region of Western Canada, in the Rocky Mountains and coastal regions. The differences in Western Canada can be used as an indicator of tectonic movements in the region. The differences in the Rockies might be a sign of lower amount and quality level of gravity measurements in the region. The range of the indirect effect changes between -0.019 m and -1.163 m and represents the effect of the topographical pattern to the geoid model.

The combined model M6 is depicted in Figure 5.14. The geoid ranges between -50 and 40 m and it changes very smoothly as it is expected. In the coastal areas it is close to zero whereas in the Hudson Bay and the Great Lakes area it is located below the reference ellipsoid.

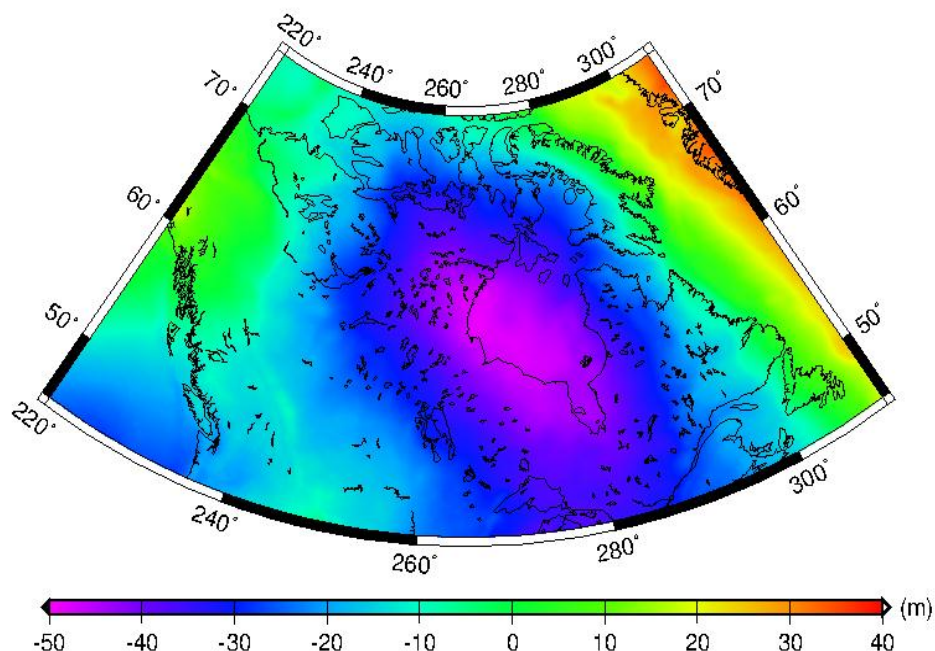


Figure 5.14: The combined model M6.

The statistics of the 11 models are given in Tables 5.7, 5.8 and 5.9 for Canada, the Great Lakes region and the Rocky Mountains, respectively. The removal of outliers improves the agreement of the EGM2008 model with GPS/leveling-derived geoid undulations; compare Table 5.1, where the statistics are shown before the removal of the outliers to the M2 columns in Tables 5.7 to 5.9 which show results after the removal of the outliers. The geoid agreements with GPS/leveling-derived geoid undulations are improved from 13.2 to 12.2 for Canada, 4.6 to 4.1 in the Great Lakes region and 7.8 to 6.8 in the Rockies. The comparisons, explanations and interpretations of the 11 models are given in Table 5.10.

Table 5.7: Comparisons of the combined models with the GPS/leveling-derived geoid undulations in Canada. The values in parenthesis are obtained after the 4-parameter corrector surface is applied. The statistics are given in meter.

Models	M1	M2	M3	M4	M5	M6	M7	M8	M9	M10	M11
Max	0.197	0.006	0.755	0.006	0.001	0.012	0.009	0.010	0.049	-0.012	0.056
	(0.675)	(0.417)	(1.646)	(0.417)	(0.407)	(0.408)	(0.407)	(0.408)	(0.432)	(0.427)	(0.479)
Min	-1.600	-0.779	-2.285	-0.801	-0.792	-0.795	-0.791	-0.798	-0.773	-0.789	-0.829
	(-0.124)	(-0.341)	(-1.608)	(-0.359)	(-0.348)	(-0.343)	(-0.350)	(-0.343)	(-0.218)	(-0.351)	(-0.362)
Mean	-0.421	-0.382	-0.542	-0.366	-0.374	-0.374	-0.373	-0.374	-0.334	-0.375	-0.361
	(0)	(0)	(0)	(0)	(0)	(0)	(0)	(0)	(0)	(0)	(0)
Std	0.232	0.122	0.426	0.115	0.120	0.120	0.120	0.121	0.117	0.122	0.115
	(0.201)	(0.077)	(0.364)	(0.074)	(0.075)	(0.075)	(0.075)	(0.076)	(0.077)	(0.078)	(0.081)
Rms	0.481	0.401	0.690	0.384	0.393	0.393	0.392	0.393	0.386	0.394	0.379
	(0.201)	(0.077)	(0.364)	(0.074)	(0.075)	(0.075)	(0.075)	(0.076)	(0.077)	(0.078)	(0.081)

Table 5.8: Comparisons of the combined models with the GPS/leveling-derived geoid undulations in the Great Lakes area. The values in parenthesis are obtained after the 4-parameter corrector surface is applied. The statistics are given in meter.

Models	M1	M2	M3	M4	M5	M6	M7	M8	M9	M10	M11
Max	0.197	-0.149	0.749	-0.104	-0.105	-0.107	-0.107	-0.111	-0.075	-0.133	-0.081
	(0.497)	(0.12)	(1.142)	(0.149)	(0.152)	(0.150)	(0.150)	(0.146)	(0.177)	(0.134)	(0.172)
Min	-0.803	-0.414	-1.183	-0.411	-0.455	-0.454	-0.455	-0.453	-0.458	-0.490	-0.409
	(-0.505)	(-0.137)	(-0.837)	(-0.143)	(-0.185)	(-0.184)	(-0.185)	(-0.184)	(-0.189)	(-0.221)	(-0.147)
Mean	-0.295	-0.278	-0.345	-0.268	-0.272	-0.272	-0.272	-0.271	-0.270	-0.274	-0.267
	(0)	(0)	(0)	(0)	(0)	(0)	(0)	(0)	(0)	(0)	(0)
Std	0.144	0.041	0.338	0.042	0.046	0.046	0.047	0.046	0.050	0.054	0.049
	(0.143)	(0.037)	(0.335)	(0.038)	(0.043)	(0.043)	(0.043)	(0.043)	(0.045)	(0.052)	(0.045)
Rms	0.328	0.281	0.484	0.272	0.276	0.276	0.276	0.275	0.274	0.279	0.272
	(0.143)	(0.037)	(0.335)	(0.038)	(0.043)	(0.043)	(0.043)	(0.043)	(0.045)	(0.052)	(0.045)

Table 5.9: Comparisons of the combined models with the GPS/leveling-derived geoid undulations in the Rocky Mountains region. The values in parenthesis are obtained after the 4-parameter corrector surface is applied. The statistics are given in meter.

Models	M1	M2	M3	M4	M5	M6	M7	M8	M9	M10	M11
Max	0.080	-0.181	0.755	-0.194	-0.212	-0.208	-0.210	-0.207	-0.226	-0.191	-0.183
	(0.808)	(0.285)	(1.520)	(0.222)	(0.223)	(0.226)	(0.225)	(0.227)	(0.213)	(0.236)	(0.234)
Min	-1.600	-0.657	-2.284	-0.626	-0.669	-0.666	-0.669	-0.663	-0.646	-0.689	-0.637
	(-0.950)	(-0.178)	(-1.360)	(-0.178)	(-0.197)	(-0.194)	(-0.198)	(-0.192)	(-0.190)	(-0.226)	(-0.200)
Mean	-0.516	-0.463	-0.885	-0.443	-0.465	-0.466	-0.465	-0.467	-0.450	-0.471	-0.429
	(0)	(0)	(0)	(0)	(0)	(0)	(0)	(0)	(0)	(0)	(0)
Std	0.284	0.068	0.465	0.066	0.068	0.069	0.068	0.070	0.067	0.070	0.072
	(0.225)	(0.066)	(0.449)	(0.061)	(0.062)	(0.062)	(0.062)	(0.063)	(0.062)	(0.063)	(0.065)
Rms	0.589	0.468	0.999	0.448	0.470	0.471	0.470	0.472	0.455	0.476	0.435
	(0.225)	(0.066)	(0.449)	(0.061)	(0.062)	(0.062)	(0.062)	(0.063)	(0.062)	(0.063)	(0.065)

Table 5.10: Explanation, comparison and interpretation of result of each model developed.

Models	Explanation	Comparison and interpretation
M1	Model is developed to provide comparisons with satellite-only geoid models.	Due to the omission error this model is not expected to provide a good agreement with GPS/leveling-derived geoid. It allows us to compare a satellite-only model with a high degree satellite and terrestrial data combined model and observe the contribution of the surface data.
M2 (EGM08)	Model is developed to provide comparisons with a global combined geoid model published and GOCE and terrestrial data combined geoid models.	This model is the best available global combined gravity model. It is used in the comparisons of the combined GOCE models. According to the comparisons made with EGM2008, GOCE combined models are proved to be compatible with EGM2008.
M3	Model is developed to provide comparisons with satellite-only geoid models.	Due to the omission error, this model is not expected to provide a good agreement with GPS/leveling-derived geoid. It allows us to compare a satellite-only model with a high degree satellite and terrestrial data combined model and observe the contribution of the surface data.
M4	Model is developed to observe if the currently available Canadian terrestrial data can improve the EGM2008 model.	This model shows if Canadian terrestrial gravity data components above spherical harmonic degree 360 can improve EGM2008 geoid model in Canada. It slightly agrees more (11.5 cm) with the GPS/leveling-derived geoid undulations on benchmarks than the EGM2008 model only expanded up to s.h.d 2190 (12.2 cm). There is no significant improvement observed in the Great Lakes and Rocky Mountains.
M5	Model is developed to take the advantages of GOCE and EGM2008 models as well as the terrestrial data in the development of an optimum combined regional model.	It makes use of HTW01 for the lower and medium degree components up to s.h.d. 150 and HEGM2008 from s.h.d. 151 to 360 to account for the far-zone contribution. In our investigations, this model does not show improvement compared to M2 (EGM2008 geoid) and other combined models developed here.

M6	Model is developed to form an optimally combined geoid model from GOCE and terrestrial data only.	This model provides about the same level of agreement as M5 does. Figures 5.11 to 5.14 show its components. This model is expected to be improved by including GRACE and other geodetic techniques obtained low degree gravity field components.
M7	Model is developed to take the advantages of GOCE and EGM2008 models as well as the terrestrial data in the development of an optimum combined regional model.	It is slightly modified version of M5. It makes use of HTW01 for the lower and medium degree components up to s.h.d. 150 and HEGM2008 from s.h.d. 151 to 2190 to account for the far-zone contribution. It does not indicate any improvement compared to M2 and other combined models developed here.
M8	Model is developed to form an optimally combined geoid model from GOCE and terrestrial data only.	This model is expected to be affected by the truncation error compared to the other models. However, there is no significant difference in statistics indicating the truncation error.
M9	Model is developed to form an optimally combined geoid model from GOCE and terrestrial data only.	This model is a slightly modified version of M6. The truncation degree has been changed from 150 to 120 to find out the optimum truncation degree of GOCE model and terrestrial data. Again, there is not any improvement (cm level) indicating GOCE contribution to the existing geoid.
M10	Model is developed to form an optimally combined geoid model from GOCE and terrestrial data only.	Same as M9 but the truncation is made at s.h.d. 180. There is no significant improvement (cm level) compared to EGM2008 and other combined models.
M11	Model is developed to form an optimally combined geoid model from GOCE and terrestrial data only.	Same as M9 but the truncation is made at s.h.d. 90. There is no significant improvement (cm level) compared to EGM2008 and other combined models.

In general, GOCE is expected to improve the geoid in the areas lacking gravity data (e.g. Yukon region in Canada). Our results suggest that GOCE combined models (e.g., M9, M11) may provide slightly better geoid agreement with GPS/leveling-derived ones for Canada compared to the EGM2008 and other combined models developed.

In the Great Lakes area, we do not see any improvement coming from GOCE solution. It is known that in this region there is already good coverage with high quality terrestrial data which was already included in EGM2008. Thus it can be said that it is sufficient to use M2 only, i.e., EGM2008 expanded up to spherical harmonic degree 2190, in this area as the geoid model.

In the Rocky Mountains region, there is also no improvement observed coming from GOCE solution. Since we look for a cm accurate geoid, mm level of better results do not confirm that the GOCE combined model is more accurate or agrees better. As mentioned before, GOCE is expected to improve the knowledge mostly in the medium and medium to short wavelength components of the gravity field; however, in the Rocky Mountains region, better short wavelength information is needed in order to improve the geoid model in the area.

The difference between EGM2008 expanded up to spherical harmonic degree 2190 and M6 is depicted in Figure 5.15. In general, M6 agrees well with EGM2008 except for some areas such as the north-east of Canada, the Yukon Territory, and mountainous areas in the west, eastern and western coastal regions and parts of Greenland where we see slight differences due to the possible impact of the GOCE data or the differences of the terrestrial data included in EGM2008 and M6. The differences seen in the Atlantic Ocean are possibly due to the ocean current information coming from the GOCE. According to Huang and Véronneau (2010), GOCE improves the realization of the geoid in Yukon Territory. However, it is to be further investigated if the differences shown in Figure 5.15 correspond to any improvement associated with GOCE.

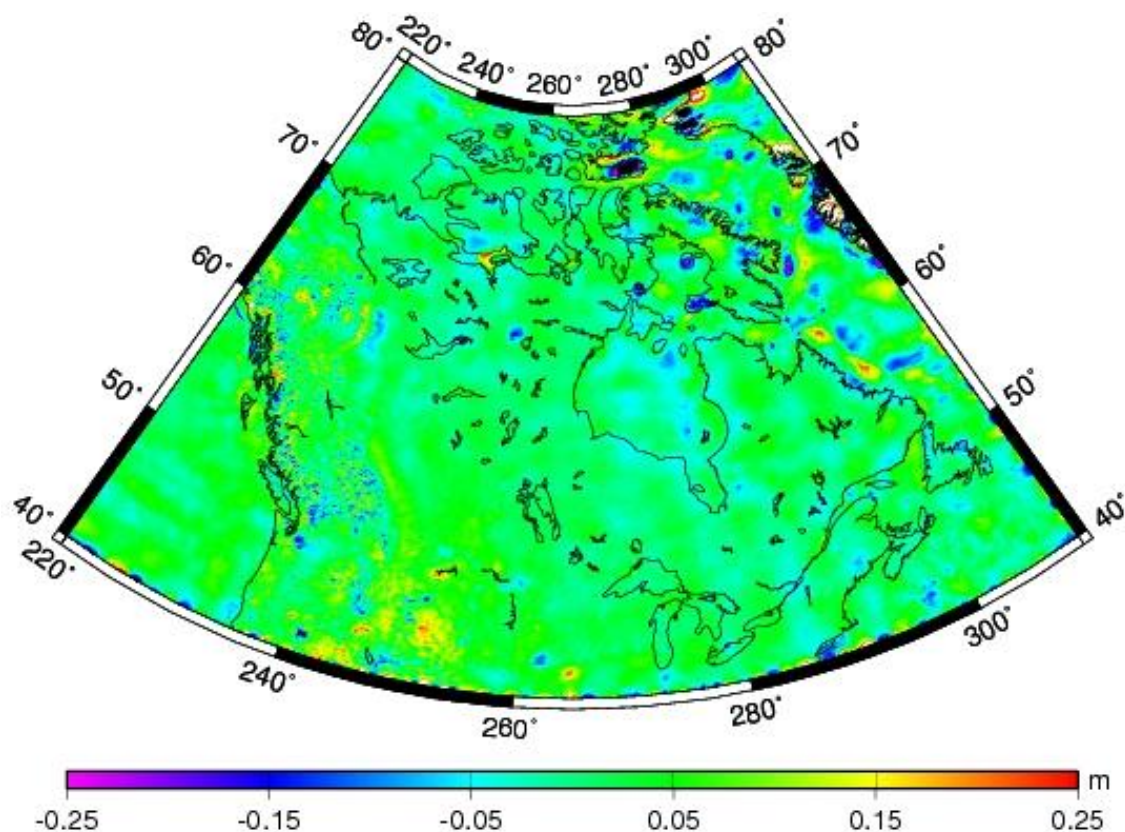


Figure 5.15: The difference between EGM2008 and M6.

5.4. Summary

In summary, the comparisons of the combined models $h_{GNSS} - H - N_{grav}$ made with the Canadian GPS/leveling suggest a geoid agreement of 11.5-12 cm for Canada, 4.1-5.0 cm for the Great Lakes area, and 6.6-7.2 cm for the Rockies. These results indicate the best achievable results thus far by the contribution of the GOCE data to the existing Canadian terrestrial gravity data. The statistics of the recently released latest official Canadian Gravimetric Geoid of 2010, CGG2010, suggests 11.6 cm of geoid agreement with GPS/leveling-derived geoid undulations (Véronneau and Huang, 2011). Considering the fact that the GOCE solution used in the combined models was developed from only the first two-month observations cycle, upcoming GOCE solutions obtained from longer period observations are expected to improve the results in Canada and in some sub-regions such as Yukon (Huang and Véronneau, 2010). Our preliminary investigations on

the second generation GOCE models also support the idea that upcoming GOCE models may provide more accurate geoid model and agreement with GPS/leveling-derived geoid undulations. In addition, GOCE data used here should be replaced with GRACE-based data for the lower degree components or GRACE and GOCE combined satellite-only based datasets (such as GOCO01S and GOCO02S) might be other options to be used in the development of the new combined geoid models.

CHAPTER 6

6. CONCLUSIONS AND RECOMMENDATIONS

In this final chapter, the conclusions and recommendations of the thesis are given. The requirement of a precise regional geoid model to be used as a vertical reference surface in transforming the GPS ellipsoidal heights into the physical heights in Canada has been the starting point of this study. The investigations on the satellite-only and satellite and terrestrial data combined regional geoid models have been performed with the aim of developing a highly accurate gravimetric geoid model in Canada. Besides accurate terrestrial gravity data, the contribution of the GOCE-only and GRACE-GOCE based satellite-only global gravity field models are important in the development of the combined regional geoid models.

The investigations in the thesis are conducted in three main steps:

- The existing heights and vertical datums in North America are explored; the problems with them are investigated and a new vertical datum based on a geoid model is introduced.
- The GOCE and GRACE-GOCE combined satellite-based global gravity models are evaluated by comparing them to GPS/leveling-derived geoids.
- The new combined regional gravimetric geoid models are developed from a GOCE-only model and Canadian terrestrial data and evaluated with the GPS/leveling-derived geoids, as well as with the existing global and regional geoid models.

The main tests are made by using GPS/leveling benchmarks in all of Canada. Also two specific areas representing different topographical features of Canada, the flat Great Lakes area and the rough Rocky Mountains region, are included in the evaluation to assess the influence of the roughness of the gravity field on the results.

6.1. Conclusions

The conclusions can be given in three parts.

Conclusions on the geoid-based height system in Canada:

- A geoid-based height system in Canada is necessary because the current height system does not meet the requirements of modern GNSS-based height determination and the needs of the users, and it includes known systematic errors.
- A regional gravimetric geoid model, computed from satellite-only based models and Canadian terrestrial data, is proposed to be used as a vertical reference surface in Canada.
- A conventional geopotential value obtained from global computations by the use of altimetry observations or determined from regional tide-gauge sea level observations, conventional constants and a reference ellipsoid defined in a tide-free/zero tide reference system together with accurate global gravity models and epoch information are necessary to define a geoid-based reference system in Canada.

Conclusions on the contributions of satellite-only gravity field models:

- GOCE-only and GRACE and GOCE combined satellite-only models show a good agreement with EGM2008 up to spherical harmonic degree 150-180, 120-150 and 150-180 in Canada, the Great Lakes and the Rocky Mountains, respectively, but none of the satellite-only models shows a significant improvement over EGM2008 for any of the three regions considered.
- In general, GOCE solutions show a good agreement with GPS/leveling-derived geoid undulations up to spherical harmonic degrees of about 120-180 where they start showing a rapid increase of the commission error.
- In general, second generation GOCE based models show better agreement with the GPS/leveling-derived geoid undulations than the first generation GOCE based models except DS01.
- Assessment of the relative accuracy of the GOCE-only solutions suggests that the geoid differences over baselines shorter than 80-100 km are not modeled well by the GOCE observations due to the limited satellite data resolution.

Conclusions on the investigations of the combined regional geoid models:

- In general, the combined models show comparable agreements to EGM2008 in Canada and the two sub regions.
- Model M4 developed from the EGM2008 expansion up to spherical harmonic degree 360 and the complementary Canadian terrestrial data shows an improvement in terms of the standard deviation of the agreement of the geoid undulations compared to the EGM2008-only geoid obtained from its highest expansion, from 12.2 to 11.5 cm in Canada, whereas it does not show any improvement in the sub-regions. This may indicate that the EGM2008 model does not include all terrestrial Canadian datasets currently available, i.e., that there were new gravity measurements included in the Canadian terrestrial data after the development of EGM2008 or the high resolution terrestrial data included in the combined model may be the reason of the improvement.
- No visible improvement coming from GOCE solutions is observed in the Great Lakes and Rocky Mountains regions compared to EGM2008 and CGG2005. This was expected in the Great Lakes area since the region has a good coverage of high quality terrestrial data which was already included in EGM2008.
- The combined model M6 agrees well with EGM2008 except for some areas such as the north-east of Canada, the Yukon Territory, the mountainous areas in the west, eastern and western coastal regions, and parts of Greenland where there are small differences due to the possible impact of the GOCE data or the differences of the terrestrial data included in EGM2008 and M6.
- GOCE is expected to improve the knowledge in the oceans. The differences in the Atlantic Ocean coast are possibly due to the update coming from the GOCE data.
- The comparisons $h_{GNSS} - H - N_{grav}$ of the combined models made with the Canadian GPS/leveling data suggest a geoid agreement of 11.5-12 cm for Canada, 4.1-5.0 cm for the Great Lakes area, and 6.6-7.2 cm for the Rockies.

In summary:

- One important contribution of this study is to provide a GOCE-only and complementary terrestrial data combined geoid model in Canada. The current studies include the information from GOCE and GRACE together (e.g., CGG2010) and the investigations may not be enough to dictate if and how much, and in which wavelength interval of the gravity field, GOCE can contribute and improve the current geoid model in Canada and sub-regions. This study provides an interpretation of the usage of the first generation GOCE time-wise solution to a regional combined geoid model without including any other satellite data information.
- Another contribution is to assess the results regarding the accuracy of the satellite-only models. Satellite-only models are potentially expected to be used in the development of a unified Canadian and global vertical datum alone rather than in combined models with terrestrial data. This study will help the construction of the regional and Canadian geoid models by investigating the quality of the recent GOCE solutions.

6.2. Recommendations

- A geoid-based vertical datum in Canada is to be realized by a globally or regionally determined W_0 value and a surface defining the geoid.
- Tide gauge records can be used to determine the W_0 value; however, an accurate sea surface topography model is necessary to correct the observed sea level records for the sea surface topography.
- The improvement of the geoid can be obtained by the recent and future GOCE-only and GOCE-GRACE combined satellite-only models and the recently collected altimetry/shipborne based gravity data in the oceans.
- GOCE models do not provide accurate information for the lower degree components of the gravity field. Therefore, GRACE-based models and/or data from other geodetic techniques (e.g., SLR) should be incorporated in the solutions.

- There is no plan for more land surveys in Canada. Updates on the treatment and the realization of the terrestrial gravity data (e.g., topographical reduction by using a denser and more accurate DEM) might be an option to improve the accuracy of the geoid.
- Any improvement in the methodology (e.g., using another function instead of the cosine function to obtain transition coefficients can provide more smooth transition in the modified Stokes band) can help to develop a more accurate geoid model.
- The best accuracy can only be obtained by making use of the best available datasets, and none of the existing datasets is perfect. North American agencies working on the geoid-based vertical datum and improvement of the geoid need to cooperate in data sharing and updating.
- The new geoid model of Canada can be realized as a vertical datum through the following steps:
 - The best static geoid model in Canada should be developed by using the most recent and accurate satellite and terrestrial datasets available. The possible satellite model suggested to be used in the combined model can be a product of GRACE, GOCE and other combined geodetic techniques, rather than using a GOCE model alone.
 - This geoid needs to be estimated for a specific epoch and the change of the geoid in time should be observed and modeled.
 - Depending on how big the temporal change is, updates with need to be applied to the static geoid. This updating will provide a long-term geoid as a reference surface. Previous studies indicated that the change of the estimated geoid height from combined terrestrial gravity rates and GPS vertical velocities agree with each other within 0.1 to 0.2 mm/year due to the post glacial rebound effect. Accordingly, geoid model in Canada should be updated every decade (Rangelova, 2007).

- If new, unique and more accurate datasets are obtained, or new geodetic techniques used in the data collection are developed, it will be necessary to compute a new static geoid model and its temporal variation.
- Lastly, besides the GPS/leveling datasets, another independent set of data can be used in the evaluation of the geoid models. Many of the Canadian GPS/leveling benchmarks deteriorate rapidly, are not stable anymore, and the land movement due to the post-glacial rebound needs to be considered in the comparisons. Accordingly, other independent datasets not included in the development of the geoid model (e.g., airborne deflections of vertical data) can provide additional independent data sets for the validation procedure of the existing and future Canadian geoid models. The GSD has already collected such datasets and has performed a preliminary validation.

REFERENCES

- Amos, M.J. and Featherstone, W.E., (2009):** Unification of New Zealand's local vertical datums: iterative gravimetric quasigeoid computations, *Journal of Geodesy*, vol. 83, number 1, pp. 57-68.
- Ardalan, A.A., Karimi, R., and Poutanen, M., (2009):** A bias-free geodetic boundary value problem approach to height datum unification, *Journal of Geodesy*, vol. 84, number 2, pp. 123-124.
- Augath, W. and Ihde, J., (2002):** Definition and realization of vertical reference systems – The European Solutions EVRS/EVRF 2000-, FIG XXII International Congress, Washington, D.C., USA, 19-26 April.
- Bajracharya, S., (2003):** Terrain Effects on Geoid Determination, *MSc Thesis*, Report No. 20181, University of Calgary, Canada.
- Balasubramania, N., (1994):** Definition and Realization of a Global Vertical Datum. Department of Geodetic Science and Surveying, Report No. 427, The Ohio State University, Columbus, USA.
- Balmino, G., Perosanz, F., Rummel, R., Sneeuw, N., Sünkel, H., and Woodworth, P., (1998):** European views on dedicated gravity field missions: GRACE and GOCE, An Earth Sciences Division Consultation Document, European Space Agency Report ESA-MAG-REP-CON-001.
- Barthelmes, F., (2009):** Definition of Functionals of the Geopotential and Their Calculation from Spherical Harmonic Models, Theory and formulas used by the calculation service of the International Centre for Global Earth Models (ICGEM), Scientific Technical Report STR09/02, GFZ, Potsdam.
- Bruinsma, S.L., Marty, J.C., Balmino, G., Biancale, R., Förste, C., Abrikosov, O., and Neumayer, H., (2010):** GOCE gravity field recovery by means of the direct numerical method, presented at the ESA Living Planet Symposium, Bergen, Norway, 27 June - 2 July.
- Burša, M., (1995):** Report of special commission SC3, Fundamental Constants, Presented at the 21st General Assembly of the International Association of Geodesy, Boulder, CO, USA, 2-14 July.

- Burša, M., Kenyon, S., Kouba, J., Šima, Z., Vatrt, V., and Vojtíšková, M., (2004):** A global vertical reference frame based on four regional vertical datums, *Studia Geophysica et Geodaetica*, vol. 48, pp. 493-502.
- Burša, M., Kenyon, S., Kouba, J., Šima, Z., Vatrt, V., Vitek, V., and Vojtíšková, M., (2007):** The geopotential value W_0 for specifying the relativistic atomic time scale and a global vertical reference system, *Journal of Geodesy*, vol. 81, number 2, pp. 103-110.
- Cannon, J. B., (1929):** Adjustments of the precise level net of Canada 1928. Publication No. 28, Geodetic Survey Division, Earth Sciences Sector, Natural Resources Canada, Ottawa, Canada.
- Colombo, O.L., (1980):** A World Vertical Network, Department of Geodetic Science and Surveying, Report No. 296, The Ohio State University, Columbus, USA.
- Colombo, O.L., (1981):** Numerical Methods for Harmonic Analysis on the Sphere, Department of Geodetic Science and Surveying, Report No. 310, The Ohio State University, Columbus, USA.
- de Bruijne, A., Haagmans, R., and de Min, E., (1997):** A preliminary North Sea Geoid Model GEONZ97, Project report, Directoraat-Generaal Rijkswaterstaat, Meetkundige Dienst.
- de Min, E., (1990):** On the Computation of the Geoid and Its Errors: With Special Attention to the Inner Zone, *MSc Thesis*, Technical University of Delft, The Netherlands.
- Drinkwater, M.R., Floberghagen, R., Haagmans, R., Muzi, D., and Popescu, A., (2003):** GOCE ESA's first Earth Explorer Core mission. In Beutler, G.B., Drinkwater M., Rummel R., and von Steiger R. (Eds.), *Earth Gravity Field from Space - from Sensors to Earth Sciences*, In the Space Sciences Series of ISSI, Vol. 18, 419-432, Kluwer Academic Publishers, Dordrecht, Netherlands, ISBN: 1-4020-1408-2.
- Ellmann, A. and Vaníček, P. (2007):** UNB application of Stokes-Helmert's approach to geoid computation, *Journal of Geodynamics*, vol. 43, pp. 200-213.

- Erol, B., (2007):** Investigations on local geoids for geodetic applications, *PhD. Thesis*, Istanbul Technical University, Istanbul, Turkey.
- ESA, (2005):** The European Programme for Global Navigation Services. European Space Agency, BR-186, ESA Publications Division, The Netherlands.
- ESA, (2010):** European Space Agency-Living Planet Programme, The Gravity Field and Steady-State Ocean Circulation Explorer (GOCE) mission website, <http://www.esa.int/SPECIALS/GOCE/index.html>.
- Featherstone, W.E., (1998):** Do we need a gravimetric geoid or a model of the Australian height datum to transform GPS Heights in Australia? *The Australian Surveyor*, vol. 43, number 4, pp. 273-280.
- Featherstone, W.E., Evans, J.D., and Olliver, J.G., (1998):** A Meissl-modified Vaníček and Kleusberg kernel to reduce the truncation error in gravimetric geoid computations, *Journal of Geodesy*, vol. 72, number 3, pp. 154-160.
- Featherstone, W.E. and Kuhn, M., (2006):** Height systems and vertical datums: a review in the Australian context, *Journal of Spatial Science*, vol. 51, number 1, pp. 21-42.
- Featherstone, W.E., Kirby, J.F., Hirt, C., Filmer, M.S., Claessens, S.J., Brown, N.J., Hu, G., and Johnston, G.M., (2010):** The AUSGeoid09 model of the Australian Height Datum, *Journal of Geodesy*, vol. 85, number 3, pp. 133-150.
- Forsberg, R., (1994):** Terrain Effects in Geoid Computations, In International School for the Determination of the Geoid, Lecture Notes, Milan, Italy, 10-15 October
- Forsberg, R. and Madsen, F., (1990):** High-precision geoid heights for GPS leveling, Presented GPS-90 Symposium, Ottawa.
- Fotopoulos, G., (2003):** An Analysis on the Optimal Combination of Geoid, Orthometric and Ellipsoidal Height Data, *PhD Thesis*, Report No. 20185, University of Calgary, Canada.
- Förste, C., Flechtner, F., Schmidt, R., Stubenvoll, R., Rothacher, M., Kusche, J., Neumayer, H., Biancale. R., Lemoine, J-M., Barthelmes, F., Bruinsma, S., Koenig, R., and Meyer. Ul., (2008):** EIGEN-GL05C - A new global combined

high-resolution GRACE-based gravity field model of the GFZ-GRGS cooperation, *Geophysical Research Abstracts*, vol. 10, EGU2008-A-03426.

Fu, R., Del Genio, A.D., and Rossow, W.B., (1994): Influence of ocean surface conditions on atmospheric vertical thermodynamic structure and deep convection, *Journal of Climate*, vol. 7, pp. 1092-1108.

GOCE, (2008): GOCE Level 2 Product Data Handbook prepared by the GOCE Gravity Consortium EGG-C.

Goiginger, H., Hoeck, E., Rieser, D., Mayer-Guerr, T., Maier, A., Krauss, S., Pail, R., Fecher, T., Gruber, T., Brockmann, J.M., Krasbutter, I., Schuh, W.-D., Jaeggi, A., Prange, L., Ausleitner, W., Baur, O., and Kusche, J.: The combined satellite-only global gravity field model GOCO02S, presented at the 2011 General Assembly of the European Geosciences Union, Vienna, Austria, 4-8 April.

Grafarend, E.W. and Ardalan, A.A. (1997): W_0 : an estimate in the Finnish Height Datum N60, epoch 1993.4, from twenty-five GPS points of the Baltic Sea Level Project, *Journal of Geodesy*, vol. 71, number 11 pp. 673-679.

Grebenitcharsky, R.S., (2004): Numerical Solutions to altimetry-gravimetry boundary value problems in coastal regions, *PhD Thesis*, Report No. 21095 University of Calgary, Canada.

Gruber, T., (2009): Evaluation of the EGM2008 gravity field by means of GPS-Leveling and sea surface topography solutions: In External quality evaluation reports of EGM2008, *Newton's Bulletin*, vol. 4, pp. 3-17.

Heck, B., (1990): An evaluation of some systematic error sources affecting terrestrial gravity anomalies. *Bulletin Géodésique*, vol. 64, pp. 88-108.

Heck., B., (2003): On Helmert's methods of condensation, *Journal of Geodesy*, vol. 77, numbers 3-4, pp. 155-170.

Heck, B. and Grüninger, W., (1987): Modification of Stokes formula by combining two classical approaches, *Proceedings of XIX. IUGG General Assembly*, Vancouver, pp. 299-337.

- Heck, B. and Rummel, R., (1990):** Strategies for solving the vertical datum problem using terrestrial and satellite geodetic data. *International Association of Geodesy Symposia*, vol. 104, Sünkel H and Baker T (Eds.), Springer-Verlag, pp. 116-128.
- Hofmann-Wellenhof, B. and Moritz, H., (2005):** Physical Geodesy. Springer-Verlag, Wien.
- Huang, J. and Véronneau, M., (2004):** GPS-leveling and CHAMP&GRACE geoid models, Joint CHAMP/ GRACE meeting, GFZ, Postdam, Germany, 6 July.
- Huang, J. and Véronneau, M., (2005):** Applications of downward-continuation in gravimetric geoid modeling: case studies in Western Canada, *Journal of Geodesy*, vol. 79, numbers 1-3, pp. 135-145.
- Huang, J. and Véronneau, M., (2006):** Spherical harmonic spectral response of different Stokes kernel modifications, The 2006 Joint Assembly, Baltimore Maryland, USA, 23-26 May.
- Huang, J., Fotopoulos, G., Cheng, M.K., Véronneau, M., and Sideris, M.G., (2007):** On the Estimation of the Regional Geoid Error in Canada, *In International Association of Geodesy Symposia*, pp. 273-279.
- Huang, J. and Véronneau, M., (2009):** Evaluation of the GRACE-based Global Gravity Field Models in Canada, In: External quality evaluation reports of EGM2008, *Newton's Bulletin*, vol. 4, pp. 66-72
- Huang, J. and Véronneau, M., (2010):** Methods of using the satellite-based global gravity field models to model the geoid in Western Canada and Alaska. In: Second International Symposium of the International Gravity Field Service, Fairbanks, Alaska, USA, 20-22 September
- Huang, J., Véronneau, M., Henton, J., and Héroux, P., (2011):** A Prototype of a Geoid-Based Height System in Canada, XXV IUGG General Assembly, Earth on the Edge: Science for Sustainable Planet, Melbourne, Australia, IAG G06: Towards a unified World Height System, 28 June-7 July.
- ICGEM, (2010):** International Centre for Global Earth Models, <http://icgem.gfz-potsdam.de/ICGEM/ICGEM.html>.

- IGLD, (1979):** Establishment of IGLD55, Second Edition” prepared by the Coordinating Committee.
- IGLD, (1991):** International Great Lakes Datum, Update Letter No: 76, November 4
- IGLD, (1995):** Establishment of International Great Lakes Datum (1985), by The Coordinating committee on Great Lakes Basic Hydraulic and Hydrologic Data.
- Ihde et al., (2007):** Conventions for the Definition and Realization of a Conventional Vertical Reference System (CVRS) IAG inter-commission project, ICP1.2 Vertical Reference Frames.
- Ihde, J. and Sánchez, L., (2005):** A unified global height reference system as a basis for IGGOS, *Journal of Geodynamics*, vol. 40, pp. 400-413.
- Jekeli, C., (1979):** Global Accuracy Estimates of Point and Mean Undulation Differences Obtained from Gravity Disturbances, Gravity Anomalies and Potential Coefficients, Department of Geodetic Science and Surveying, Report No. 288, The Ohio State University, Columbus, USA.
- Jekeli, C., (2000):** Heights, the Geopotential, and Vertical Datums. Ohio State University, Department of Geodetic Science and Surveying, Report No. 459, The Ohio State University, Columbus, USA.
- Kaula, W. M., (1966):** Theory of Satellite Geodesy, Blaisdell Publishing Company, USA.
- Klees, R. and van Gelderen, M., (1997):** The Fiction of the Geoid. Presented at the *Staring Symposium, Royal Academy of Sciences*, Amsterdam, Netherlands, 12 Oct., 1997. Also in Delft Institute for Earth-Oriented Space Research (DEOS) Progress Letters, 97.1, pp. 17-26.
- Kotsakis, C. and Sideris, M.G., (1999):** On the adjustment of combined GPS/levelling/geoid networks. *Journal of Geodesy*, vol. 73, number 8, pp. 412–421.
- Kotsakis, C., Katsambalos, K., and Gianniou, M., (2009):** Evaluation of EGM08 based on GPS and orthometric heights over the Hellenic mainland, In: External quality evaluation reports of EGM2008, *Newton's Bulletin*, vol. 4, pp. 144-163

- Lehmann, R., (1999):** Boundary-value problems in the complex world of geodetic measurements, *Journal of Geodesy*, vol. 73, number 9, pp. 491- 500.
- Lehmann, R., (2000):** Altimetry-gravimetry problems with free vertical datum. *Journal of Geodesy*, vol. 74, numbers 3-4, pp. 327-334.
- Lemoine, F.G., Kenyon, S.C., Factor, J.K., Trimmer, R.G., Pavlis, N.K., Chinn, D.S., Cox, C.M., Klosko, S.M., Luthcke, S.B., Torrence, M.H., Wang, Y.M., Williamson, R.G., Pavlis, E.C., Rapp, R.H., and Olson, T.R. (1998):** The development of the joint NASA GSFC and the National Imagery and Mapping Agency (NIMA) geopotential model EGM96. NASA Technical Publication -1998 - 206861, July.
- Mainville, A., Forsberg, R., and Sideris, M.G., (1992):** Global Positioning System testing of geoids computed from geopotential models and local gravity data. *Journal of Geophysical Research*, vol. 97, no.B7, pp. 11,137-11,147.
- Martensen, E. and Ritter, S., (1997):** Potential theory. in *Lecture Notes in Earth Sciences, vol. 65, Geodetic Boundary Value Problems in View of the 214 One Centimeter Geoid*, pp. 19-66, Eds. F. Sanso and R. Rummel, Springer-Verlag, Berlin.
- Martinec, Z., (1998):** Boundary-Value Problems for Gravimetric Determination of a Precise Geoid, *Lecture Notes in Earth Sciences*.
- Martinec, Z., Matyska, C., Gradarend, E.W., and Vaniček, P., (1993):** On the Helmert's 2nd condensation method, *manuscript geodaetica*, vol. 18, pp.417-421.
- Mather, R. S., (1978):** The role of the geoid in four-dimensional geodesy, *Marine Geodesy*, vol. 1, number 3, pp.217-252.
- Mayer-Guerr, T., Kurtenbach, E., and Eicker A., (2010):** The GRACE-only gravity field model ITG-Grace2010s,
<http://www.igg.uni-bonn.de/apmg/index.php?id=itg-grace2010>.
- Meissl, P., (1971):** Preparation for the numerical evaluation of second-order Molodensky-type formulas, Department of Geodetic Science and Surveying, Report No. 163, The Ohio State University, Columbus, USA.

- Migliaccio, F., Reguzzoni, M., Sanso, F., Tscherning, C. C., and Veicherts, M., (2010):** GOCE data analysis: the space-wise approach and the first space-wise gravity field model. Proceedings of the ESA Living Planet Symposium, Bergen, Norway, 28 June–2 July.
- Moritz, H., (1980):** Advanced Physical Geodesy. Herbert Wichmann Verlag, Karlsruhe, Abacus Press, Tunbridge Wells, Kent.
- Moritz, H., (1992):** Geodetic Reference System 1980. *Bulletin Geodesique*, vol. 66, pp. 187-192.
- Nahavandchi, H. and Sjöberg, L.E., (1997):** Terrain correction to power H^3 in gravimetric geoid determination, *Journal of Geodesy*, vol 72, number 3, pp.124-135.
- Novak, P., (2000):** Evaluation of Gravity Data for the Stokes Helmert Solution to the Geodetic Boundary-value Problem, *PhD. Thesis*, Report No. 207, University of New Brunswick, Canada.
- NRCan, 2011:** Height Reference System Modernization, Geodetic Survey Division, Earth Sciences Sector, Natural Resources Canada, http://www.geod.nrcan.gc.ca/hm/index_e.php.
- Omang, O.C.D. and Forsberg, R., (2000):** How to handle topography in practical geoid determination: three examples, *Journal of Geodesy*, vol. 74, number 6, pp. 478-488.
- Pail, R., Metzler, B., Preimesberger, T., and Wermuth, M., (2006):** GOCE Quick-Look Gravity Field Analysis in the Framework of HPF, Proc. 3rd GOCE User Workshop, Frascati, ESA.
- Pail, R., Goiginger, H., Mayrhofer, R., Schuh, W., Brockmann, J. M., Krasbutter, I., Hoeck, E., and Fecher, T., (2010a):** GOCE gravity field model derived from orbit and gradiometry data applying the time-wise method. Proceedings of the ESA Living Planet Symposium, Bergen, Norway, 28 June – 2 July 2010.
- Pail, R., Goiginger, H., Schuh, W.-D, Hock, E., Brockmann, M., Fecher, T., Gruber, T., Mayer-Gurr, T., Kusche, J., Jaggi, A., and Rieser, D., (2010b):** Combined

satellite gravity field model GOCO01S derived from GOCE and GRACE, *Geophysical Research Letters*, vol. 37, L20314.

- Pail, R., Bruinsma, S., Migliaccio, F., Förste, C., Goiginger, H., Schuh, W.-D, Hoeck, E, Reguzzoni, M., Brockmann, J.M, Abrikosov, O., Veicherts, M., Fecher, T., Mayrhofer, R., Krasbutter, I., Sanso, F., and Tscherning, C.C., (2011):** First GOCE gravity field models derived by three different approaches, *Journal of Geodesy*, in review.
- Pan, M. and Sjöberg, L.E., (1998):** Unification of vertical datums by GPS and gravimetric geoid models with application to Fennoscandia, *Journal of Geodesy*, vol. 72, number 2, pp. 64-70.
- Pavlis, N.K., (1997):** Development and Applications of Geopotential Models, prepared for the Second International School for the Determination and use of the Geoid, Rio de Janeiro, Brazil, 10-16 September.
- Pavlis, N.K., (2006):** Global Gravitational modeling, An Overview Considering current and Future Dedicated Gravity Mapping Missions, prepared for the IGes Geoid School 2006, The Determination and Use of the Geoid, University of Copenhagen, Denmark, 19-23 June
- Pavlis, N.K., Holmes, S.A., Kenyon, S.C., and Factor, J.K., (2008):** An Earth Gravitational Model to Degree 2160: EGM 2008, presented at Session G3: "GRACE Science Applications", EGU Vienna.
- Pavlis, N.K., (2010):** Lecture presentation, Determination and use of the geoid, 10th International Geoid School Lecture Notes, Concern CSRI Elektropribor, JSC, Saint Petersburg, Russia, 28 June- 2 July.
- Rangelova, E.V., (2007):** A Dynamic Geoid Model for Canada, *PhD. Thesis*, Report No. 20261, University of Calgary, Canada.
- Rapp, R.H., (1997):** Use of potential coefficient models for geoid undulation determinations using a spherical harmonic representation of the height anomaly/geoid undulation difference, *Journal of Geodesy*, vol. 71, number 5, 282-289.

- Rapp, R.H. and Rummel, R., (1975):** Methods for the Computation of Detailed Geoids and their Accuracy. Department of Geodetic Science and Surveying, Report No. 233, The Ohio State University.
- Reigber, Ch., Lühr, H., and Schwintzer, P., (2003):** First CHAMP mission results for gravity, magnetic and atmospheric studies, Springer-Verlag, 563.
- Reigber, Ch., Schwintzer, P., Lühr, H., and Wickert, J. (2004):** CHAMP: Mission Status & Development. Joint CHAMP/GRACE Science Meeting, Potsdam, Germany.
- Rizos, C., (1979):** An efficient computer technique for the evaluation of geopotential from spherical harmonics, *Australian Journal of Geodesy Photogrammetry and Surveying*, vol. 31, pp. 161-169.
- Roman, D.R. and Smith, D. A., (2000):** Recent investigations toward achieving a one centimeter geoid, presented at GGG2000 session 9 of the IAG Symposium in Banff, Alberta, Canada, 31 July–4 August.
- Rummel, R. and Teunissen, P., (1988):** Height datum definition, Height datum connection and the role of the geodetic boundary value problem, *Bulletin Géodésique*, vol. 62, pp. 477-498.
- Rummel, R. and Sanso, F., (1993):** Satellite Altimetry in Geodesy and Oceanography, Lecture notes Earth Science., 50, Berlin, Springer Verlag, pp. 479.
- Rummel, R. and Ilk, K.H., (1995):** Height datum connection – the ocean part, *Allgemeine Vermessungsnachrichten, Wichmann, Helf* 8-9, pp. 321-329.
- Rummel, R., Balmino, G., Johannessen, J., Visser, P., and Woodworth, P., (2002):** Dedicated gravity field missions-principles and aims. *Journal of Geodynamics*, vol. 33, pp. 3-20.
- Sánchez, L., (2007):** Definition and realisation of the SIRGAS vertical reference system within a globally unified height system, In *Dynamic Planet: Monitoring and Understanding a Dynamic Planet with Geodetic and Oceanographic Tools*, 130, pp. 638-645.
- Sánchez, L., (2009):** Strategy to establish a Global Vertical Reference System, *International Association of Geodesy Symposia*, 2009, vol. 134, part 5, 273-278

- Sanso, F. and Venuti, G., (2002):** The height datum/geodetic datum problem, *Geophysical Journal International*, 149, pp.768-775.
- Schwarz, K.P., Sideris, M.G., and Forsberg, R., (1987):** Orthometric heights without levelling, *Journal of Surveying Engineering*, vol. 113, number 1, pp. 28-40.
- Seeber, G., (1993):** *Satellite Geodesy: Foundations, Methods and Applications*. Walter de Gruyter, New York.
- Shum, C.K., Woodworth, P.L., Andersen, O.B., Egbert, E., Francis, O., King, C., Klosko, S., Le Provost, C., Li, X., Molines, J.M., Parke, M., Ray, R., Schlax, M., Stammer, D., Thierney, C., Vincent, P., and Wunsch, C., (1997):** Accuracy assessment of recent ocean tide models. *Journal of Geophysical Research*, vol. 102, C11, pp. 173-194.
- Sideris, M.G., (1994):** Geoid determination by FFT techniques, In *Lecture Notes, International School for the Determination and Use of Geoid*, DIIAR, Politecnico di Milano, Italy, 10-15 October.
- Sideris, M.G. and Forsberg, R., (1991):** Review of Geoid Prediction methods in Mountainous regions. in *International Association of Geodesy Symposia*, vol. 106, *Determination of the Geoid: Present and Future*, pp. 51-62, Eds. Rapp, R.H. and Sanso, F., Springer-Verlag.
- Sideris, M.G., Mainville, A., and Forsberg, R., (1992):** Geoid testing using GPS and leveling (or GPS testing using leveling and the geoid?). *Australian Journal of Geodesy, Photogrammetry and Surveying*, number.57, pp. 62-67.
- Sideris, M.G. and She, B.B., (1995):** A new high-resolution geoid for Canada and part of the U.S. by 1D-FFT method. *Bulletin Geodesique*, vol. 69, pp. 92–108.
- Sjöberg, L.E., (1984):** Least-squares modification of Stokes's and Vening Meinesz's formula by accounting for truncation and potential coefficient errors. *Manuscripta Geodaetica*, vol. 9, pp. 229–248.
- Sjöberg, L.E., (1986):** Comparison of some methods of modifying Stokes formula, *Bollettino di Geodesia e Scienze Affini*, vol. 46, pp. 229–248.
- Sjöberg, L.E., (1991):** Refined least squares modification of Stokes's formula. *Manuscripta Geodaetica*, vol. 16: pp. 367-375.

- Sjöberg, L.E., (1998):** The exterior Airy/Heiskanen topographic-isostatic gravity potential anomaly and the effect of analytical continuation in Stokes's formula. *Journal of Geodesy*, vol. 72, number 11, pp. 654–662.
- Stokes, G.G., (1849):** On the variation of gravity at the surface of the Earth. *Trans. Cambridge Philos. Soc.* VIII, 672-695.
- Tapley, B.D. and Reigber, C., (2004):** The GRACE Mission: Status and Early Results, *Eos Trans. AGU*, 85(17), Jt. Assem. Suppl., Abstract U31A-01, Montreal, Canada May
- Torge, W., (2001):** *Geodesy*, Walter de Gruyter, Berlin New York, 3rd edition.
- UTEX CSR, (2004):** <http://www.csr.utexas.edu/grace/gravity>.
- van Gelderen, M., (1991) :** The geodetic boundary value problem in two dimensions and its iterative solutions, *Publications on Geodesy* 35, Delft, 1991. 143.
- van Onselen, K., (1997):** Quality Investigation of Vertical Datum Connection. Delft University of Technology, DEOS Report No. 97.3.
- Vaniček, P., (1991):** Vertical Datum and NAVD88. *Surveying and Land Information Systems*, vol. 51, number. 2, pp. 83-86.
- Vaniček, P. and Kleusberg, A., (1987):** The Canadian geoid- Stokesian approach. *Manuscripta Geodaetica*, vol. 12, pp. 86-98.
- Vaniček, P. and Sjöberg, L., (1991):** Reformulation of Stokes's Theory for Higher than Second-Degree Reference Field and Modification of Integration Kernels, *Journal of Geophysical Research*, vol. 96, number B4, pp. 6529-6539.
- Vaniček, P., Najafi, M., Martinec, Z., Harrie, H., and Sjöberg, E., (1995):** Higher-degree reference field in the generalized Stokes-Helmert scheme for geoid computation, *Journal of Geodesy*, vol. 70, number 3, pp. 176-182.
- Vaniček, P. and Featherstone, W.E., (1998):** Performance of three types of Stokes's kernel in the combined solution for the geoid, *Journal of Geodesy*, vol. 72, number 12, pp. 684-697.
- Vaniček, P., Huang, J., Novak, P., Pagiatakis, S., Véronneau, M., Martinec, Z., and Featherstone, W.E., (1999):** Determination of the boundary values for the Stokes-Helmert problem, *Journal of Geodesy*, vol. 73, pp. 180-192.

- Véronneau, M., (report):** Height Reference Systems in North America and Gravity, NRCan internal report, Geodetic Survey Division, Earth Sciences Sector, Natural Resources Canada, Ottawa, Canada.
- Véronneau, M., (1994):** Determination of Mean Helmert Gravity Anomalies in a Plane Approximation, Internal Report, Geodetic Survey Division, Earth Sciences Sector, Department of Natural Resources Canada, Ottawa, Canada.
- Véronneau, M., (2001):** The Canadian Gravimetric Geoid Model of 2000 (CGG2000): http://www.geod.nrcan.gc.ca/publications/papers/abs26_e.php, accessed 19 July 2010.
- Véronneau, M., Duval, R., and Huang, J., (2006):** A gravimetric geoid model as a vertical datum for Canada. *Geomatica*, vol. 60, number 2, pp. 165-172.
- Véronneau, M. and Héroux, P., (2007):** Canadian Height Reference System Modernization: Rational, Status and Plans, Geocongres, Québec, Canada, 2-5 October.
- Véronneau, M. and Huang, J. (2007):** The Canadian Gravimetric Geoid Model 2005 (CGG2005), report, Geodetic Survey Division, Earth Sciences Sector, Natural Resources Canada, Ottawa, Canada.
- Véronneau, M. and Huang, J. (2011):** A new Gravimetric Geoid Model for Canada: CGG2010, CGU Annual Scientific Meeting, Banff, Alberta, Canada, 15-18 May.
- Wong, L. and Gore, R. (1969):** Accuracy of geoid heights from modified Stokes kernel. *Geophysical Journal*, *Astron Soc* 18:81-91.
- Yang, Z.J., (1998):** Precise Determination of Local geoid and its Geophysical Interpretation, *PhD Thesis*, The Hong Kong Polytechnic University, Hong Kong.
- Zilkoski, D. B., (1991):** "North American Vertical Datum and International Great Lakes Datum: They are One and the Same," National Geodetic Survey, Silver Spring, Maryland, USA.

Appendix A

Illustration of the spherical harmonic coefficients and their errors for the first generation GOCE-only solution TW01 is given in Appendix A.

```

begin_of_head =====
product_type          gravity_field
modelname            EGM_GOC_2_20091101T000000_20100111T000000_0002
earth_gravity_constant 3.9860044150000000E+14
radius                6.3781362999999998E+06
max_degree           224
errors                formal
norm                  fully_normalized
tide_system           tide_free

key   L   M           C           S           sigma C           sigma S
end_of_head =====
gfc  0  0   1.0000000000000000   0.0000000000000000   0.0000000000000000   0.0000000000000000
gfc  1  0   0.0000000000000000   0.0000000000000000   0.0000000000000000   0.0000000000000000
gfc  2  0  -4.8416512626965743E-04   0.0000000000000000   5.8737841985093265E-11   0.0000000000000000
gfc  3  0   9.5718902423203781E-07   0.0000000000000000   5.2548171712564754E-11   0.0000000000000000
gfc  4  0   5.3987992612476683E-07   0.0000000000000000   8.2526178088664044E-11   0.0000000000000000
gfc  5  0   6.8621231048452158E-08   0.0000000000000000   7.1285791761116760E-11   0.0000000000000000
gfc  6  0  -1.5040126751902623E-07   0.0000000000000000   1.0572426239560897E-10   0.0000000000000000
gfc  7  0   9.0584842067375286E-08   0.0000000000000000   8.8904520864562271E-11   0.0000000000000000
gfc  8  0   4.9058628174311774E-08   0.0000000000000000   1.2885499860465435E-10   0.0000000000000000
gfc  9  0   2.8096440576346767E-08   0.0000000000000000   1.0650532279631679E-10   0.0000000000000000
gfc 10  0   5.2972788449325223E-08   0.0000000000000000   1.5232475664520664E-10   0.0000000000000000
gfc 11  0  -5.0587495626466319E-08   0.0000000000000000   1.2424625616526455E-10   0.0000000000000000
gfc 12  0   3.5799772442760225E-08   0.0000000000000000   1.7629525672018542E-10   0.0000000000000000
.....
gfc 224 220  9.4317227819836165E-11  3.8155828065789548E-11  2.3136017983503712E-10  2.3136067563242492E-10
gfc 221 221 -1.2418688967690073E-12 -1.19328856260213411E-10  2.3536455027100898E-10  2.3536245576055740E-10
gfc 222 221  3.6060976322153436E-11  1.6200602055850622E-10  2.3457352556351729E-10  2.3457660998956442E-10
gfc 223 221 -1.5847675403494332E-10  1.7142183165991714E-10  2.3315244986408458E-10  2.3315461392189332E-10
gfc 224 221 -6.6060364133969971E-11 -3.3211050877401752E-11  2.3169567518195092E-10  2.3169690951401384E-10
gfc 222 222  4.2623116676538802E-11 -1.1504396702497329E-10  2.3438995919243534E-10  2.3439312632130752E-10
gfc 223 222 -6.6712426549789665E-11  2.6748491086065515E-11  2.3355892512965538E-10  2.3355709172638170E-10
gfc 224 222  2.6093118812320527E-11 -1.0162235655293725E-10  2.3211629744084678E-10  2.3211332906853087E-10
gfc 223 223  3.3557331675088150E-12  5.1666351291710744E-11  2.3336550235318848E-10  2.3336443813735866E-10
gfc 224 223  1.3273887275761105E-11 -3.0381840520759108E-11  2.3247892203988380E-10  2.3248030222509910E-10
gfc 224 224 -3.9022923623328819E-11 -2.8596025423486236E-11  2.3228223136431407E-10  2.3228463425389471E-10

```